



ADVANCED PROCESS SIMULATION MODELLING FOR HYDROGEN APPLICATION IN STEEL AND CEMENT

A Technical and Economic Assessment



HYDROGEN H₂

Advanced Process Simulation Modelling for Hydrogen Application in Steel and Cement – A Technical and Economic Assessment

DST Ref – DST/TMD-EWO/AHFC-2021/2021/185

Murali Ramakrishnan Ananthakumar

Ramprasad Thekkethil

Vengdhanathan Srinivasan

Center for Study of Science, Technology and Policy (CSTEP)

December 2024



Edited and Designed by CSTEP

Disclaimer

Every effort has been made to ensure the correctness of data and information used in this document. However, the authors or CSTEP does not accept any legal liability for the accuracy or inferences of the material contained in this document and for any consequences arising from the use of this material.

©2024 CSTEP

Any reproduction in full or part of this document must mention the title and/or citation, which is given below. Due credit must be provided to the copyright owners of this product.

Suggested citation: CSTEP. 2024. *Advanced process simulation modelling for hydrogen application in steel and cement – A technical and economic assessment*. (CSTEP-RR-2024-11).

December 2024

Editors: Veena P, Reghu Ram R

Designer: Bhawna Welturkar

Bengaluru

No. 18, 10th Cross, Mayura Street
Papanna Layout, Nagashettyhalli
RMV Stage 2, Bengaluru 560094
Karnataka (India)

Noida

1st Floor, Tower-A
Smartworks Corporate Park
Sector 125, Noida 201303
Uttar Pradesh (India)

Tel.: +91 (80) 6690 2500

Email: cpe@cstep.in





सत्यमेव जयते

दूरभाष / Tel. : 26962819, 26567373,
26562134, 26562122 (EPBAX)

फैक्स / Fax : 26569908, 26515637,
26863847, 26862418

वेबसाइट/website : www.dst.gov.in

भारत सरकार
विज्ञान और प्रौद्योगिकी मंत्रालय
विज्ञान और प्रौद्योगिकी विभाग
टेक्नोलॉजी भवन, नया महरौली मार्ग
नई दिल्ली-110 016

GOVERNMENT OF INDIA
MINISTRY OF SCIENCE AND TECHNOLOGY
DEPARTMENT OF SCIENCE AND TECHNOLOGY
TECHNOLOGY BHAVAN, NEW MEHRAULI ROAD
NEW DELHI-110 016

Foreword

Green hydrogen could be the silver bullet to hard-to-abate industries, where matured technologies find it challenging to decouple energy and emissions. Hard-to-abate industries require a scalable and clean solution, which will not drastically change the layout of a plant. As a nation, we continue to aspire for innovative solutions to help decarbonise hard-to-abate segments. Under the Advanced Hydrogen and Fuel Cell (AHFC) programme, several projects aim to develop and demonstrate the application of green hydrogen.

Steel and cement are important commodities, and the performance of these sectors are closely linked with the performance of the economy. These sectors are also closely tied with the energy sector, considering their ever-growing energy requirements (currently at 4,250 petajoules). More than two-third of this demand is met through the combustion of coal and natural gas, among other fossil fuels.

The Center for Study of Science, Technology and Policy (CSTEP) was granted a project centred around the modelling of green hydrogen application in steel and cement manufacturing. They have undertaken this exercise to develop analytical models and use them to adjudge green hydrogen use in blast furnace (iron) and kiln (cement), in addition to providing commentary for alternative resources within the ecosystem. While there are relevant studies that showcase projected hydrogen demand in steel and cement industries, this will be a first-of-a-kind research report that delves into the practicality of green hydrogen application in blast furnace and rotary kiln processes. The findings will inform policymakers about the opportunities and challenges in adopting hydrogen in steel and cement manufacturing.

I congratulate the research team at CSTEP for conducting a comprehensive examination of green hydrogen use in steel and cement manufacturing. The team has incorporated technical reasoning (via modelling) and considered practical limitations (plant visits and stakeholder engagement) to arrive at validated (academia) results.

Dr Ranjith Krishna Pai
Scientist F / Senior Director
Climate, Energy and Sustainable Technology (CEST) Division
Department of Science and Technology (DST)
Ministry of Science and Technology, Government of India

You can also follow us on

@IndiaDST or www.facebook.com/IndiaDST
 @IndiaDST or www.twitter.com/IndiaDST

Acknowledgement

We would like to thank the Department of Science and Technology (DST), Government of India, for providing us the opportunity to conduct this exercise. Special thanks to Dr Anita Gupta, Head of Scientific Division, Climate, Energy and Sustainable Technology (CEST) Division, DST, and Dr Ranjit Krishna Pai, Scientist F, CEST Division, DST, for their leadership and support. We would also like to thank other staff members at DST for offering their time and assistance during the execution of the project. Additional thanks to the leadership support issued at CSTEP from the Committee of Directors (CoD) team.

Technical leadership and advisory

We would be remiss if we did not mention the guidance from Mr N C Thirumalai, Sector Head, Strategic Studies (CSTEP); Dr Sanjay Chandra, Professor of Practice, IIT Bombay; and Dr N Rajalakshmi, Former Senior Scientist, International Advanced Research Centre for Powder Metallurgy and New Materials (ARCI). We also acknowledge the guidance from Dr Max Åhman, Associate Professor, Lund University. Special thanks to Dr S B Hegde, Professor, Jain College of Engineering and Technology, for guiding our researchers on a periodic basis.

Our sincere gratitude to officers from both Tata Steel Ltd, Jamshedpur, and Dalmia Bharat Cements Ltd, Mudhol, for imparting key plant-specific knowledge to our team during plant visits. From Tata Steel Ltd, we would like to thank Dr Samik Nag, Chief – Iron Making Research Group, Research and Development; Mr Sujan Hazra (for his advice to strengthen the technical quality of the report); Mr Girish S; and Mr Supratim Sengupta for productive discussions around hydrogen adoption in steel plants. Similarly, our thanks are due to the team from Dalmia Bharat Cements Ltd—Mr Prabhat Kumar Singh, Mr Shreedhar, and Mr Sameer.

Research and assistance

Our team of researchers would like to appreciate the efforts of Mr Dhiraj Kumar, Mr Gopala Krishnan, Ms Aparna Sharma, Mr Sairam Thandra, Mr Ramanaidu Merla, and Mr Srinu Nagaraju at CSTEP for their contributions in completing this project. Our gratitude to the communication and policy engagement team (Ms Veena P, Ms Bhawna Welturkar, and Mr Reghu Ram R) at CSTEP for helping us refine and improve the quality of the report. We would also like to thank Ms Rajeshree Menon, Chief Financial Officer (CFO), CSTEP, and the accounts team (Mr Mahesh Kumar and Ms Lalitha Naganandan) at CSTEP for supporting us throughout the project duration.



Executive Summary

Decarbonising hard-to-abate sectors calls for measures that can reduce emissions from both fuel combustion and different processes. These measures can yield incremental emission savings for abating emissions at scale. As the last frontier towards the net-zero goal, hard-to-abate sectors such as steel and cement manufacturing units must look to transition to scalable solutions that can offer energy saving opportunities and emissions reduction. In this study, we examine whether hydrogen can play a pivotal role in decarbonising steel and cement sectors. Studies indicate that hydrogen and carbon capture technologies are not silver bullet solutions to these problems. However, applicability and scale of implementation are areas that remain unexplored, especially in Indian conditions. This study estimates the amount of hydrogen that can be used in steel manufacturing and provides a series of options that can be incorporated alongside hydrogen to further amplify emissions reduction. Furthermore, it outlines proven ways of blending hydrogen with other fuels in cement manufacturing to increase the share of alternative fuel resources (AFRs) and reduce coal dependency.

Further, the study delves into rationalising the global and regional outlook for both steel and cement plants. It provides essential statistics such as production, installed capacity, energy consumption, and emissions intensity required to justify the current and projected growth of these sectors. The growing demand for these commodities has a direct impact on energy requirements and consequent emissions. Hence, there is an opportunity and a need for hydrogen as a decarbonisation measure. The thermal energy dependency of these sectors allows us to consider alternative options that can play a substitutive role in the interim, and possibly in the long run, with necessary design modifications.

This report also introduces current technology routes and decarbonisation pathways in the steel sector to emphasise the role of the blast furnace–basic oxygen furnace. It further discusses options available to save energy and reduce emissions, including but not limited to energy efficiency, fuel substitution, and renewable energy. A zero-dimensional perturbation-fluctuation model was developed to demonstrate the threshold of hydrogen injection into a blast furnace. Prior to that, a dynamic process modelling–based approach outlines challenges and shortcomings experienced by the research team in choosing the zero-dimensional approach. After completing mass and energy balance, we estimated that 18–25 kg (with 21 kg as mean value) of hydrogen can be used to produce one tonne of hot metal, resulting in 8%–9% reduction in emissions. Further, we estimated that the levelised cost of hydrogen (LCOH) used in the blast furnace is INR 444 per kg hydrogen, where the levelised cost of electricity is assumed to be INR 7 per kWh. The premium related with the injection of hydrogen in the blast furnace is around 39% higher than a conventional blast furnace. Further, amortisation of incentives under the Strategic Interventions for Green Hydrogen Transition (SIGHT) scheme yields a marginal benefit of 2% reduction in the cost of steel for every tonne of steel produced.

Coming to the cement sector, this report discusses rotary kiln–based cement manufacturing in detail, capturing the thermal and electrical specific energy consumption of various sub-processes involved. Further, indirect decarbonisation measures (such as waste heat recovery and energy efficiency) and direct decarbonisation measures (such as clinker substitution) are discussed. Estimation of the emission reduction potential of carbon management techniques, including carbon capture and utilisation, calcium looping, and the use of molten carbonate fuel cells, along with relatively nascent approaches, such as the electrification of cement manufacturing and electrochemical cement manufacturing, are also examined.



The application of hydrogen as an AFR that can substitute conventional carbon-intensive fuel, such as the coal and pet coke combination, is demonstrated by developing a mass and energy-based perturbation model. It was found that 12 to 18 kg of hydrogen can be injected as fuel for every tonne of clinker produced, depending on whether it is introduced in the rotary kiln or in the pre-calciner. The maximum emission reduction potential of hydrogen was estimated to be 32%, and it has the potential to completely mitigate fuel-based emissions. The study also provides an in-depth analysis of the use of AFRs such as meat and bone meal, glycerine, paint sludge, biomass, and municipal solid waste. Finally, the technical, operational, economic, and social challenges associated with the adoption of these decarbonisation measures are discussed.

Further, all current policies related to steel, cement, and green hydrogen segments are enlisted. These are policies that aid in transitioning to envisaged sustainable pathways (in conjunction with the subject of interest here), thereby helping in achieving production goals. Any improvements or new policy measures that can aid in hydrogen use in these manufacturing units are explained. Iron slime beneficiation, green steel taxonomy, innovative business models to reduce renewable electricity tariff (INR 2 per kWh for breaking even from an investment standpoint) for electrolyzers, pull mechanisms (such as advanced market commitments), energy efficiency measures (such as waste heat recovery systems), R&D-based next-generation technologies, and policy measures are discussed briefly.

In conclusion, the price of hydrogen will need to fall significantly for its greater adoption in steelmaking. The findings suggest that hydrogen adoption in steelmaking is expected to foray into direct reduced iron in the coming years and then transition to blast furnace operations in the next decade. To reduce emissions at scale, all decarbonisation measures will have to play a decisive role. After all, the whole (achieving the goal) is always greater than the sum of its parts (choices and options undertaken).



Contents

1. Introduction.....	15
1.1. Global steel and cement sector outlook.....	15
1.2. Indian steel and cement sector outlook.....	16
1.3. Need for hydrogen as a decarbonisation measure.....	17
2. Steel.....	20
2.1. Technology pathways.....	20
2.2. Decarbonisation pathways.....	24
2.3. Data analysis and scope of analysis.....	26
2.4. Blast furnace modelling.....	26
2.5. Techno-economic assessment.....	49
2.6. Limitations.....	53
3. Cement.....	56
3.1. Cement manufacturing process.....	56
3.2. Energy requirements in a cement plant.....	60
3.3. Need for decarbonising the Indian cement industry.....	61
3.4. AFRs and hydrogen.....	62
3.5. Other decarbonisation measures.....	62
3.6. Challenges to decarbonising the cement industry.....	65
3.7. Process methodology.....	67
3.8. Results and discussion.....	76
3.9. Limitations.....	85
4. Policy Discussions.....	88
4.1. Enabling policy measures.....	89
5. Way Forward and Conclusion.....	92
6. References.....	94
7. Appendix.....	104
7.1. Types of cement.....	104
7.2. Other electrification technologies.....	104
7.3. Decentralised renewable energy sizing: Green hydrogen (HOMER Pro).....	106



List of Tables

Table 1: Steel-consuming sectors	16
Table 2: Reaction scheme in a blast furnace.....	22
Table 3: Decarbonisation measures in steel.....	25
Table 4: Reaction scheme in a blast furnace	30
Table 5: Typical constituents in Indian iron ore	32
Table 6: Iron-bearing material proportion.....	33
Table 7: Iron-bearing material composition.....	33
Table 8: Compositions of fluxing agents	34
Table 9: Hot metal composition.....	35
Table 10: Typical slag composition.....	35
Table 11: Iron reduction mechanism using hydrogen	38
Table 12: Direct, indirect, and hydrogen reduction of wustite	38
Table 13: General operating parameters for RAFT and TGT	44
Table 14: Operating expenses.....	50
Table 15: Various reactions occurring within the pyroprocessing system.....	58
Table 16: Types of cement and their properties	59
Table 17: Calorific values of different AFRs.....	62
Table 18: Emission reduction potential of different decarbonisation measures	65
Table 19: Bogue formula	70
Table 20: Cement quality control formula.....	70
Table 21: Particle input and output sizes for various attrition equipment.....	73
Table 22: Pyroprocessing system assumptions.....	74
Table 23: Scaled-up plant assumptions	75
Table 24: Pre-heater configuration and plant CUF	75
Table 25: Materials for producing 1 kg of clinker	76
Table 26: Comparison of theoretical and practical drive requirement	79
Table 27: Calciner assumptions	83
Table 28: Current policies in steel, cement, and hydrogen	88
Table A 1: Electrification technologies in cement manufacturing.....	104
Table A 2: Case set-up.....	106
Table A 3: Assumptions.....	106
Table A 4: Energy balance - base case.....	108
Table A 5: Energy balance - 100% renewable energy case.....	110



List of Figures

Figure 1: Share in total final energy requirements (authors' analysis).....	18
Figure 2: Steelmaking pathways	20
Figure 3: The BF–BOF process	21
Figure 4: The DRI process	23
Figure 5: Aspen flowsheet.....	31
Figure 6: Composition of coke and coal	34
Figure 7: RIST diagram	37
Figure 8: Bauer–Glaessner diagram (adopted from de Castro et al., 2023)	38
Figure 9: Extent of reduction of ferrous material.....	39
Figure 10: Methodology	41
Figure 11: Mass balance (base case)	42
Figure 12: Material balance (industry standards)	42
Figure 13: Energy balance with ARA.....	43
Figure 14: Base case (slag properties)	43
Figure 15: Industry standards (slag properties)	44
Figure 16: Top gas composition	44
Figure 17: Effect of hydrogen injection on RAFT and TGT	45
Figure 18: Hydrogen as ARA (mass balance).....	46
Figure 19: Hydrogen as ARA (energy balance).....	46
Figure 20: Hydrogen as ARA (slag properties).....	47
Figure 21: Hydrogen as ARA (top gas composition in kg/tHM)	47
Figure 22: Percentage of hydrogen reacted versus injected	48
Figure 23: Levelised cost of steel (various sources)	51
Figure 24: Cost of steel (hydrogen injection)	52
Figure 25: Steel price variation with green hydrogen electricity cost	53
Figure 26: Cement plant layout.....	60
Figure 27: Electrical SEC breakup	61
Figure 28: CaL in the cement industry	63
Figure 29: Decarbonisation measures in the cement industry	65
Figure 30: Baseline value chain	68
Figure 31: System boundary of the pyroprocessing unit.....	68
Figure 32: Ore composition.....	69
Figure 33: Raw meal composition	69
Figure 34: Coal composition.....	69
Figure 35: Pre-heater configurations	71
Figure 36: Plant capacity vs thermal SEC	72
Figure 37: Work indices of different materials (kWh/t)	73
Figure 38: Degree of calcination vs fuel injection rate	74
Figure 39: Mass balance for 1 kg of clinker	77
Figure 40: Clinker composition	77
Figure 41: Clinker composition in terms of C ₂ S, C ₃ S, C ₃ A, and C ₄ AF	78



Figure 42: Pre-heater exhaust composition.....	78
Figure 43: Energy balance	79
Figure 44: 5-Stage pre-heater electrical SEC	80
Figure 45: 6-Stage pre-heater electrical SEC.....	81
Figure 46: Theoretical fuel requirement for different fuel	82
Figure 47: Impact of hydrogen injection	84
Figure 48: Scaled-up cement plant.....	85
Figure A 1: Base case (Grid + PV)	107
Figure A 2: 100% Renewable energy case.....	107
Figure A 3: Time series plot - base case (screenshot).....	109
Figure A 4: Time series plot - 100% renewable energy (screens)	111



Abbreviations

AFR	Alternative Fuel Resource
AMC	Advanced Market Commitment
ARA	Auxiliary Reducing Agent
BAT	Best Available Technology
BF-BOF	Blast Furnace-Basic Oxygen Furnace
BIS	Bureau of Indian Standards
C ₂ S	Dicalcium Silicate (Belite)
C ₃ A	Tricalcium Aluminate
C ₃ S	Tricalcium Silicate (Alite)
C ₄ AF	Tetracalcium Aluminoferrite
CaL	Calcium Looping
CC	Composite Cement
CCS	Carbon Capture and Sequestration
CCUS	Carbon Capture, Utilisation, and Storage
CF	Clinker Factor
CII	Confederation of India Industry
CPCB	Central Pollution Control Board
CPP	Captive Power Plant
CUF	Capacity Utilisation Factor
DRI	Direct Reduced Iron
EAF	Electric Arc Furnace
ELV	End-of-Life Vehicle
Gcal	Gigacalorie
GCV	Gross Calorific Value
GHG	Greenhouse Gas
GJ	Gigajoule
Gt	Gigatonne
IF	Induction Furnace
ILC	In-Line Calciner
IPPU	Industrial Process and Product Use
ISTS	Inter-State Transmission Charges
Kcal	Kilo Calorie
kWh	Kilo Watt Hour
LC ³	Limestone Calcined Clay Cement



LCOE	Levelised Cost of Energy
LCOH	Levelised Cost of Hydrogen
LSF	Lime Saturation Factor
MBM	Meat and Bone Meal
MCFC	Molten Carbonate Fuel Cell
MJ	Megajoule
MNRE	Ministry of New and Renewable Energy
MSW	Municipal Solid Waste
Mt	Million Tonne
MTPA	Million Tonne Per Annum
NGHM	National Green Hydrogen Mission
OPC	Ordinary Portland Cement
PCI	Pulverised Coal Injection
PLI	Production Linked Incentive
PPC	Portland Pozzolana Cement
PSC	Portland Slag Cement
RAFT	Raceway Adiabatic Flame Temperature
RDH	RotoDynamic Heater
RPO	Renewable Power Obligation
SCM	Supplementary Cementitious Material
SEC	Specific Energy Consumption
SIGHT	Strategic Interventions for Green Hydrogen Transition
SLC	Separate-Line Calciner
tCS	Tonne of Crude Steel
TGT	Top Gas Temperature
tHM	Tonne of Hot Metal
TPD	Tonnes Per Day
TSR	Thermal Substitution Rate
VRM	Vertical Roller Mill
WHR	Waste Heat Recovery



1. Introduction

Globally, the decarbonisation of hard-to-abate sectors is one of the biggest current challenges because of two reasons. First is process emissions, which is often referred to as industrial process and product use (IPPU) in various classification frameworks. Second is the dependency on fossil fuels to meet thermal (heat) energy requirements. Hard-to-abate sectors include the industry (that are energy intensive because of the use of pyroprocessing technology) and transport (freight, shipping, and aviation) sectors, where emission reduction measures are limited because of fossil fuel dependency. Both steel and cement manufacturing are considered hard-to-abate industries, owing to their IPPU emissions and fossil fuel dependency.

Typically, industries find it difficult to reduce process emissions because of their reliance on heat energy and thermodynamic limitations. These industries include cement, steel, aluminium, fertilisers, pulp and paper, and other allied industries, which account for more than 30% of India's overall greenhouse gas (GHG) emissions (MoEFCC, 2021).

1.1. Global steel and cement sector outlook

Steel is one of the most essential commodities for construction, industry, and many other sectors of the contemporary economy. The alloy's main component is iron, but it also contains carbon and other elements that improve its strength, durability, and malleability.

As of 2023, global crude steel output stood at 1,892 million tonne (Mt) (Ministry of Steel, 2024b). With 1,019.1 Mt of crude steel produced in 2023, China leads the world in steel production. India comes in second with 144.2 Mt, followed by Japan with 87.0 Mt, and the United States with 80.7 Mt (World Steel Association, n.d.). However, there are notable differences in the worldwide per capita consumption of finished steel: For the fiscal year 2022–23, India consumed 86.7 kg, China 649 kg, and the rest of the world 224 kg (Ministry of Steel, n.d.-a). This gap underscores India's immense potential for growth in steel consumption.

However, there are serious environmental problems associated with the production of steel, especially when it comes to GHG emissions. Because of the energy-intensive nature of the steelmaking process, which entails reducing iron ore to iron and turning that iron into steel, the sector is one of the biggest producers of industrial emissions. Therefore, the mitigation of environmental problems is contingent upon the adoption of cleaner technology and innovations in manufacturing processes.

Further, a significant portion (11%) of the world's carbon dioxide (CO₂) emissions comes from the steel industry, with the conventional blast furnace–basic oxygen furnace (BF–BOF) route being carbon intensive (Hasanbeigi, 2022). Reducing the industry's carbon footprint on a worldwide scale requires investment in an array of decarbonisation measures such as energy efficiency; fuel substitution; and carbon capture, utilisation, and storage (CCUS) technology, in addition to switching to less carbon-intensive processes such as the electric arc furnace (EAF).

The cement industry stands as the second-largest contributor to industrial GHG emissions globally. According to McKinsey & Company, the cement sector was responsible for approximately 7% of CO₂ emissions in 2023 (Fabian et al., 2023). Driven by increasing demand in emerging and developing countries, global annual cement production is expected to reach 4.8 billion tonnes by 2030 and 6 billion tonnes by 2050.

Emissions from the cement sector is expected to reach as high as 3.8 gigatonne (Gt) in 2050.

Emissions from the cement sector can be classified into process- and energy-based emissions. Energy-based emissions can be further classified as coal-based (pyroprocessing) and electrical energy-based (thermal power plant) emissions. Limestone, the primary raw material in cement manufacturing, contains a significant amount of carbon that is released as CO₂ during the cement manufacturing process. Moreover, the production of cement demands a substantial energy input, often relying on coal and pet coke as fuel sources. This further amplifies the emission intensity of cement production, underscoring the importance of decarbonising the sector to combat climate change.

1.2. Indian steel and cement sector outlook

The steel industry contributes ~2% to India's gross domestic product (GDP) and employs 6 lakh people directly (JSW Steel, n.d.). In 2023–24, India's crude steel capacity was estimated to be 179.5 Mt, with production data indicating a strong upward trend. Moreover, 144.2 Mt of crude steel and 138.83 Mt of finished steel, including stainless, alloy, and non-alloy varieties, were produced in 2023–24 (Ministry of Steel, 2024a). The dominant steel-consuming sectors are construction, infrastructure, capital goods, and automobiles (Table 1), accounting for almost 87% of total demand (Gupta et al., 2023).

Table 1: Steel-consuming sectors

Category	Percentage	Production in Mt (2022–23)
Construction	43	51.5
Infrastructure	25	30
Automobile	10	12
Capital good	9	11
Consumer durable	6	7.2
Intermediate product	7	8.4

India's industrial sector plays an important role in driving up CO₂ emissions, accounting for 24% of the country's total emissions (IEA, 2022). The iron and steel sector is considered a vital pillar of the Indian economy; however, it is a significant contributor to the country's industrial emissions, making up around 34% of the emissions from manufacturing industries and construction categories (MoEFCC, 2021). Moreover, the sector accounts for nearly 12% of the nation's CO₂ emissions (Ministry of Steel, 2022). The emissions from the steel industry depend on the production route. The emission intensity of the BF–BOF route is 2.5 kg CO₂/tonne of crude steel (tCS), while the direct reduced iron–electric arc furnace (DRI–EAF) route has an intensity of 2.2 kg CO₂/tCS for the coal-based process (Bhardwaj et al., 2024). The gas-based DRI process has an emission intensity of 1.3–1.8 kg CO₂/tCS. India's rapid development is expected to drive a significant increase in steel demand. According to the Ministry of Steel, the nation's steel demand is projected to triple by 2030 and increase fivefold by 2050 (Hall et al., 2020; Ministry of Steel, n.d.-b; National Steel Policy, 2017). Therefore, to lessen its impact on the environment and yet fulfil the nation's expanding need for steel, the government and industry stakeholders are

concentrating on using cleaner manufacturing techniques and innovative technology (Ministry of Steel, 2023).

India is the second largest cement manufacturer in the world after China (GCCA, 2022). As of 2022–23, the installed capacity of cement plants in India was about 594.14 Mt, with cement production in 2022 being 298 Mt per annum (GCCA & Global CCS Institute, 2024; Vipin et al., 2023). The major cement consumers in the country are the housing and real estate sectors (67%), the infrastructure sector (13%), the commercial construction sector (11%), and the industrial sector (9%; AEEE, 2021). Today, India has about 333 cement manufacturing units in operation. These units encompass a mix of 150 large integrated cement plants, 116 grinding units, 62 mini cement plants, and 5 clinkerisation units (GCCA & Global CCS Institute, 2024). About 59% of the cement production in the country happens in 134 cement plants, owned by 13 companies (Nitturu et al., 2023).

From 2024 to 2032, the cement sector in India is expected to grow at 4.7% compound annual growth rate (CAGR; IBEF, 2024). The demand for cement is anticipated to rise significantly, with the market expected to reach 599.7 Mt by 2032. This growth is fuelled by government initiatives aimed at enhancing infrastructure, housing, and urban projects, which are critical for India's economic development. However, the cement sector in India is responsible for 5.63% of the country's total GHG emissions, with the third Biennial Update Report (BUR), submitted in 2021, noting that the sector contributed 106.59 Mt under the industrial processes and product-use category and 53.47 Mt under the energy-use category in 2016. Today, the average emission intensity from the Indian cement sector is about 0.617 tCO₂/t of cement (GCCA & Global CCS Institute, 2024). If left unattended, the total emissions from the cement industry could double in the next 8 years.

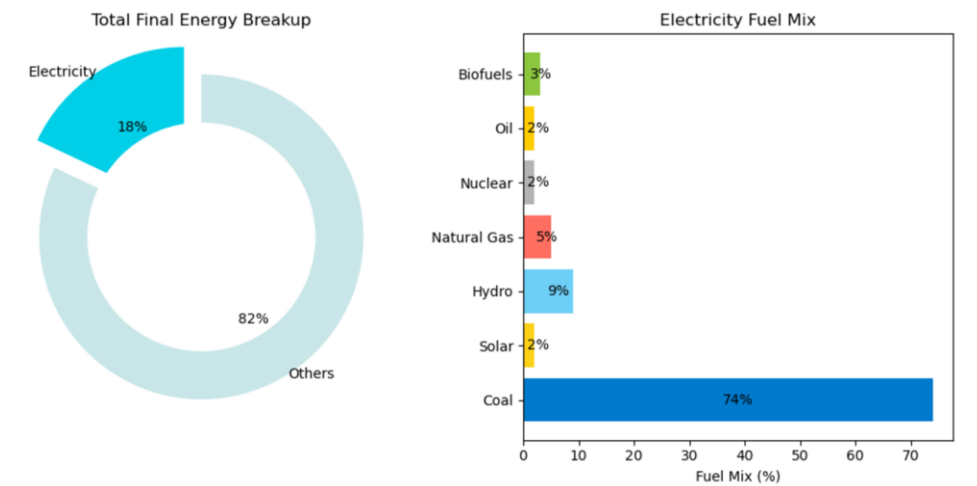
Hence, the cement industry faces a pressing need to decarbonise its operations. As the sector grows, balancing increased production with sustainable practices will be essential for minimising environmental impacts and meeting global climate goals.

1.3. Need for hydrogen as a decarbonisation measure

To achieve our climate goals and reduce emissions beyond the climate pledges, hard-to-abate sectors such as steel and cement need to be decarbonised by adopting clean technologies. Given the complexities and linkages of the Index of Industrial Production with the GDP of the sectors, it is important to assess the strengths and opportunities of hydrogen in these sectors in a systematic manner. Further, the combination of energy-efficiency measures and the shift to a clean fuel has the potential to significantly reduce carbon emissions.

Typically, more than 80% of India's final energy requirements are from non-electricity-based needs (Figure 1). This is often thermal energy derived from fossil fuels such as coal, oil (and derivatives), and natural gas. The types of applications dependent on thermal energy include coal-fired boilers of thermal power plants, petrol or diesel used in internal combustion engines (automobiles), and natural gas vehicles powered by compressed natural gas or liquefied natural gas. Therefore, decarbonising thermal energy applications can unlock opportunities to further reduce emissions.

Figure 1: Share in total final energy requirements (authors' analysis)



The cement and steel industries rely heavily on coal for thermal energy. For every tonne of clinker produced, the Indian cement industry consumes 3.1 gigajoules (GJ) of thermal energy compared with the global norm of 3.5 GJ (AEEE, 2021). This indicates that the overall fleet of cement plants in India is more efficient than global plants. However, this is not the case with iron and steel plants. For instance, integrated steel plants in India typically consumes 6.5 gigacalories (Gcal) to produce one tonne of crude steel in comparison with the 5 Gcal treated as the global average (Ministry of Steel, 2021). In total, the cement and steel sector collectively consume 4,250 petajoules of thermal energy. More than two-third of this energy is supplied through the combustion of fossil fuel, predominantly coal.

To decarbonise these hard-to-abate industries, energy demand from cement, steel, and other sectors should be shifted to a scalable fuel such as hydrogen, owing to its improved gross calorific value (GCV). Hydrogen can also be used as a feedstock and fuel—feedstock for iron ore reduction and fuel to meet thermal energy demand—but the differences in thermal energy norms and feedstock applicability will require a deeper examination (discussed in subsequent chapters). The hard-to-abate industries where hydrogen can be used as a feedstock include fertilisers, iron and steel, glass manufacturing, metals processing, chemicals, and petrochemical industries. Moreover, using hydrogen as a fuel for thermal energy can be realised in industries that use rotary kilns for the pyroprocessing technique.



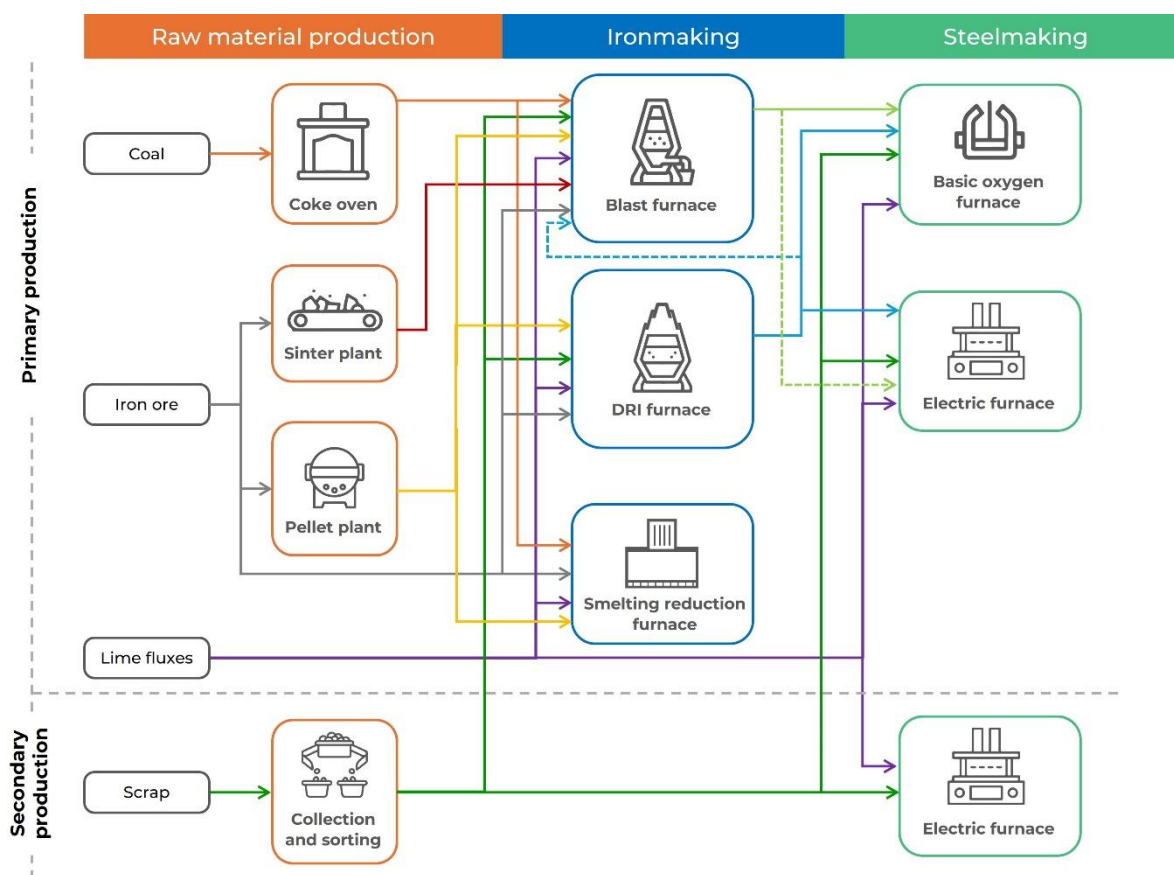
2. Steel

2.1. Technology pathways

In India, the production of iron and steel is carried out through the following pathways (Figure 2):

1. **BF-BOF**
2. **Coal-based and gas-based direct reduction of iron** with **EAFs and induction furnaces (IFs)**, along with secondary steel production

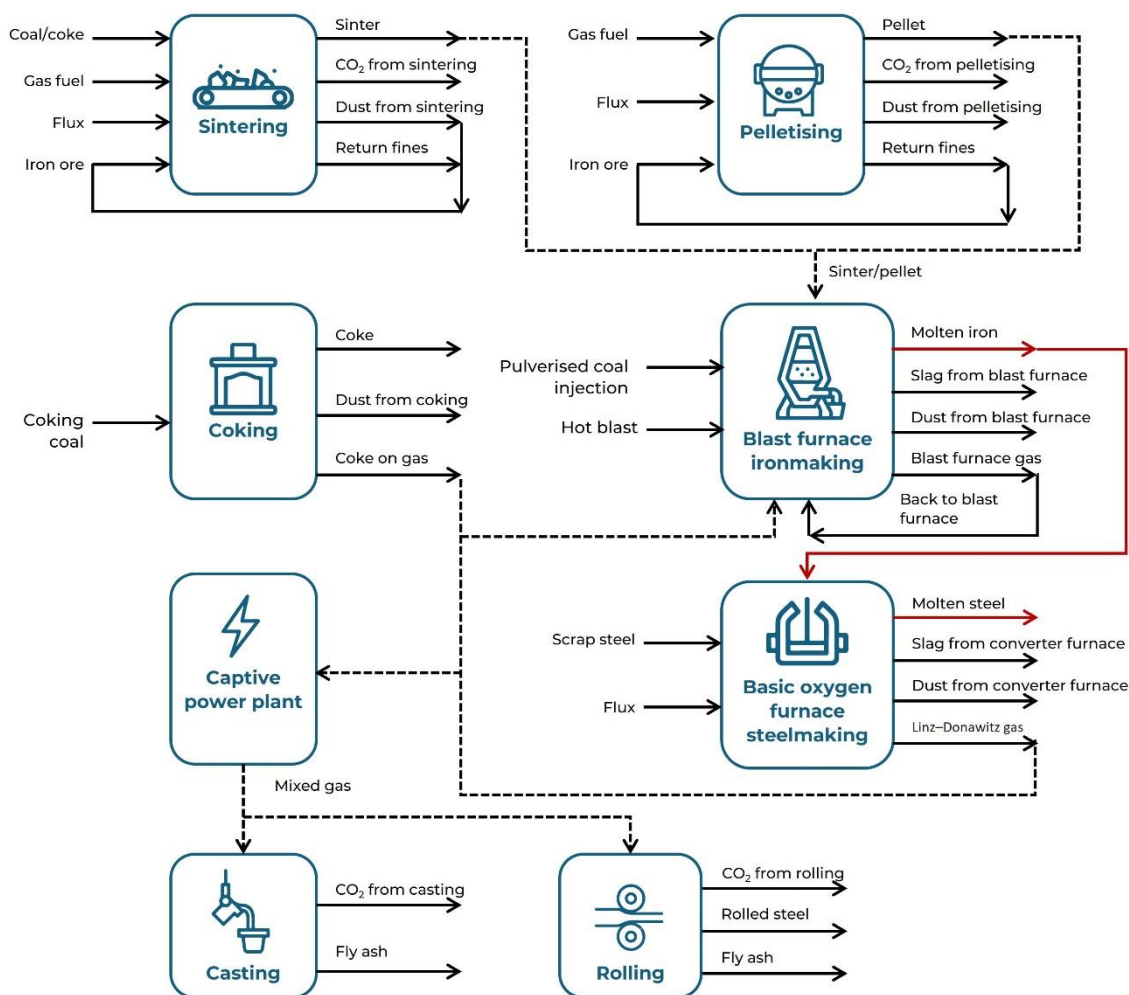
Figure 2: Steelmaking pathways



In 2023–24, 22% of steel production came from EAFs and 35% from IFs. The remaining 43% was produced using BOFs (Ministry of Steel, 2024a). According to the Ministry of Steel, India is the world's largest producer of DRI since 2003, with production close to 51.5 Mt (Ministry of Steel, 2024a). Blast furnace remains the largest pathway to produce iron (hot metal), accounting for more than half of the country's iron production.

Modern blast furnaces (Figure 3) can produce up to 10,000 tonnes of hot metal per day, with furnace dimensions reaching 50 feet in diameter and 120 feet in height (Yang, Y., et al., 2014). Temperature variations within the furnace are significant, with the top at around 200 °C and the bottom exceeding 1,500 °C (Kildahl et al., 2023). The furnace is charged with alternating layers of iron ore and coke while air or oxygen-enriched air (the 'blast') is injected from the bottom after being preheated to 1,100–1,350 °C by hot stoves (Yang, Y., et al., 2014). This preheated blast supplies most of the heat required for furnace operation.

Figure 3: The BF-BOF process



As the hot blast passes through layers of coke, it reacts to form carbon monoxide (CO), which ascends through the furnace. CO reduces iron ore (Table 2) to metallic iron while transferring heat to the material higher in the furnace. Once reduced, liquid iron accumulates at the bottom and is tapped from the furnace. To remove impurities from iron ore, additives such as limestone are introduced. Limestone helps eliminate sulphur by converting iron sulphide (FeS) to metallic iron and calcium sulphide (CaS; Kildahl et al., 2023). Being less dense than iron, CaS rises to form a layer of molten slag, which also contains other impurities such as silicon dioxide (SiO₂), aluminium oxide (Al₂O₃), magnesium oxide (MgO), and calcium oxide (CaO). This slag, tapped at 1,650 °C, allows for heat recovery, with up to 65% being recovered (Barati et al., 2011). Approximately, 0.275 tonnes of slag are generated per tonne of steel produced.

Table 2: Reaction scheme in a blast furnace

Height (feet)	Temperature zone (°C)	Reaction	ΔH (kJ/mol)
70–75	400 °C	$3\text{Fe}_2\text{O}_3 + \text{CO} \rightarrow 2\text{Fe}_3\text{O}_4 + \text{CO}_2$	-27,800
		$2\text{Fe}_2\text{O}_3 + 8\text{CO} \rightarrow \text{CO}_2 + \text{Fe} + \text{C} + \text{CO}$	-67,900
55–70	700 °C	$\text{Fe}_3\text{O}_4 + \text{CO} \rightarrow 3\text{FeO} + \text{CO}_2$	5,900
45–55	850 °C	$\text{FeO} + \text{CO} \rightarrow \text{Fe} + \text{CO}_2$	-3,900
		$\text{CaCO}_3 \rightarrow \text{CaO} + \text{CO}_2$	41,800
35–45	1,000 °C	$\text{C} + \text{CO}_2 \rightarrow 2\text{CO}$	41,500
0–35	1,500 °C	$\text{SiO}_2 + 2\text{C} \rightarrow \text{Si} + 2\text{CO}$	1,45,000
		$\text{FeS} + \text{CaO} + \text{C} \rightarrow \text{CaS} + \text{Fe} + \text{CO}$	34,800
		$\text{P}_2\text{O}_5 + 5\text{C} \rightarrow 2\text{P} + 5\text{CO}$	2,34,000
		$\text{MnO} + \text{C} \rightarrow \text{Mn} + \text{CO}$	64,400
		$\text{H}_2\text{O} + \text{C} \rightarrow \text{H}_2 + \text{CO}$	31,400
		$2\text{C} + \text{O}_2 \rightarrow 2\text{CO}$	-58,230

The furnace off gas, also known as top gas, exits the furnace at 200–300 °C and consists mainly of CO and CO₂. This recovered heat, combined with energy from top gas combustion, is used to reheat the blast to over 1,100 °C.

In terms of material flows, the BF–BOF steelmaking route requires approximately 1,370 kg of iron ore, 780 kg of metallurgical coal, 270 kg of limestone, and 125 kg of recycled steel to produce 1,000 kg of crude steel (World Steel Association, 2011). The blast process involves injecting 1,500 kg of air into the furnace through tuyeres (Kildahl et al., 2023). Metallurgical coal must undergo a pre-treatment process, involving heating to 1,250 °C for 12 hours, using heat from top gas and coke oven gas (COG). COG is generally composed of 60% hydrogen, 24% methane (CH₄), 6% CO, 6% nitrogen (N₂), and 4% CO₂.

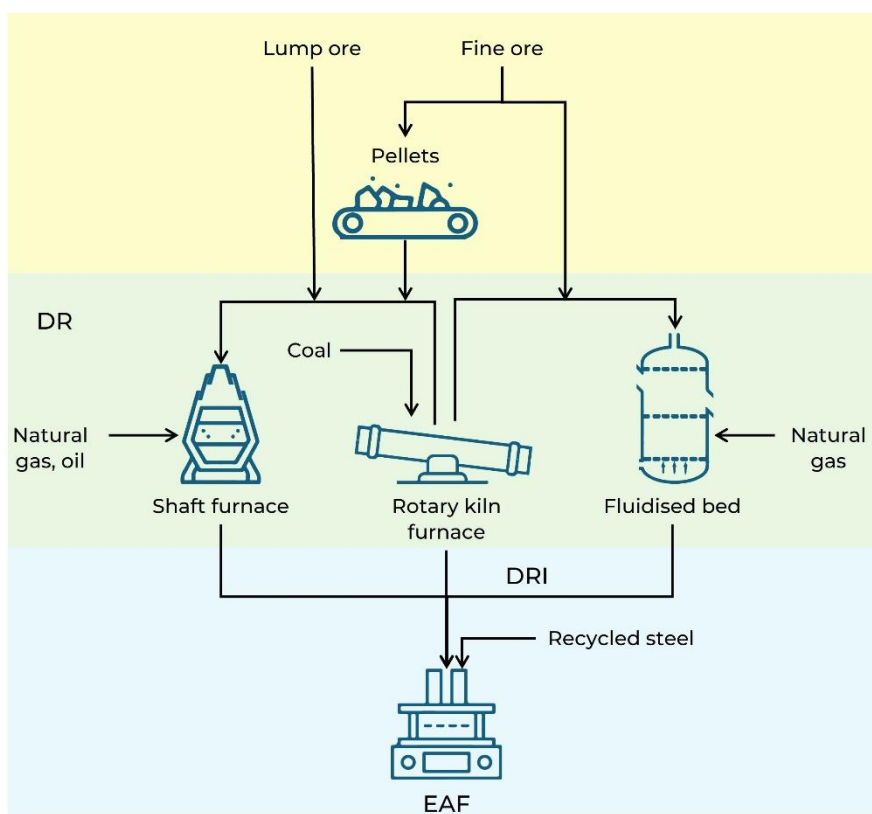
Treated coke plays several critical roles in the blast furnace operation. It serves as a primary energy source, providing 20%–40% of the total energy through combustion. Moreover, coke reacts with oxygen to produce CO, which reduces iron ore. The Boudouard reaction further increases CO levels when CO₂ reacts with coke. Coke also adds carbon to molten iron and provides structural support to iron ore layers, facilitating gas flow through the furnace. To reduce coke consumption, alternative reducing agents such as pulverised coal, hydrocarbons, waste plastics, and biomass can be injected into the furnace.

The DRI process (Figure 4) is an important route for producing iron in the steelmaking industry, especially where traditional blast furnaces are not viable. Using this process, high-grade iron ore pellets are first produced and then reduced using natural gas or coal to create sponge pellets. In terms of material flows, the DRI–EAF steelmaking route

requires approximately 2,024 kg of iron ore, 1,355 kg of non-coking coal, and 127 kg of dolomite to produce 1,000 kg of crude steel (Bhardwaj et al., 2024).

The gas-based DRI process relies on natural gas, which acts as the primary reductant. This creates a mixture of hydrogen and CO (syngas) through reforming of natural gas by using a steam oxygen mixture at around 800 °C in the presence of a nickel catalyst. Iron ore, in the form of pellets or lumps, is reduced to metallic iron without melting by using this reducing gas (syngas). The reduction takes place in a vertical shaft furnace, where reducing gases are maintained at temperatures between 760 °C and 950 °C with iron oxides in a countercurrent flow, resulting in the formation of sponge iron. This process is advantageous in regions with abundant natural gas as it is highly efficient and less emission intensive compared with coal-based methods. However, the gas-based approach requires access to cost-effective natural gas, which may not be available in all regions, and the requirement of a reformer adds to the process complexity. It is particularly suitable for producing high-quality DRI that can be used in EAFs for steelmaking, thus supporting a low-carbon pathway for steel production.

Figure 4: The DRI process



On the other hand, the coal-based DRI process is used primarily in regions where natural gas is not available but non-coking coal is plentiful. This process requires high-grade iron ore. The unit consists of a rotary kiln followed by a rotary cooler. In this method, iron ore and coal are injected into a rotary kiln, where coal serves as both the reductant and the energy source. The process operates on a countercurrent principle where the gases flow opposite to the solid flow. The reduction occurs through reactions between the iron ore and CO and carbon from the coal, leading to the production of sponge iron. This process operates at temperatures between 950 °C and 1,050 °C. A flux is added to remove the impurities (e.g. sulphur separated as its sulphide). The product extracted from the kiln is

cooled to room temperature in an indirectly cooled rotary cooler and separated using magnetic separators. Minor modifications are made to the standard coal DRI process and indigenised as required in an Indian context (Battle et al., 2014).

In India, the DRI pathway primarily relies on coal (almost 82% of DRI) instead of natural gas (Hall et al., 2020; Ministry of Steel, n.d.-c). In general, the energy intensity of both BF–BOF and DRI pathways exceeds global averages. This is primarily attributed to the use of coal with high ash content, which has a lower energy density, and the age of certain plants (IEA, 2020).

Because of only one main conversion step, EAF mills are often referred to as mini mills. Molten steel is treated in a ladle furnace before being cast and rolled to its final form. In the past, mini mills primarily provided lower-quality products, especially when it came to reinforcing bars. Nevertheless, they have managed to secure a greater portion of the steel market in recent times (El Hagggar, 2005).

Prior research has examined the decrease of CO₂ emissions in BF–BOF and EAF configurations in terms of enhanced energy efficiency, both with and without the use of renewable energy sources and with and without the use of carbon capture. To attain the net-zero emissions objective, many decarbonisation strategies are required as we cannot accomplish deep decarbonisation using just one strategy (Zang et al., 2023).

2.2. Decarbonisation pathways

The growth projection of the steel industry necessitates the need for pathways to decarbonise processes (Table 3).

2.2.1. Energy efficiency measures

Improving energy efficiency is one of the most immediate and cost-effective ways to reduce emissions in steel production. This involves optimising existing processes, modernising equipment, and adopting best practices such as heat recovery systems, waste heat utilisation, and advanced control systems. The energy efficiency measures implemented across different sub-processes of steelmaking encompass various improvements (Krishnan et al., 2013). In the sintering process, heat recovery from the sinter cooler, reduction of air leakage, utilisation of waste fuel in the sinter plant, and improvements in charging methods are employed to enhance efficiency.

For coke making, measures such as programmed heating in coke ovens, the use of variable speed drives on coke oven gas compressors, and coke dry quenching are undertaken to optimise energy usage. Within the blast furnace ironmaking process, several energy-saving strategies are applied, including the injection of pulverised coal, natural gas, oil, and coke oven gas. Additional measures involve top-pressure recovery turbines, blast furnace gas recovery, improved furnace control, and better management of hot blast stove systems. In steelmaking using BOFs, heat recovery from BOF gas, variable speed drives on ventilation fans, and efficient ladle preheating are utilised for energy efficiency. In EAF steelmaking, enhancements include converting furnace operations to ultra-high power, employing adjustable speed drives on flue gas fans, using oxy fuel burners, and improving process control.

Furthermore, measures such as using a direct current (DC) arc furnace, scrap preheating, and bottom stirring or gas injection contribute to the overall energy efficiency of the EAF process. Moreover, the iron and steel sector has seen the implementation of extra energy

efficiency measures, owing to the Bureau of Energy Efficiency's Perform, Achieve and Trade (PAT) scheme. Various methods, including coke dry quenching, waste heat recovery (WHR), and insulation, have resulted in substantial energy savings (Johnson et al., 2023). Continuing efficiency improvements will be increasingly challenging in the future. According to the International Energy Agency (IEA), ~20% emission reductions from 2020 to 2050 are expected to come from efficiency and technological improvements (IEA, 2020).

2.2.2. Fuel substitution and renewable energy

Transitioning from carbon-intensive fossil fuels to cleaner alternatives is another critical decarbonisation pathway. Replacing traditional coal and coke used in blast furnaces with lower-emission fuels such as natural gas or shifting to hydrogen and/or biochar can significantly reduce CO₂ emissions. Moreover, integrating renewable energy sources such as wind, solar, or biomass into steel production, particularly for powering EAFs, helps further reduce reliance on fossil fuels, promoting cleaner production. IEA projects the proportion of emission reduction attributable to this intervention to be around 23% between 2020 and 2050 (IEA, 2020).

Newer technologies such as HIsarna (a low-CO₂ steelmaking initiative by TATA Steel in Europe) release capturable amounts of CO₂ in high concentrations (TATA Steel, 2020). ULCORED (ultra-low CO₂ reduction) uses syngas (a mixture of CO and H₂) as a reductant in DRI to increase CO₂ concentration for ease of capture. Both these technologies can be coupled with carbon capture and sequestration (CCS) to offer up to 50% emission reduction (Abdul Quader et al., 2016). Extensive research is also underway on electrification of steelmaking using the electrochemical reduction of iron ore through processes such as ultra-low CO₂ electrolysis (ULCOLYSIS), and ultra-low CO₂ winning (ULCOWIN), with almost negligible emissions (depending on the grid emission factor).

2.2.3. Carbon management

CCUS technologies are key to managing the remaining emissions in the steel industry. CCUS involves capturing CO₂ emissions from steel production processes before they are released into the atmosphere and storing them underground or utilising them in other industrial applications. This approach can mitigate emissions from hard-to-abate processes, such as blast furnace operations, and is essential for achieving deeper decarbonisation in combination with energy efficiency and renewable energy use. Close to 20% of emission reduction is projected to be achieved through carbon management interventions.

Table 3: Decarbonisation measures in steel

Technology	Emission reduction with respect to BF-BOF	Remark/concern
BF-BOF + Top gas recovery	52%	Mature
HIsarna + CCS	20%	Major constituent of top gas is CO ₂ making CCS easier (pilot)
ULCORED + CCS	54%	-
ULCOWIN and ULCOLYSIS + CCS	~90%	Early stages

Biomass-based (Fan & Friedmann, 2021)	19%-38% (Fan & Friedmann, 2021)	Availability of biomass
CCS coupled with BF-BOF/other processes	-	-
Coal bed methane injection (TATA Steel, 2022)	-	Early stage

2.3. Data analysis and scope of analysis

As explained earlier, fuel substitution is one of the important levers for decarbonisation. Considering emissions from ironmaking and steelmaking are hard to abate, hydrogen, especially green hydrogen, is a crucial component of fuel substitution efforts. In the DRI process, there are pilots that show the feasibility of hydrogen and hydrogen-rich gases in vertical shaft furnaces to produce low-carbon steel (HYBRIT, n.d.; Leadership Group for Industry Transition, n.d.).

Considering the reliance on blast furnace in ironmaking, the use of green hydrogen in blast furnace is the primary focus of this work.

Data analysis and dataset preparation are crucial in creating the complete model in the BF–BOF method of steel production. To initiate the dataset preparation, a complete understanding of the material flow of the BF–BOF route is required. Hydrogen is modelled to be injected to the blast furnace.

2.4. Blast furnace modelling

Many complexities regarding modelling a blast furnace stem from the multitude of physical and chemical processes occurring simultaneously inside it (Abhale et al., 2020; K. Yang et al., 2010). Several multiphase (solid, liquid, and gas), multi-component reactions that occur inside the furnace make it challenging and hard to understand and predict the furnace behaviour.

2.4.1. Why analytical modelling

- **Complexity of the process involved:** Analytical models have evolved over the years to various complexities driven by advancements in computational power and a deeper understanding of the underlying physical and chemical phenomena. These modelling techniques help breakdown the furnace mechanism into various levels of complexities, depending on the end-use/purpose that they are developed for. They also allow us to mathematically represent complex flows (heat and mass) within the furnace.
- **Process optimisation:** These models help operators and engineers identify bottlenecks in furnace operations by analysing the internal structure of the furnace and evaluate the impact of change in operating parameters such as temperature, pressure, and composition.
- **Control strategies:** Models allow operators to deploy advanced control strategies in the furnace to extract the desired quality of output.
- **New experimentation:** The addition of alternative feedstock and fuel, such as hydrogen, can change the entire internal operation within the furnace. These models help in studying such impacts, as done in this study.

- **Limitations of physical experimentation:** Finally, the biggest advantage of these mathematical models is that they can help save time by providing near-accurate results when experimenting with relatively new feedstock/fuel such as hydrogen. The present study uses a similar analytical model to identify the feasibility of hydrogen injection into the blast furnace. While accurate results can be obtained using pilot studies, an analytical model can provide a preliminary feasibility check and first-order results, upon which decisions can be taken. Often, actual pilot studies require additional infrastructure, cost, and time that need to be borne. This is true especially in the case of hydrogen, which costs between 1.9 and 4 USD/kg depending on the source of production. This leads to the requirement of additional retrofitting and other infrastructural modifications to realise hydrogen injection into a blast furnace.

2.4.2. Different types of analytical models

Over the years, because of the advancement in the computational power of systems and a relatively better understanding of the underlying furnace mechanisms, blast furnace models and their functionalities have evolved considerably.

Today, we have comprehensive models that look at the overall behaviour of the furnace, zone-specific models that focus on specific regions within the furnace, and data-driven models that rely on operational data (Abhale et al., 2020).

2.4.2.1. Comprehensive models

These models aim to describe the overall behaviour of the blast furnace, considering the spatial distribution of variables. They are further classified on the basis of their dimensions.

- **0D (lumped) models (e.g. Rist diagram):** These simplified models use overall mass and heat balances to analyse furnace performance without considering spatial variations.
- **1D models:** These models consider the vertical distribution of variables (along the height of the furnace), offering a more detailed representation of the furnace.
- **2D models:** These models capture both vertical and radial variations in the furnace, providing insights into phenomena such as burden distribution, gas flow patterns, and cohesive zone shape.
- **3D models:** By incorporating all three spatial dimensions, these models offer the most comprehensive representation of the blast furnace, enabling the study of asymmetric phenomena such as tuyere blanking and scaffolding.
- **CFD-DEM models:** Combining computational fluid dynamics (CFD) with the discrete element method, these models offer a highly detailed representation of the granular flow and fluid dynamics within the blast furnace. However, their high computational cost currently limits their practical application for full-scale simulations.

2.4.2.2. Zone-specific models

These models focus on specific regions of the blast furnace. For example, burden distribution models analyse the charging process, cohesive zone models study the softening and melting of iron ore, and raceway models investigate combustion phenomena.

2.4.2.3. *Data-driven models*

These models leverage statistical techniques and machine-learning algorithms to analyse operational data, identify patterns, and make predictions about furnace performance. These models are particularly useful for tasks such as hot metal quality prediction, anomaly detection, and control optimisation.

Blast furnace ironmaking is often considered to be a comprehensive, steady-state process (Emre Ertem & Gürgen, 2006). This is because the loading of ores and other materials into the furnace happens continuously, and products are tapped out at regular intervals. Hence, to effectively model blast furnaces at steady state, mass and energy balance-based studies are often highly relied upon. These models provide a fundamental framework for understanding inputs, outputs, and transformations within the system. They consider every flow in and out of the furnace, varying temperature and pressure conditions within the furnace, and reactions that occur within the furnace. However, because of the increase in computational power over the years and better understanding of furnace mechanisms, several thermodynamic simulation-based models have also been developed (Schultmann et al., 2004; Yilmaz et al., 2017; Zhang et al., 2010).

Thermodynamic process simulation software, such as DWSIM and Aspen Plus, provides prebuilt modules for common process units, such as reactors and columns, along with databases of chemical properties and algorithms to handle recycling loops (DWSIM, n.d.; Aspen Plus, n.d.). This significantly speeds up the creation of process models. Moreover, flow sheeting tools—case studies, sensitivity testing, and process optimisation—enable in-depth analysis.

2.4.3. *DWSIM*

To develop a process simulation-based mass and energy balance model, CSTEP's initial application of choice was DWSIM. DWSIM is a free and open-source chemical process simulator developed by Daniel Medeiros. It provides a user-friendly interface for modelling and simulating a wide range of chemical processes. DWSIM also offers a comprehensive library of unit operations, advanced thermodynamic models, support for reacting systems, and petroleum characterisation tools. DWSIM is widely used by students, researchers, and engineers for tasks such as process design, process modelling and optimisation, and analysis.

2.4.3.1. *Limitations*

One of the biggest limitations of DWSIM arises from the fact that most of the compounds that are part of the ironmaking process, such as Fe_2O_3 , Fe_3O_4 , FeO , SiO_2 , and Al_2O_3 , are not available by default in the in-house database. These compounds have to be manually created with the help of the compound creation wizard offered by DWSIM. Several thermo-physical property data such as the UNIFAC structure of the compound, critical properties, molecular weight, enthalpy of formation, and Gibbs energy of formation of individual compounds have to be hard-coded into the compound creation wizard. Even though DWSIM allows users to import data from external databases such as KDB, DDB, and Chemeo, these databases often do not have all the properties essential for DWSIM to use its algorithms to create the required compounds.

In addition to this, DWSIM does not offer the necessary thermodynamic package that can handle metallurgical compounds.

2.4.4. Aspen Plus

Aspen Plus is a powerful and comprehensive commercial chemical process simulation software widely used and preferred in the industry. It offers a vast array of features that make it an indispensable tool for process engineers and researchers. Some of its key features that make it preferable over DWSIM include the following:

- **Extensive unit operations library:** Aspen Plus consists of a comprehensive library of unit operations, covering a wide range of processes from distillation and absorption to reactors and heat exchangers. This enables users to accurately model complex chemical plants.
- **Extremely powerful solver:** It can perform, multicomponent, multiphase reactions easily.
- **Large database of compounds:** Unlike DWSIM, Aspen Plus hosts a larger library of compounds, which also include several metallurgical compounds.
- **Thermodynamic property models:** The software incorporates a wide range of thermodynamic property models for electrolytes, hydrocarbon, and inorganic minerals, allowing for precise calculations of phase equilibria, enthalpies, interaction parameters, and other properties (Aspen Technology, Inc., 2001; Nishioka et al., 2018)

2.4.4.1. CSTEP's Aspen Plus model

To develop a steady state mass and energy balance model using Aspen Plus, CSTEP used Aspen Plus Version 12.1.

The blast furnace is often divided into zones of varying activity to better understand the physiochemical phenomenon that occurs within the furnace. This division is usually based on the following:

- **Physical state of the materials:** Lumpy zone, cohesive zone, dripping zone, and combustion zone (Nishioka et al., 2018).
- **Temperature and the activity:** Preheating zone, chemical reserve zone, inactive zone, thermal reserve zone, indirect reduction zone, direct reduction zone, and melting zone (Biswas, 1981).

To simplify the modelling attempts, the entire blast furnace was divided into zones (see Table 4).

Table 4: Reaction scheme in a blast furnace

Zone	Lower zone (above 1,000 °C)	Middle zone (800–1,000 °C)	Upper zone (up to 800 °C)
Temperature	Above 1,000 °C	800–1,000 °C	Up to 800 °C
State of substances	Most of the substances are in a molten state, and temperature can reach above 1,400 °C.	This is an isothermal zone where the temperature of the substances is identical.	The top gas enters this zone from the middle zone where its temperature drops rapidly because of the preheating of raw materials.
Processes	The slag and molten metal get separated because of the high temperature and additives added.	Most of the indirect reduction occurs at this zone, with very little transfer of oxygen from the iron ore to gas.	The top gas is removed from the furnace in this zone and utilised for the heating of the hot air blast.
Major reactions	$\text{CaCO}_3 \rightarrow \text{CaO} + \text{CO}_2$ $\text{FeO} + \text{C} \rightarrow \text{Fe} + \text{CO}$ $\text{MnO} + \text{C} \rightarrow \text{Mn} + \text{CO}$ $\text{FeS} + \text{CaO} + \text{C} \rightarrow \text{CaS} + \text{Fe} + \text{CO}$ <p>All the reactions presented above are endothermic in nature.</p> <p>Apart from this, CO₂ generation because of the reaction of coal with air, which is exothermic, and Boudouard reaction also occurs in this zone.</p>	$\text{FeO} + \text{CO} \rightarrow \text{Fe} + \text{CO}_2$ <p>Water–gas shift reaction:</p> $\text{CO} + \text{H}_2\text{O} \rightarrow \text{CO}_2 + \text{H}_2$	<p>Decomposition of carbonates</p> <p>Partial reduction of ore</p> $2\text{CO} \rightarrow \text{CO}_2 + \text{C}$

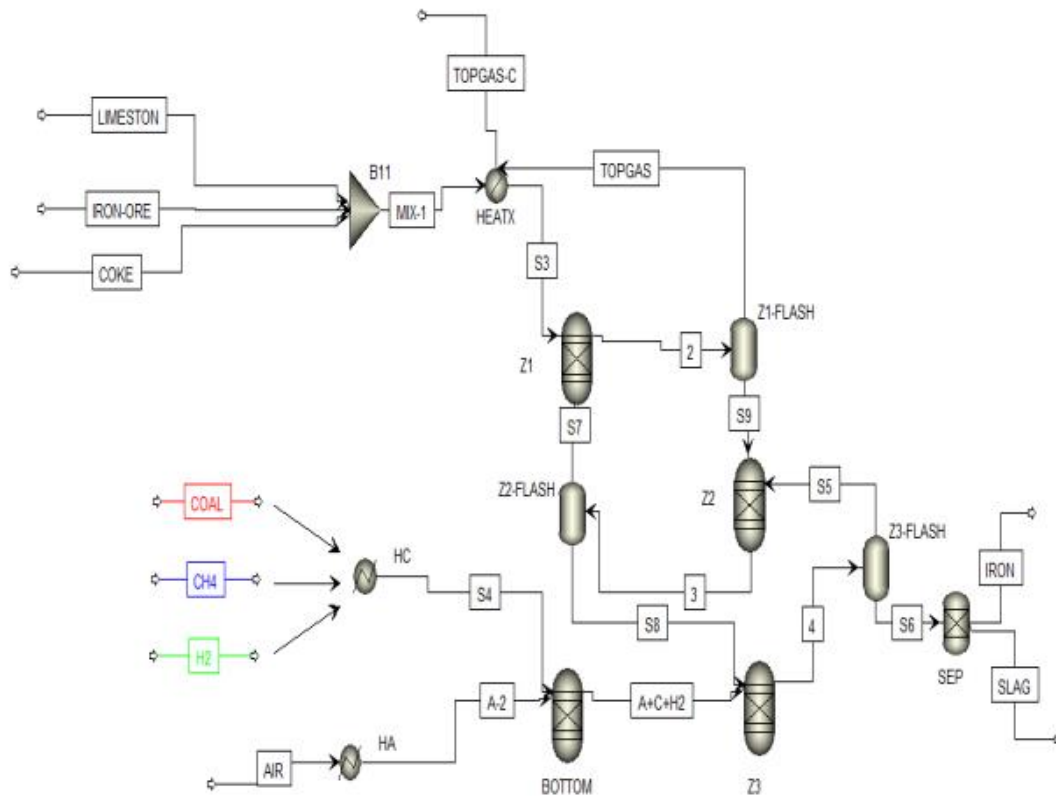
To model the zones described, the SOLIDS thermodynamic model in Aspen Plus that is capable of handling solid compounds and unit operations related to them was used in the flowsheet (Figure 5). The RGIBBS unit operation in Aspen Plus was also utilised. The RGIBBS reactor uses the multiphase Gibbs minimisation method to calculate different reaction equilibriums and phases of substances. By using three different RGIBBS reactors for three different zones (upper, lower, and middle), reaction equilibriums are established in each zone. If a single reactor was to be used for the entire furnace, the reaction equilibrium might have been established between carbon and metal oxides and not the reactions in each zone. To maintain reactor temperature according to zones, heaters and coolers were connected to inlet and outlet streams wherever necessary. An additional fourth RGIBBS reactor was used to replicate hot air blast mixing with auxiliary reducing agents (ARAs).

- RGIBBS reactors Z1, Z2, and Z3 (Figure 5) were followed by their respective flash operations to separate the solid/liquid stream from gases. This was done to create

the countercurrent action seen in the actual BF where hot air blast from the bottom rises to heat materials that are sinking to the bottom to create the zones of the BF.

- Top gas is removed from the top zone (Z1 reactor) and is used to preheat raw materials with the help of a heat exchanger operation.
- The iron and slag are removed from the bottom region (Z3) just like the actual BF.
- A separator operation was used to separate the iron and the slag mixture.

Figure 5: Aspen flowsheet



After the development, testing, and validation of the BF model, it was tested with three different types of ARAs to record the performance, difference in emission levels, and energy requirements. The ARAs were as follows:

- Pulverised coal Injection (PCI)
- H₂
- A mixture of H₂ and CH₄ in the 30:70 ratio

However, Aspen Plus was not used for subsequent analysis owing to unavailability of the licence and the high cost of acquiring a licence, which was not covered in the scope of this work.

2.4.5. Zero-dimensional perturbation-fluctuation model – blast furnace

The zero-dimensional perturbation-fluctuation model developed by CSTEP is a steady-state mass and energy balance model designed to identify the threshold for hydrogen injection into a blast furnace. This model analyses the blast furnace’s top segment, bottom segment, and the entire furnace as a unified steady-state control volume. The entire furnace was assessed to determine the mass and energy flows of various input and output streams, while the top and bottom segments were evaluated specifically to calculate the top gas temperature (TGT) and the raceway adiabatic flame temperature (RAFT), respectively.

2.4.5.1. Methodology and assumptions

To identify the threshold of hydrogen injection into the blast furnace, a baseline model had to be developed that best represents blast furnace operations in India.

2.4.5.1.1. Composition of input streams

Indian iron ore mainly occurs in the form of lumps, fines, and concentrate, which predominantly consists of hematite (Fe_2O_3) and magnetite (Fe_3O_4). The typical constituents are listed in Table 5.

Table 5: Typical constituents in Indian iron ore

Component	Composition	Range (%)
Iron oxides (Indian Bureau of Mines, n.d.-b)	Fe_2O_3 Fe_3O_4	Iron content: 60% to 72%
Silica (SiO_2) (Indian Bureau of Mines, n.d.-b)	Present in iron ores	2% to 4.5%
Alumina (Al_2O_3) (Indian Bureau of Mines, n.d.-b)	Present in iron ores	0% to 4%

Apart from phosphorus (P) in the form of P_2O_5 and oxides of magnesium, manganese and sulphur can be found in Indian iron ore.

In India, where iron ore fines make up a significant portion of the available resources, sintering and pelletisation of the ore fines are often done to effectively utilise them in the blast furnace. This is because iron ore fines cannot be directly used in blast furnaces.

Sintering involves the agglomeration of iron ore fines into larger porous clumps (sinter), improving their permeability in the blast furnace. This enhances overall productivity and reduces coke consumption.

Pelletisation, on the other hand, transforms iron ore fines into uniformly sized, high-quality pellets. These pellets have better physical and metallurgical properties than both sinter and lump ore, resulting in improved furnace efficiency and more consistent smelting. Pellets' uniform composition also allows for better control over the blast furnace operation.

Additionally, these processes have environmental benefits such as lower coke rate, lower slag rate, lower CO₂ emissions in the blast furnace, lower emissions in the agglomeration process, and an overall lower fuel requirement to produce hot metal.

Based on literature survey and discussions with industry experts, the ratio of sinter, pellets, and ore lumps in the burden mix were assumed as per Table 6 (Indian Bureau of Mines, n.d.-b).

Table 6: Iron-bearing material proportion

Sinter	50%
Pellet	10%
Ore lump	40%

The proportion of sinter, pellet, and iron ore in the burden mix was found to be varying in literature (Agrawal et al., 2020). We assumed the representative numbers provided in the document by the Indian Bureau of Mines (Indian Bureau of Mines, n.d.-b). Compositions of different input streams in the blast furnace were assumed after discussions with industry experts. The composition of iron-bearing materials, which is a mixture of ore, sinter, and pellets, is presented in Table 7.

Table 7: Iron-bearing material composition

	Compound (%)	Fe₂O₃	FeO	CaO	SiO₂	Al₂O₃	MgO	MnO	P₂O₅	H₂O	S	Total Fe
Iron-bearing material	Ore	94.65	0.00	0.00	2.50	2.50	0.00	0.15	0.15	0.00	0.05	66.26
	Sinter	67.85	11.03	6.88	9.10	2.75	2.29	0.10	0.00	0.00	0.00	56.07
	Pellet	93.51	0.00	2.40	3.30	0.10	0.17	0.00	0.50	0.00	0.02	65.46

Fluxing agent

Limestone and dolomite play essential roles as fluxing agents (Table 8) in the steelmaking process. They react with impurities such as SiO₂ and Al₂O₃ in iron ore to form slag, aiding in the removal of unwanted materials. Dolomite helps in desulphurisation, lowering sulphur levels to improve steel quality (Qiao-kun et al., 2023). These fluxing agents also reduce the melting point of the mixture, decreasing energy consumption during smelting (Ghosh & Chatterjee, 2010). For our analysis based on interactions with industry experts, we assumed 50% limestone and 50% dolomite to be utilised as fluxing agents. See Table 8 for detailed composition.

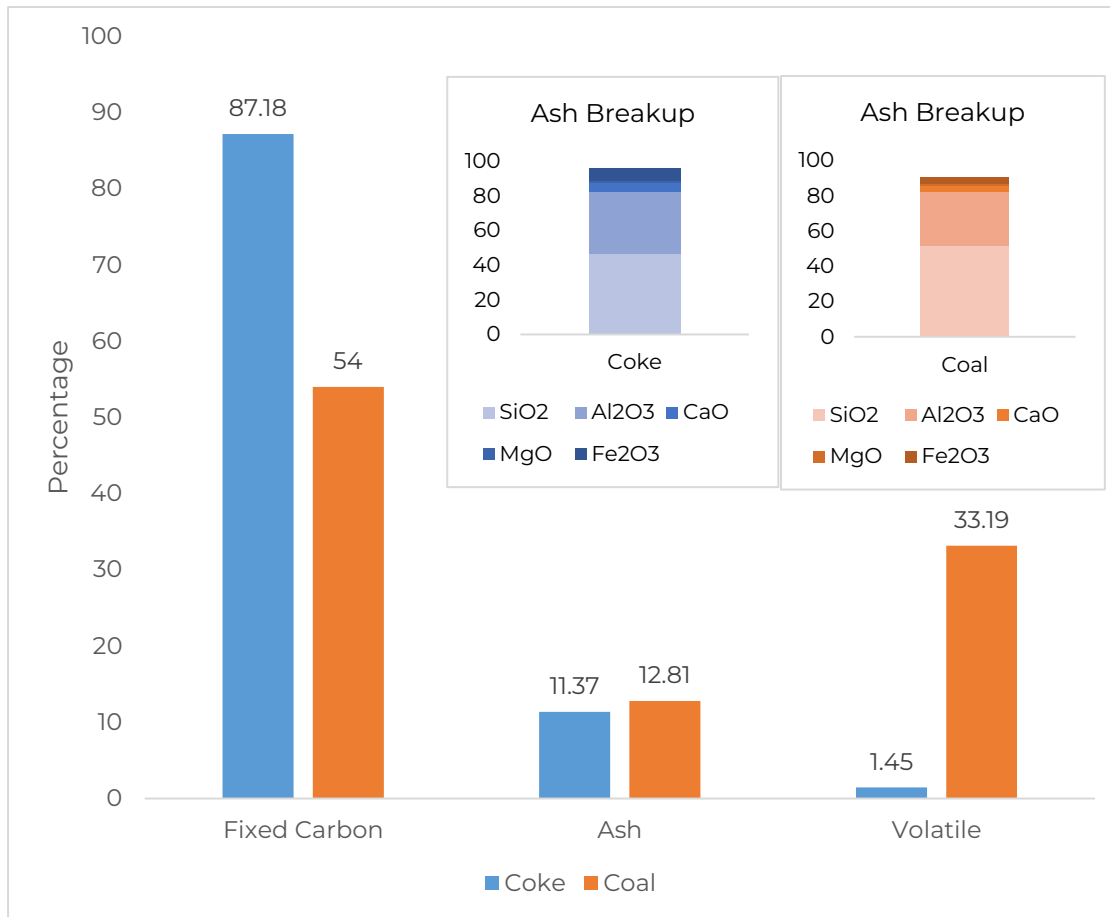
Table 8: Compositions of fluxing agents

Fluxing agent	Compound (%)	Fe ₂ O ₃	FeO	CaO	SiO ₂	Al ₂ O ₃	MgO	MnO	P ₂ O ₅	H ₂ O	S	Total Fe	Loss (CO ₂)
	Limestone	0.00	1.00	53.59	1.82	0.13	0.42	0.00	0.00	0.02	0.00	0.10	42.92
Dolomite	0.00	1.00	29.16	4.79	2.20	18.98	0.00	0.00	0.00	0.00	0.00	0.70	43.17

Coke and coal (ARAs)

For our analysis, we considered the following composition, as illustrated in Figure 6.

Figure 6: Composition of coke and coal



Hot air blast was assumed to enter the furnace at 1,000 °C, with a mass fraction of 77% nitrogen and 23% oxygen.

2.4.5.1.2. Quality control parameters

The iron quality that exits the furnace (typically, cast iron or pig iron) is characterised by specific properties, such as its carbon content, sulphur levels, and temperature. These properties are controlled within well-defined ranges to ensure that iron is suitable for

further steelmaking processes. The hot metal composition was fixed (see Table 9) after interactions with industry stakeholders and literature review (Davenport et al., 2019).

Table 9: Hot metal composition

Compound	Fe	Mn	Si	P	S	C
Hot metal composition (%)	94.2	0.1	0.8	0.2	0.06	4.64

Like hot metal composition, other parameters that are often predetermined and used as quality control measures are slag properties. About 300 to 540 kg of slag is produced for every tonne of hot metal (tHM) produced (Indian Bureau of Mines, n.d.-a). The typical composition of various oxides that are removed as slag is presented in Table 10 (Indian Bureau of Mines, n.d.-b).

Table 10: Typical slag composition

Component	Percentage (%)
SiO ₂	30–35
CaO	35–40
Al ₂ O ₃	18–22
MgO	2–10
Mn	0.1–1.2
Fe	0.2–0.4
S	1.0–2.0

Slag basicity: It is defined as the ratio of weight of CaO to that of SiO₂ in the slag and is often expected to be between 0.95 and 1.

Weight fraction of CaO, SiO₂, and Al₂O₃ in slag: The combined weight fraction of CaO, SiO₂, and Al₂O₃ should often be greater than 94%.

TGT: One of the most important operational parameters that can be used for validation of the model is the top gas or blast furnace gas temperature. Blast furnace top gas is highly useful as it contains significant energy in the form of CO and hydrogen. After cleaning, it is reused as a fuel to power hot blast stoves, which preheat air for the furnace and generate electricity in gas turbines, reducing the need for external energy sources. This recycling of energy not only improves the overall efficiency of the blast furnace process but also helps lower fuel consumption and GHG emissions, making operations more sustainable. Based on our interaction with industry experts, we came to know that the blast furnace is operated in such a way that the TGT falls in between 100 and 250 °C. Any temperature lower than this means WHR is not plausible and any temperature higher than this can damage the piping infrastructure pertaining to gas processing.

2.4.5.2. Determination of input and output flowrates

The zero-dimensional perturbation-fluctuation model was developed for three different cases.

Base case: Coke is the only reductant that is utilised in the blast furnace. The hydrogen-based reduction reactions are not considered. Only direct carbon reductions and indirect CO-based reductions are modelled.

Industry standards: PCI is used as an ARA. Hydrogen-based reduction reactions are also considered along with carbon-based reductions.

Hydrogen as ARA: Along with PCI, the impact of introducing hydrogen as an ARA was modelled in this case.

Hydrogen is recognised as a superior reductant compared with CO in the blast furnace process for iron ore reduction because of its smaller molecular size and higher diffusivity, which significantly enhance reaction kinetics and efficiency. Hydrogen's small molecules can penetrate the porous structure of iron ore pellets more effectively than CO, reaching reaction sites faster and facilitating quicker chemical reactions. Its high diffusivity, particularly at temperatures above 850 °C, allows hydrogen to overcome transport limitations within the blast furnace, ensuring efficient interaction with iron oxides and accelerating reduction rates. Unlike CO, hydrogen also offers environmental benefits by reducing iron oxides without producing harmful CO₂ emissions, making it a more sustainable option for modern steelmaking processes as industries strive to minimise their carbon footprint.

Hydrogen injection can serve as a transitional technology while the steel industry gradually shifts to more advanced hydrogen-based methods, such as hydrogen-based direct reduction (H-DR). This allows existing blast furnace infrastructure to remain operational while reducing its environmental footprint.

The RIST diagram (Figure 7) is a graphical representation of carbon, oxygen, and hydrogen balances of the blast furnace along an operational line (Kundrat et al., 1991). It also provides the heat balance (especially below the thermal reserve zone) for the bottom half of the furnace. Its primary significance lies in its ability to predict changes in blast furnace operations when various parameters are modified, such as the coke rate, injectant (ARA) amount, the oxygen amount, and the temperature of the blast/injectant. The salient features of the RIST diagram are as follows:

- **Active reductant participation:** The slope of the RIST diagram indicates the amount of all active reductants (carbon + hydrogen) involved in the reactions within the blast furnace, expressed in kmol/kmol of product Fe (Bailera et al., 2021). This helps in assessing how effectively carbon is being utilised for reduction.
- **Oxygen supplied by blast:** The RIST diagram can be used to evaluate the amount of oxygen supplied by the hot blast, including oxygen enrichment and oxygen from ARA, which is critical for maintaining combustion and ensuring efficient operation.
- **Top gas (O+ H₂)/(C+ H₂) ratio:** The diagram helps determine the oxygen-to-carbon ratio in the top gas, which is essential for understanding combustion efficiency and optimising gas compositions.
- **Impact of injectants:** By modifying parameters such as injectant amounts (e.g. hydrogen or other reducing agents), operators can predict how these changes will affect overall furnace performance.

- Temperature effects:** The RIST diagram can illustrate how variations in blast temperature influence gas compositions and reaction dynamics, aiding in thermal management within the furnace.

In our analysis, the RIST diagram was developed for two cases:

- PCI as ARA**, where PCI along with coke is used as the reductant and the impact of hydrogen-based reactions are accounted for
- PCI + H₂**, where along with coke, PCI and H₂ are injected into the furnace as reductants and their combined impact is analysed

Based on the RIST diagram, it can be inferred that hydrogen injection increases the oxygen requirements in the blast. This is because, hydrogen injection affects the furnace's heat balance. While hydrogen combustion releases heat, the largely endothermic reactions involving hydrogen may require additional oxygen to maintain the temperature (RAFT) needed for efficient operation.

By partially replacing carbon-based reductants such as coke and coal with hydrogen, the process generates water vapour instead of CO₂ as a byproduct (Table 11), reducing GHG emissions. This can contribute to achieving the industry's decarbonisation goals.

Figure 7: RIST diagram

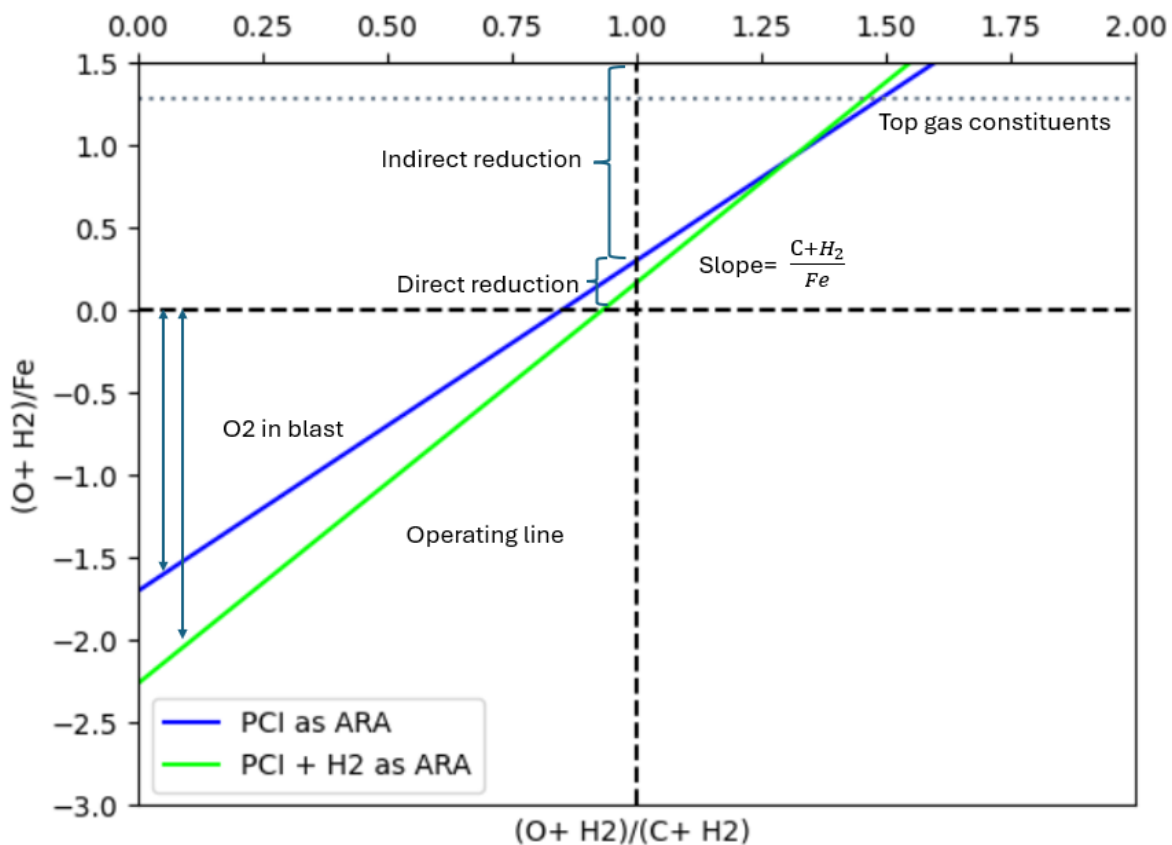
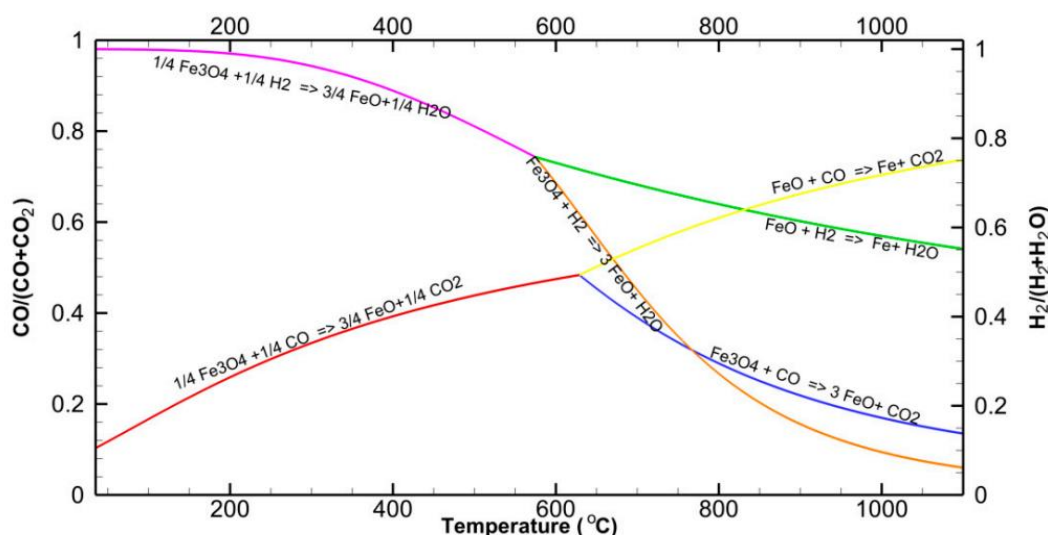


Table 11: Iron reduction mechanism using hydrogen

Reaction	Equation
Haematite to magnetite	$3 \text{Fe}_2\text{O}_3 + \text{H}_2 = 2 \text{Fe}_3\text{O}_4 + \text{H}_2\text{O}$
Magnetite to wustite	$\text{Fe}_3\text{O}_4 + \text{H}_2 = 3 \text{FeO} + \text{H}_2\text{O}$
Wustite to iron	$\text{FeO} + \text{H}_2 = \text{Fe} + \text{H}_2\text{O}$
Water-gas shift reaction	$\text{CO} + \text{H}_2\text{O} \rightleftharpoons \text{CO}_2 + \text{H}_2$

Hydrogen is injected at the tuyere level alongside PCI. This is because the hydrogen-based reduction of FeO is endothermic in nature. In addition to this, the Bauer–Glaessner diagram (Figure 8), which illustrates the reduction reactions of iron oxides with H₂ and CO at different temperatures, depicts the relative concentrations of CO/CO₂ and H₂/H₂O, highlighting the temperature-dependent efficiency of H₂ and CO as reducing agents in ironmaking processes. The hydrogen-based reduction of iron ore is also thermodynamically plausible at higher temperatures (de Castro et al., 2023).

Figure 8: Bauer–Glaessner diagram (adopted from de Castro et al., 2023)



Literature reviews and interactions with industry stakeholders made us understand that hydrogen-based reduction of iron ore and direct carbon-based reduction of iron ore are endothermic and require high temperatures (Table 12). Therefore, to model hydrogen injection effectively, we had to identify the reductant that dominated the overall reduction of iron ore to iron among CO, C, and H₂.

Table 12: Direct, indirect, and hydrogen reduction of wustite

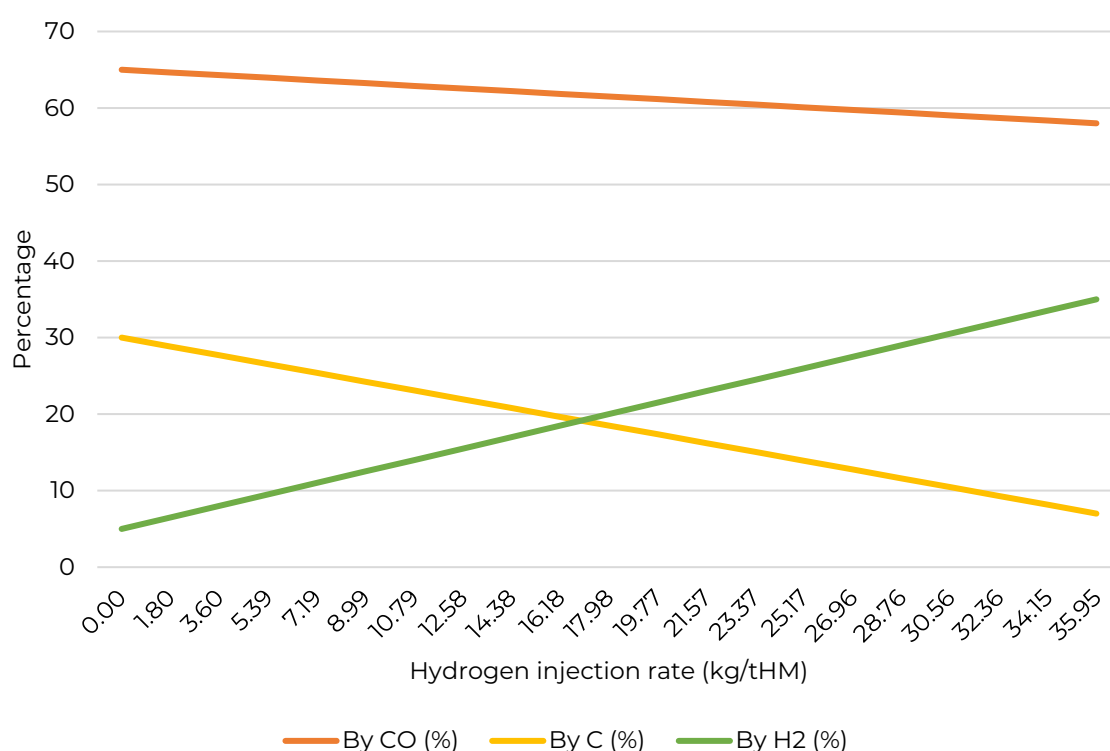
Reaction	Temperature (°C)	$\Delta H_{\text{Reaction}}$ (kcal/mole)
$\text{FeO(s)} + \text{CO(g)} \rightarrow \text{Fe(s)} + \text{CO}_2\text{(g)}$	927	-3.85
$\text{FeO(s)} + \text{C(s)} \rightarrow \text{Fe(s)} + \text{CO(g)}$	1,427	27.48
$\text{FeO(s)} + \text{H}_2\text{(g)} \rightarrow \text{Fe(s)} + \text{H}_2\text{O(g)}$	927	3.73

The complex multiphase, multicomponent, multitemperature reaction environment often makes it difficult to estimate the dominant reactant and necessitates the need for advanced thermodynamic process simulators to identify it.

Over the years, several studies have been conducted to develop advanced models using process simulation and numerical modelling tools to identify the hydrogen injection limit into the blast furnace (Yilmaz et al., 2017).

In this work, to identify the relative extent of reduction by the reactants CO, C, and H₂, we adapted results from Kamijo et al. (2022), where the authors analysed the impact of injecting hydrogen into a 12 m³ experimental blast furnace. The paper discussed the relative extent of reduction of the reductants CO, C, and H₂ with respect to the rate of hydrogen injected (Figure 9).

Figure 9: Extent of reduction of ferrous material



The flowrates and compositions of each of the input and output streams were predetermined based on our interaction with industry stakeholders and by referring to the literature.

The quality control parameters mentioned (Section 2.4.3.1.2) are common for all the three cases of the model that we developed. A parameter called RAFT—the maximum theoretical temperature achieved at the point where hot blast air and injected fuels react within the raceway, reflecting the energy available for subsequent reduction reactions in the furnace—was employed while incorporating the hydrogen-based interaction into the model.

Injecting hydrogen into a blast furnace significantly influences both RAFT and the TGT. Hydrogen injection tends to lower RAFT, which is critical for maintaining optimal melting and reduction processes. As hydrogen replaces coke, it alters the combustion dynamics within the furnace. Studies indicate that at higher hydrogen injection rates, RAFT can

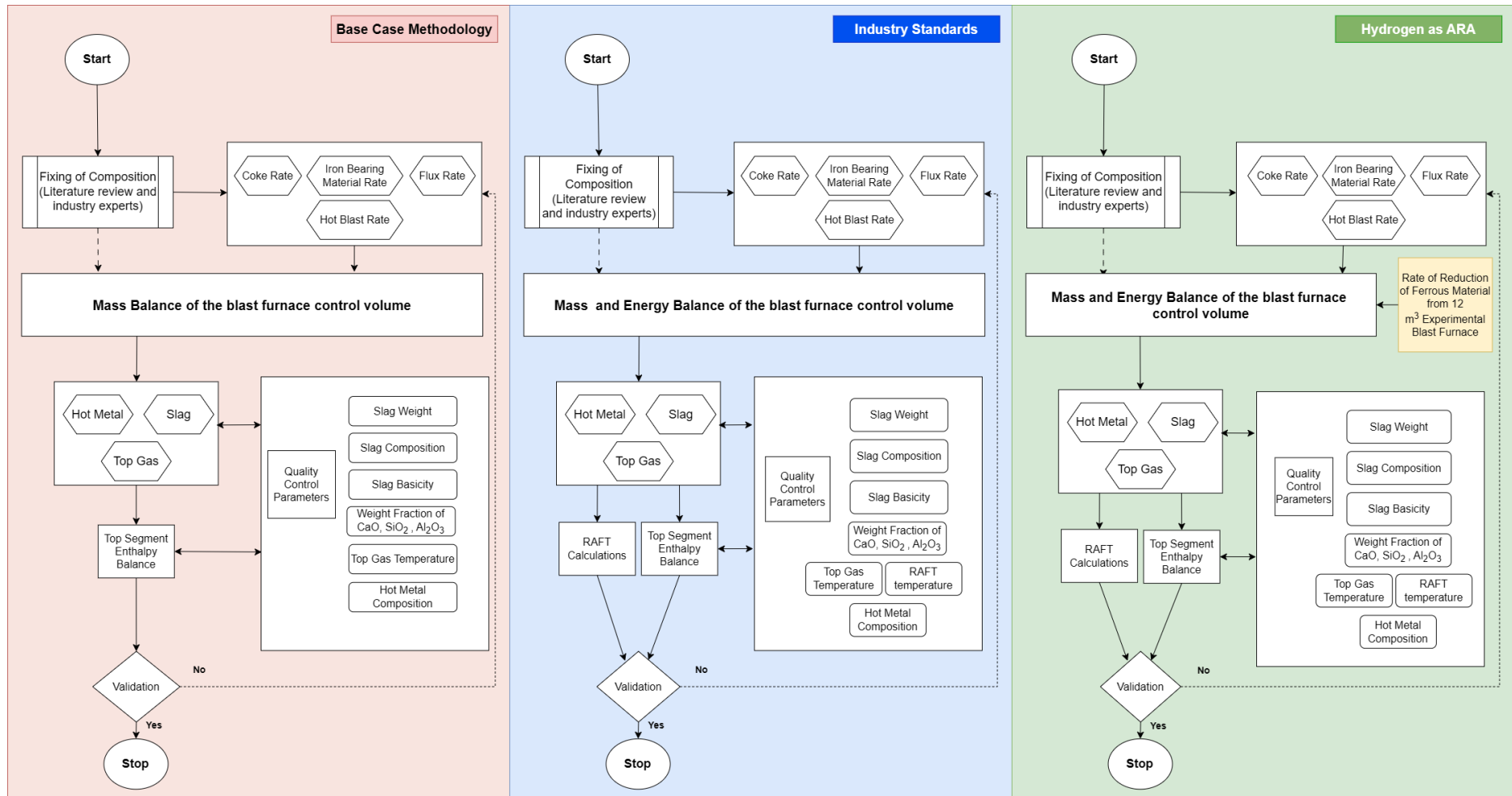
decrease by up to 200 °C compared with base-case scenarios. This drop occurs because hydrogen has a lower heat generation capacity than coke, necessitating adjustments in operational parameters, such as oxygen enrichment, to stabilise RAFT (Barrett et al., 2022; Gao et al., 2022).

The TGT also experiences changes because of hydrogen injection. As hydrogen is introduced, the overall volume of gas injected increases, which can counteract the decrease in TGT caused by reduced coke usage. However, if hydrogen injection exceeds certain thresholds, it may lead to a significant drop in TGT because of insufficient thermal energy from combustion processes (Barrett et al., 2022; Shatokha, 2022).

In summary, while hydrogen injection can facilitate a transition towards more sustainable steel production by reducing carbon emissions, it requires careful management of operational parameters to mitigate adverse effects on both RAFT and TGT.

A mass balance was performed to determine the constituents of each input and output streams. Flowrates and the composition of each stream were then compared with quality control parameters. The detailed methodology is illustrated in Figure 10.

Figure 10: Methodology

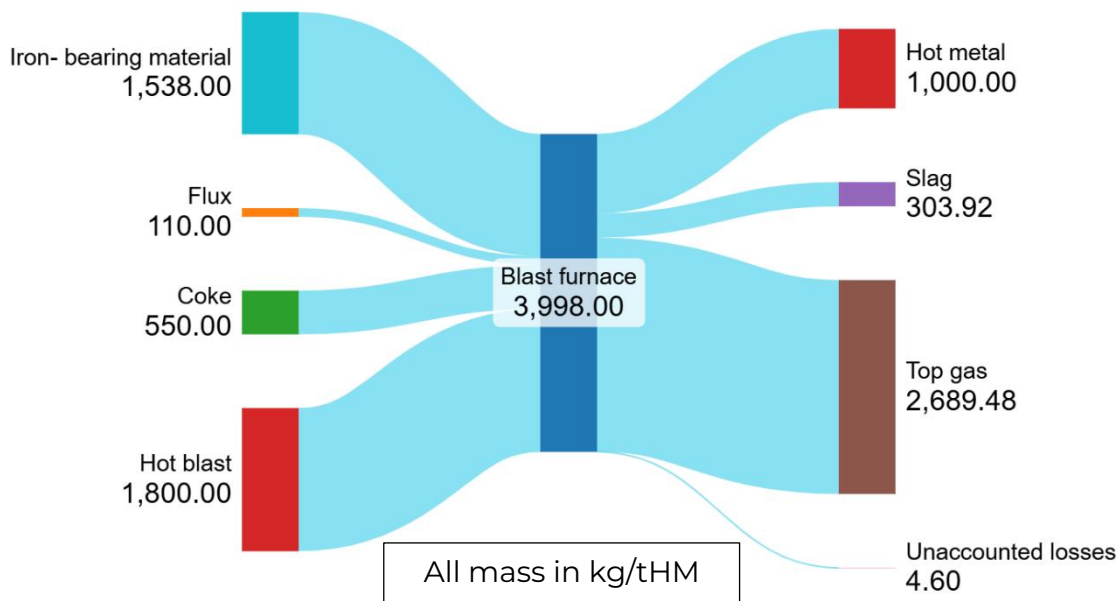


2.4.5.3. Results and analysis

The mass and energy balance aimed to evaluate the input and output streams; including raw materials, such as iron ore, coke, fluxes, and reducing agents; alongside energy flows encompassing thermal energy and chemical reactions.

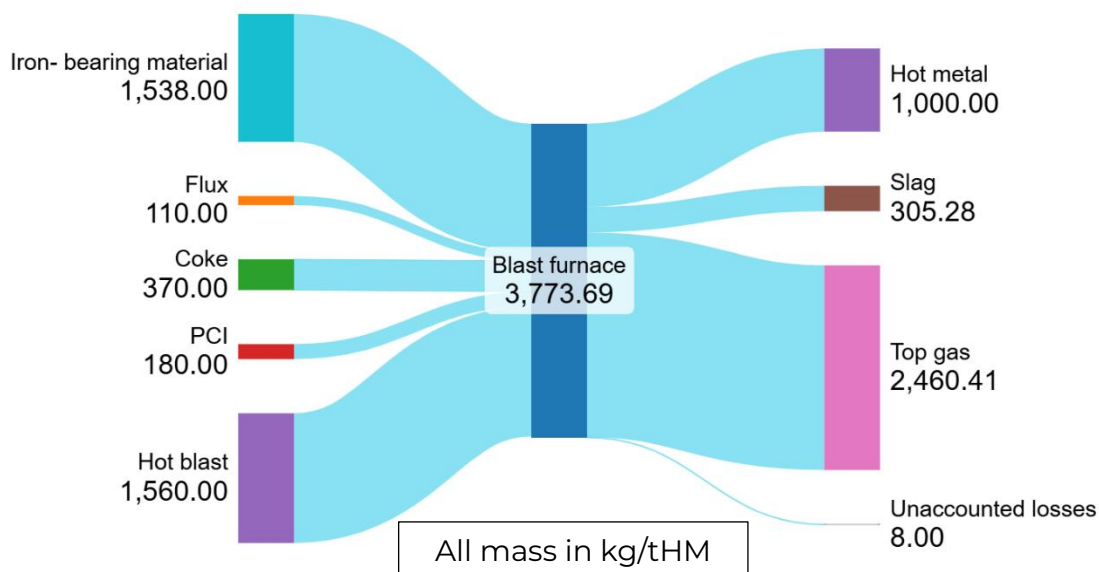
To reiterate, this analysis entails the following cases (Section 2.4.3.2): base case (Figure 11), industry standards, and hydrogen as ARA.

Figure 11: Mass balance (base case)



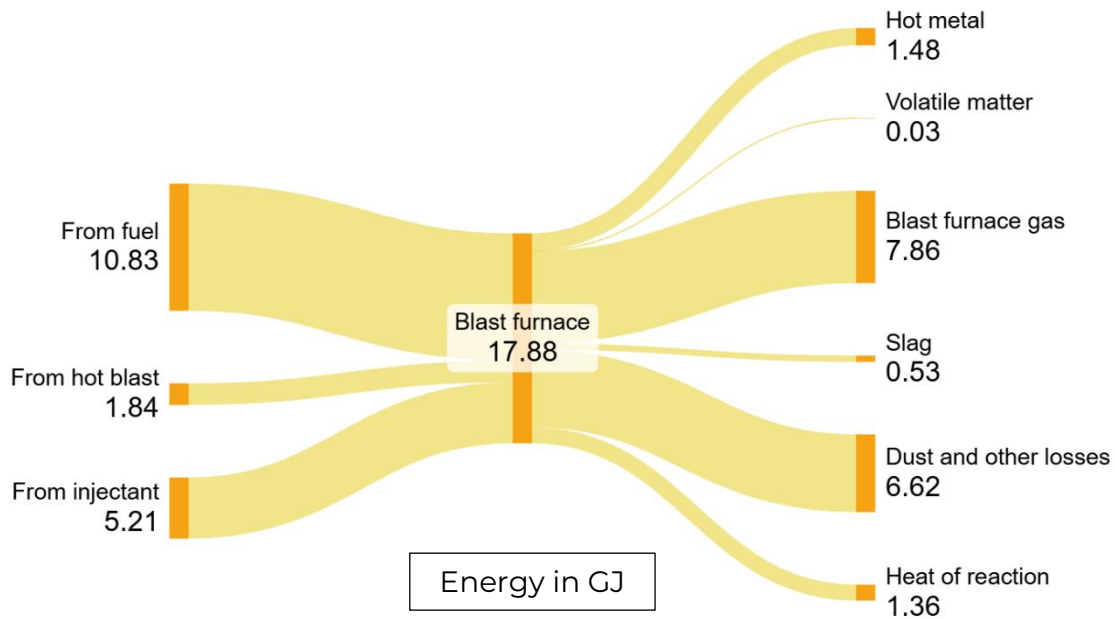
A more accurate representation, as in the industry, with the ARA is shown in Figure 12.

Figure 12: Material balance (industry standards)



As presented in Figure 13, the total heat input amounted to 17.88 GJ, which came from fuel (10.83 GJ), hot blast (1.84 GJ), and injectants (5.21 GJ).

Figure 13: Energy balance with ARA



The provided heat balance data for the blast furnace indicates that the blast furnace gas carried a significant portion of the total heat output, accounting for 7.86 GJ of the total 17.88 GJ of heat output. This represents a major pathway for energy dissipation, highlighting the high heat rate associated with the blast furnace generated during the process. The considerable energy content in the blast furnace gas points to the potential opportunity for energy recovery or reuse within the steelmaking process.

To validate the mass and energy balances developed for the base case and the industry standards case, various slag properties and additional quality control parameters, as discussed in Section 2.4.3.1.2, were computed and compared (Figure 14 and Figure 15).

Figure 14: Base case (slag properties)

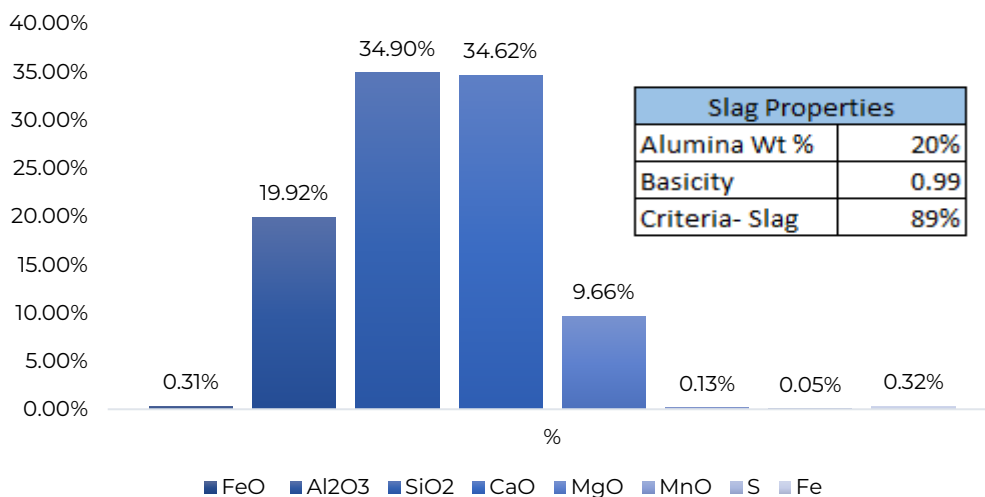
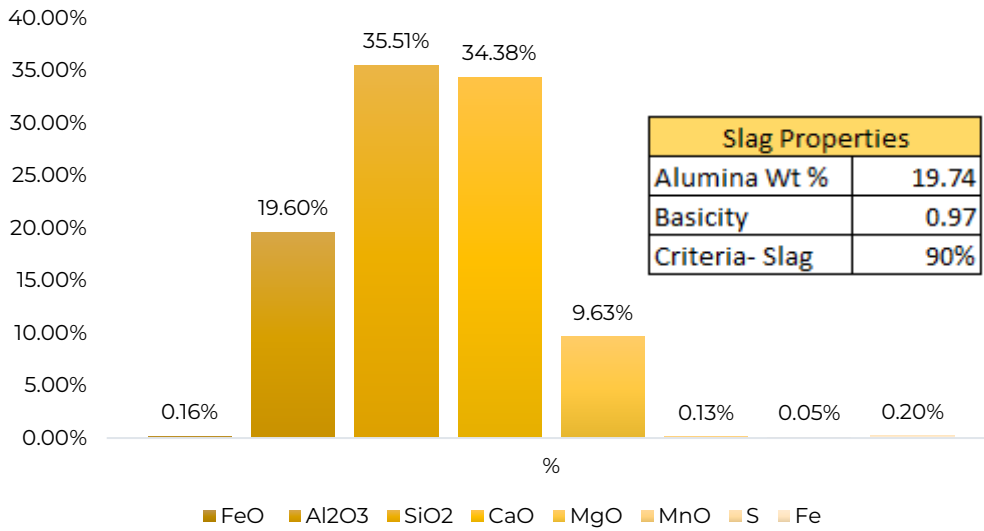


Figure 15: Industry standards (slag properties)



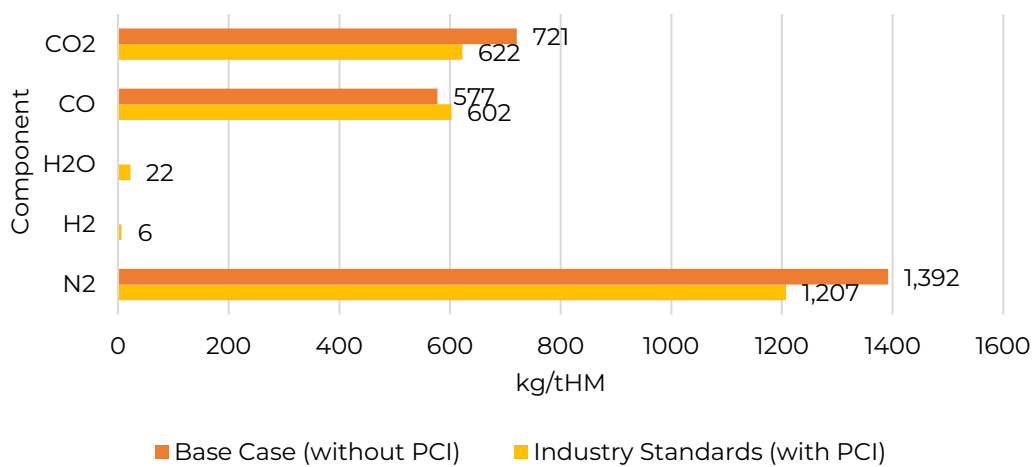
The additional quality control parameters, especially RAFT and TGT for the standard case, were calculated as per the literature and found to be well within the range (Table 13) of blast furnace operations (Davenport et al., 2019).

Table 13: General operating parameters for RAFT and TGT

TGT	Typical range: 110 to 250 °C	170 °C
RAFT	Typical range: 1,900 to 2,300 °C	2,284 °C

It was also observed from the mass balance that the addition of PCI into the system and the introduction of hydrogen-based reactions into the model changed the top composition significantly. The carbon emission (CO+ CO₂) also reduced from 1,298 to 1,224 kg/tHM (Figure 16). This can be attributed to the reduction in coke rate. Contemporary blast furnaces follow this practice to reduce their coke rate.

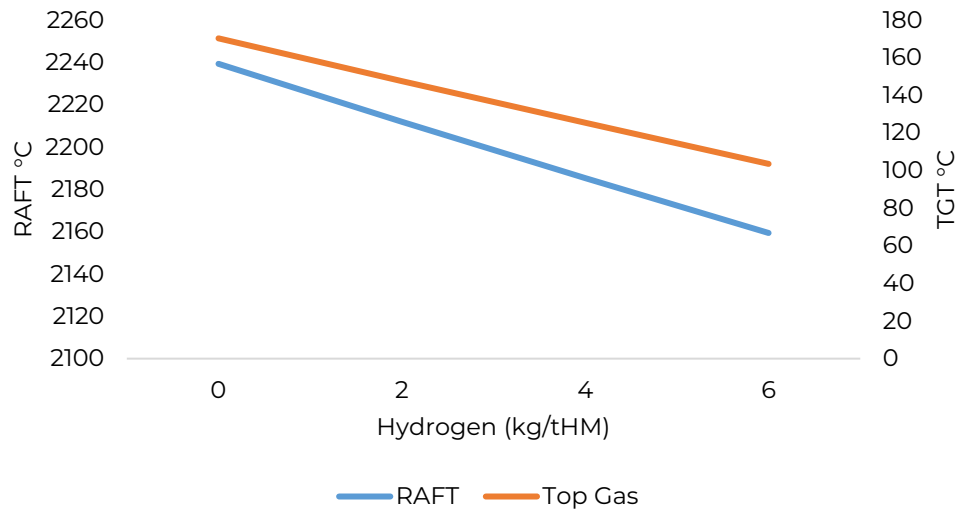
Figure 16: Top gas composition



Hydrogen as ARA

To identify the optimal hydrogen injection rate into a blast furnace, the industry standards (PCI as ARA) case, which represents typical blast furnace operations, was used. Coke and coal rates were fixed at 370 and 180 kg/tHM, respectively, and hydrogen was introduced at 25 °C. The effects on the corresponding RAFT and TGT are plotted in Figure 17.

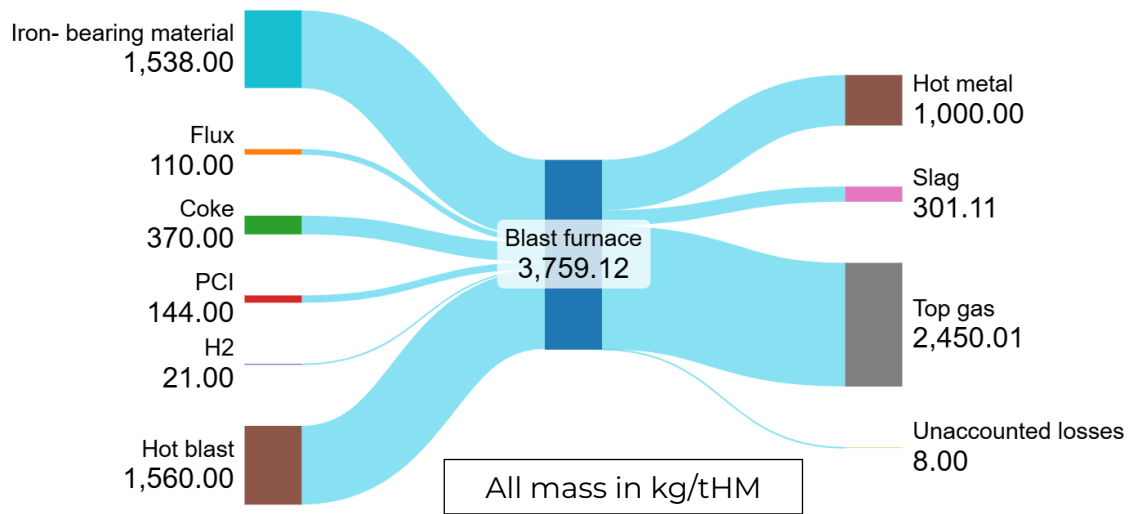
Figure 17: Effect of hydrogen injection on RAFT and TGT



When hydrogen was injected into the blast furnace at near ambient conditions, the maximum hydrogen injection rate was found to be only 6 kg/tHM. Beyond this, the injection resulted in the TGT going below the general operating parameters. This is attributed to the high specific heat capacity of hydrogen, because of which it lowers the RAFT and, subsequently, the TGT. To circumvent this issue, the amount of PCI/coke that is injected can be reduced.

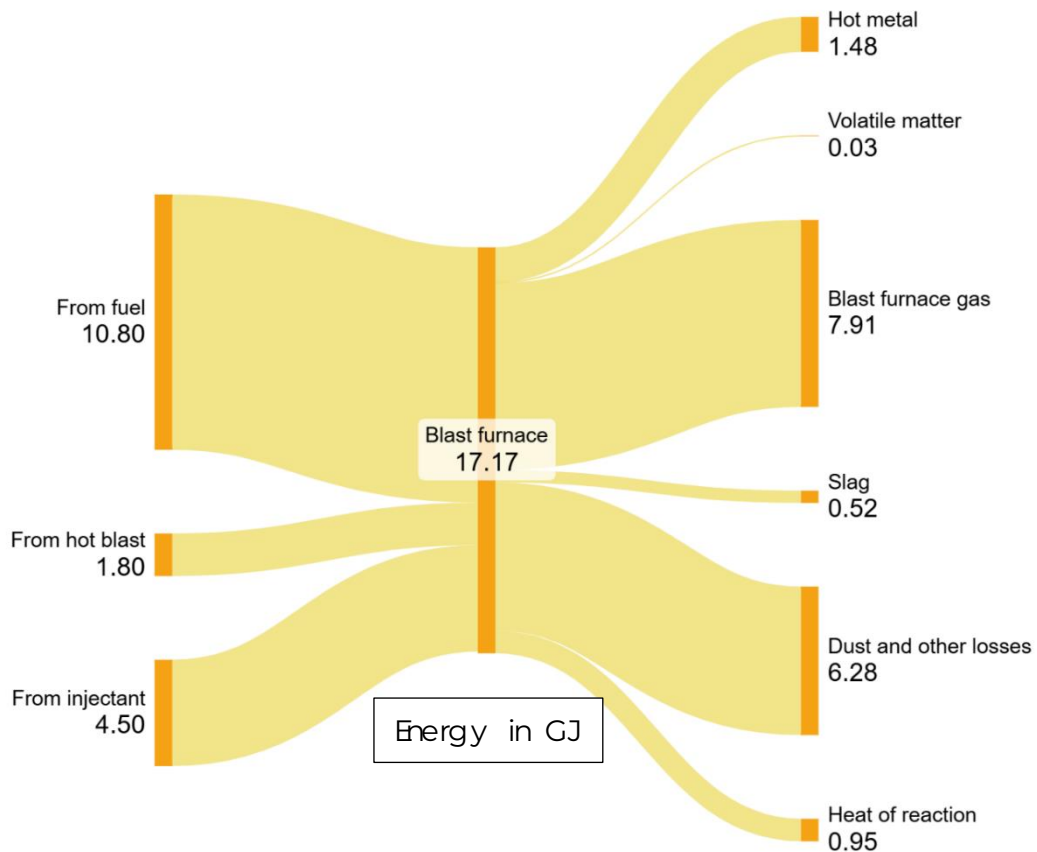
By reducing the PCI rate from 180 to 144 kg/tHM (keeping in account the other quality control parameters), the hydrogen injection rate could be improved to about 21 kg/tHM. The corresponding RAFT and TGT were obtained as 2,003 °C and 186 °C. The reduction of PCI not only enhanced the hydrogen injection rate but also reduced carbon emissions. The mass and energy balance of the blast furnace after these modifications is illustrated in Figure 18 and Figure 19, respectively.

Figure 18: Hydrogen as ARA (mass balance)



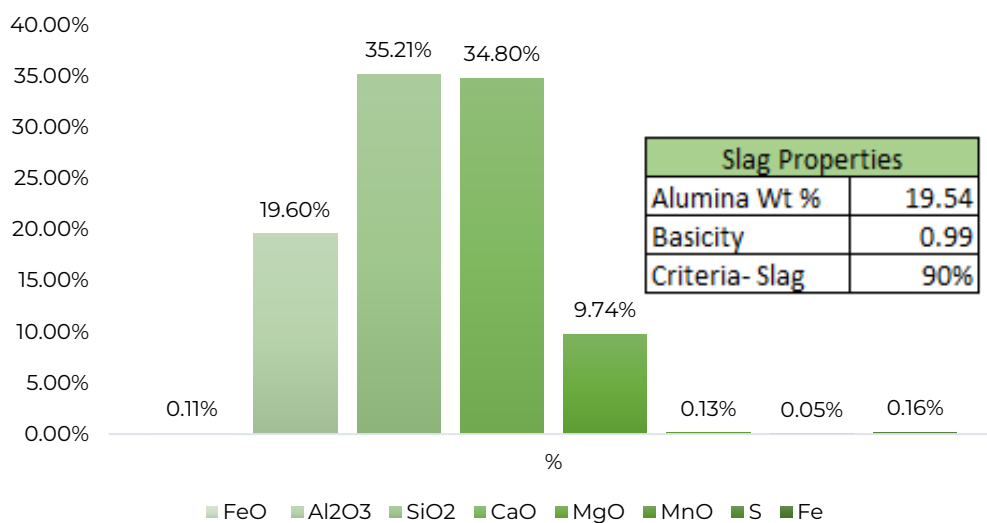
Injecting hydrogen into the blast furnace by partially substituting PCI can reduce the carbon emission from 1,224 to 1,126 kg/tHM, which translates to about 8%.

Figure 19: Hydrogen as ARA (energy balance)

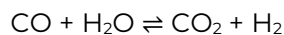


The corresponding slag properties (Figure 20) were also computed and validated using the quality control parameters.

Figure 20: Hydrogen as ARA (slag properties)

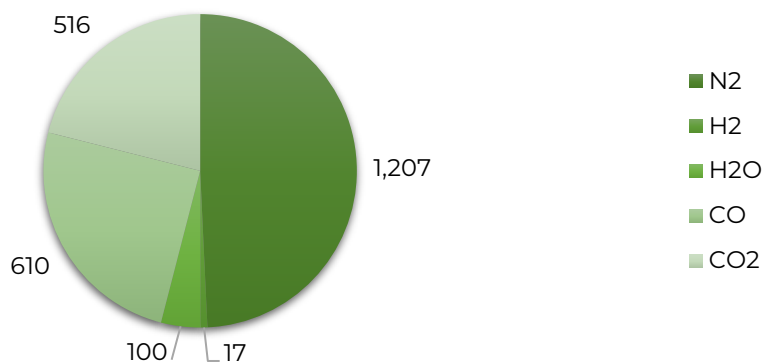


A significant portion of the hydrogen that was injected as ARA into the furnace exited through the top gas unreacted (Figure 21). This is because injecting hydrogen into the blast furnace increases the volume of reductant gases (CO and H₂) in the raising gases within the blast furnace. However, as the number of oxygen molecules that must be removed from the oxides in the burden remains the same, the amount of reductant molecules to that of reducing gases is higher. Hydrogen only partly reduces iron oxides in the blast furnace because of the thermodynamic constraints of the water–gas shift reaction.



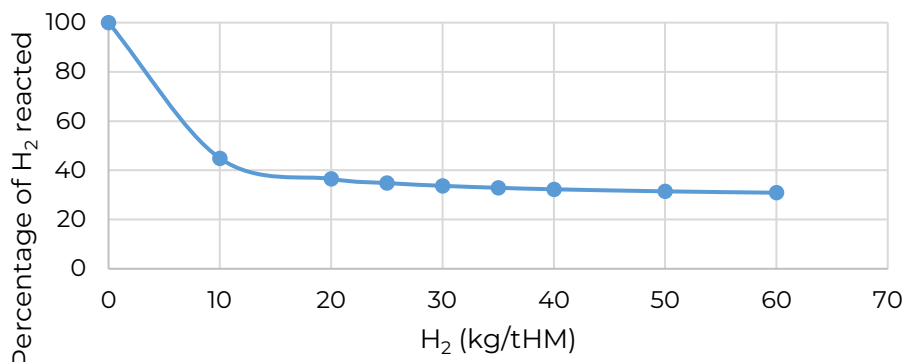
At temperatures above approximately 1,000 °C, H₂ reacts with CO₂ to form CO and H₂O instead of reducing iron oxides (Yilmaz et al., 2017). This reaction is reversible, meaning CO and H₂O are produced at lower temperatures. As a result, hydrogen's effectiveness as a reductant is limited as it competes with this reaction. The temperature-dependent nature of the water–gas shift reaction constrains hydrogen's ability to fully participate in the iron oxide reduction throughout the furnace.

Figure 21: Hydrogen as ARA (top gas composition in kg/tHM)



The ratio of the quantum of hydrogen injected as ARA to the amount of hydrogen that participates (percentage) in the reduction reaction was estimated for different injection rates (Figure 22).

Figure 22: Percentage of hydrogen reacted versus injected



Further interventions to increase hydrogen injection into the blast furnace include the following:

Injecting hydrogen at higher temperatures: Injecting hydrogen at temperatures lower than the hot blast reduces the RAFT, which negatively affects furnace efficiency. Heating injected hydrogen for blast furnace operations is, therefore, crucial as higher injection temperatures mitigate this impact, helping maintain optimal thermal conditions. However, hydrogen heating technology is still in its early stages, presenting significant logistical and financial challenges because of the complexity of heating and handling hydrogen efficiently at the required scale (Barrett et al., 2022). This has been implemented in a pilot scale in a test furnace, resulting in an emission reduction of 22% (Nippon Steel Corporation, 2023). Addressing these challenges will allow for higher hydrogen injection rates in furnaces.

Oxygen enrichment: Increasing the oxygen content in the hot blast enhances the combustion efficiency, creates a more efficient reduction atmosphere, and improves gas permeability in the furnace. Enriching oxygen improves furnace productivity and reduces coke consumption but only up to a point. This is because higher oxygen concentrations lead to excessive heat generation, requiring more coke and increasing operational costs. Additionally, at blast temperatures above 1,000–1,100 °C, the benefits of higher oxygen are outweighed by increased costs, making further enrichment economically unviable (Barrett et al., 2022). In the Indian context, oxygen enrichment in blast furnaces is typically limited to a range of 2%–4% (Sau et al., 2021). In our analysis, at 2% oxygen enrichment, we observed that hydrogen injection rate can be increased to 33 kg/tHM, with a RAFT and TGT of 2,001 °C and 249 °C, respectively. The corresponding emission reduction was found to be about 9%.

Reducing coke: Coke, in addition to acting as a fuel, serves as a structural component, providing mechanical support to the burden and facilitating gas flow. Reducing coke impacts multiple aspects simultaneously, including the permeability of the burden and the stability of the furnace. Hence, this analysis kept the coke rate constant.

However, we found that coke reduction and PCI reduction of 12 kg/tHM and 19 kg/tHM translate to a hydrogen injection rate of 19 kg/tHM, resulting in a RAFT and TGT of 2,016 °C and 205 °C, respectively. This resulted in an emission reduction of 7%.

2.5. Techno-economic assessment

The techno-economic analysis of BF–BOF steelmaking, including the introduction of hydrogen into the process, aims to provide a comprehensive understanding of production costs and their potential variations. The economic evaluation was carried out by calculating the levelised cost of steel, which considers both capital expenditures (capex) and operational expenditures (opex). This analysis was conducted within the gate-to-gate boundary of the steel plant, capturing costs associated with the entire production cycle from raw material input to steel output.

Economic parameters were sourced from a variety of references, including data provided by India's Ministry of Steel and Coal, academic literature, secondary literature, and online sources. Capital costs were determined according to methodologies outlined by Garrett, Towler, and Sinnott, with adjustments made for location factors to adapt the cost estimations for the Indian context. Capital costs were also scaled using specific scaling factors to ensure an accurate reflection of investment requirements (Johnson et al., 2023).

The life of the representative plant was assumed to be 25 years. The operation and maintenance costs and raw material costs were annualised, and the discount rate was assumed to be 10% (Bhaskar et al., 2022).

The analysis also incorporated a sensitivity assessment to account for potential variations and uncertainties in the costs associated with the introduction of hydrogen. This approach aimed to evaluate the additional costs and economic impacts of introducing hydrogen injection into the BF–BOF process, thereby enhancing the understanding of how hydrogen could influence production economics in a traditional steelmaking setup.

The analysis started with assessing the levelised cost of production for a typical steel plant of a capacity of 1 million tonne per annum (MTPA). Once the baseline was established, the changes to the price of steel with the cost of hydrogen were analysed.

2.5.1. Levelised cost of production

The levelised cost of a product (LCOP) or service aims to determine the break-even value per unit that a producer must achieve in sales revenue to justify the investment in a specific production facility. This value helps in assessing whether the investment will be financially viable, ensuring that the costs of production are covered over the lifespan of the facility. This includes all associated expenses, from the initial capital investment to ongoing operation and maintenance costs. The LCOP is calculated as follows:

$$LCOP = \frac{C(\text{capex}) * ACC + C(\text{opex}) + C(\text{maint}) + C(\text{emission})}{\text{Annual steel production}}$$

$$ACC = \frac{i * (1 + i)}{(1 + i)^n - 1}$$

where C = cost, ACC= annuity factor, and i = discount rate.

2.5.2. Results and analysis

Capex values were identified from multiple secondary literature sources and on the basis of interactions with industry experts (Davenport et al., 2019; Dowding & Whiting, n.d.; Johnson et al., 2023; Peacey & Davenport, 1979; West, 2020).

The source values provided in Table 14 showcase the material input parameters crucial for the steel production process. The key metrics include metallic input, coal consumption, and coke rate, all of which are essential in determining the overall efficiency and cost-effectiveness of the furnace operation. These data are vital as they provide a detailed view of the material and energy inputs required for steel production, laying the foundation for cost calculations and process optimisation. The scrap rate for the process was assumed to be 9% based on multiple inputs (Chattopadhyay et al., 2019; Essar Projects [India] Limited Engineering & Project Management, 2014).

Table 14: Operating expenses

Material	Consumption		Unit cost		Final cost	
	Flowrate	Unit	Amount	Unit	Amount	Unit
Flux	110	kg/tCS	1.94	INR/kg	213.4	INR/tCS
Coking coal	588	kg/tCS	10.45	INR/kg	6,148	INR/tCS
Electricity	421	kWh/tCS	5.00	INR/kWh	2,106	INR/tCS
CDI/PCI	190	kg/tCS	7.27	INR/kg	1,387	INR/tCS
Oxygen	199	kg/tCS	3.34	INR/kg	664.37	INR/tCS
Scrap steel	90	kg/tCS	29.50	INR/kg	2,655	INR/tCS
Fe ore	615.2	kg/tCS	5.65	INR/kg	3,479	INR/tCS
Sinter	769	kg/tCS	6.69	INR/kg	5,145	INR/tCS
Pellet	154	kg/tCS	8.08	INR/kg	1,243	INR/tCS
Water	2.6	m ³ /tCS	0.54	INR/m ³	1.41	INR/tCS

Opex

Table 14 reflects the costs associated with various materials and utilities required for steelmaking, such as flux, coal, electricity, and water and iron-bearing materials. For instance, the cost of flux per tonne of crude steel is INR 213, while coal, being the largest contributor, accounts for INR 6,148 per tonne of crude steel. Electricity consumption, another significant component, incurs a cost of INR 2,106 per tonne of crude steel. These figures highlight the areas where cost control measures can be implemented to improve overall profitability. The detailed cost analysis also helps in benchmarking against industry standards, enabling better financial planning and resource allocation.

Cost of steel

The final cost of steel was determined by aggregating the opex and capex along with other associated costs, such as raw material and labour costs. The table provides a comprehensive overview of these costs, breaking them down into per-unit values. For example, costs of iron ore, flux, and electricity are significant contributors to the final steel price. Understanding these costs allows for a better evaluation of the pricing strategies and competitive positioning in the market. By analysing these figures, a steel plant can identify areas for cost reduction and efficiency improvements, which are critical for maintaining profitability in a highly competitive industry.

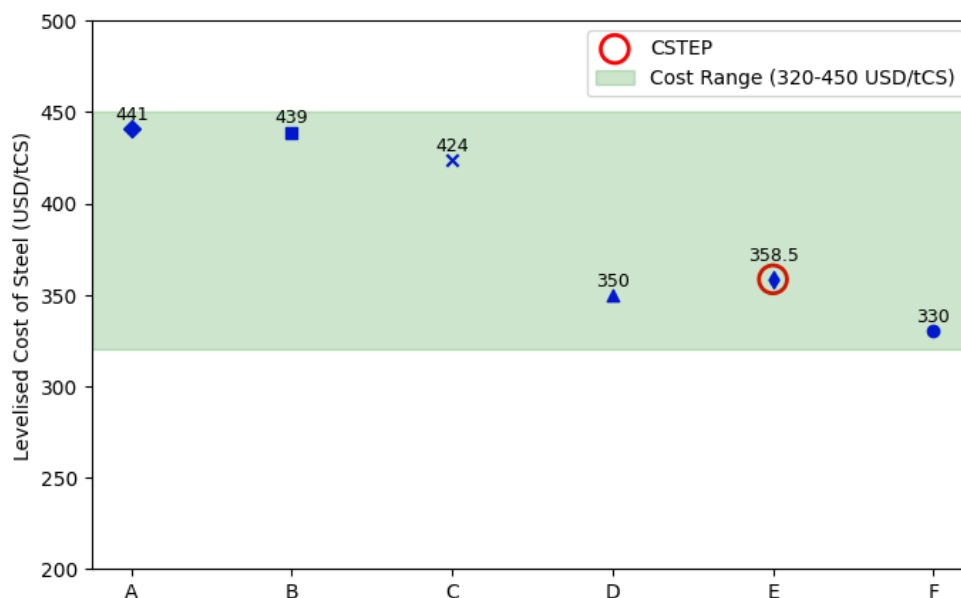
Calculations were made assuming the lifetime of the plant as 25 years, and the discount rate was calculated to be 10%.

Analysis

The analysis of the data provided in the tables provides key insights into the operational efficiency and cost structure of the steel production process. The source value table emphasises the importance of optimising material inputs and energy consumption to reduce the overall cost of production. The opex breakdown (Table 14) highlights that coal and electricity are major cost drivers, suggesting that improvements in these areas could significantly impact profitability. Capex investments, particularly in energy-efficient technology and modern infrastructure, are essential for long-term sustainability and cost reduction.

Our analysis calculated the levelised cost of production at 358.7 USD/tonne (INR 29,759 /tonne), which was validated (Figure 23) by multiple sources and industry experts.

Figure 23: Levelised cost of steel (various sources)



2.5.3. Injection of hydrogen

Once the baseline cost of the steel production was arrived at, the injection of hydrogen was evaluated. For this, the levelised cost of hydrogen (LCOH) was computed.

The assumptions used in this analysis were based on several key factors, including electricity price, electrolyser specifications, system efficiency, operational and financial parameters, and plant characteristics. These assumptions formed the basis for determining the LCOH. First, the electrolyser efficiency was assumed to be 54 kWh per kilogram of hydrogen produced, indicating that it required 54 kWh of electricity to generate 1 kg of hydrogen in the stack. This efficiency directly influenced the energy cost component of hydrogen production. The cost of electricity was assumed to be INR 7 per kWh, which was the primary determinant in the overall LCOH, given that electrolysis is a highly energy-intensive process.

The capex for the proton exchange membrane (PEM) electrolyser was assumed to be USD 800 per kW of the installed capacity (Badgett et al., 2024).

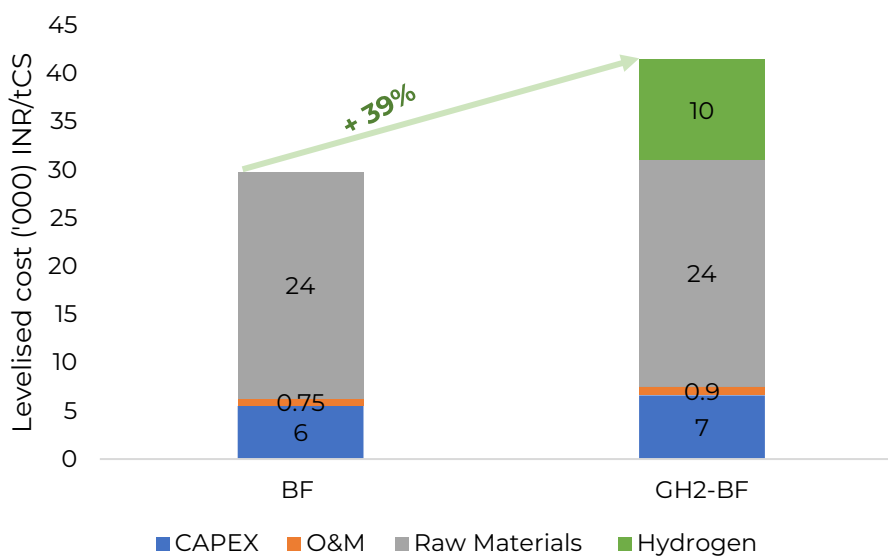
For operation and maintenance, the annual cost was estimated to be 1.5% of the initial capital cost of the electrolyser, which included maintenance activities, labour, spare parts, and other associated costs. In terms of financing, a discount rate of 11.2% was used to account for the time value of money over the project life cycle. The project was assumed to be financed with a debt-to-equity ratio of 70:30, with an interest rate of 10% on debt and a cost of equity of 14%. Additionally, stack replacement was anticipated every 7 years to ensure optimal operation and maintain efficiency throughout the plant's operational life.

Furthermore, a 20% increase in capex for steelmaking infrastructure was envisaged to accommodate the required modifications for hydrogen integration, including necessary piping, storage, and handling systems. The costs of coke and coal were also adjusted accordingly, considering the partial replacement by hydrogen, which influenced the overall cost structure of the steel production process.

These assumptions collectively provided a framework for calculating the LCOH, enabling a detailed economic evaluation of green hydrogen production using PEM electrolysers.

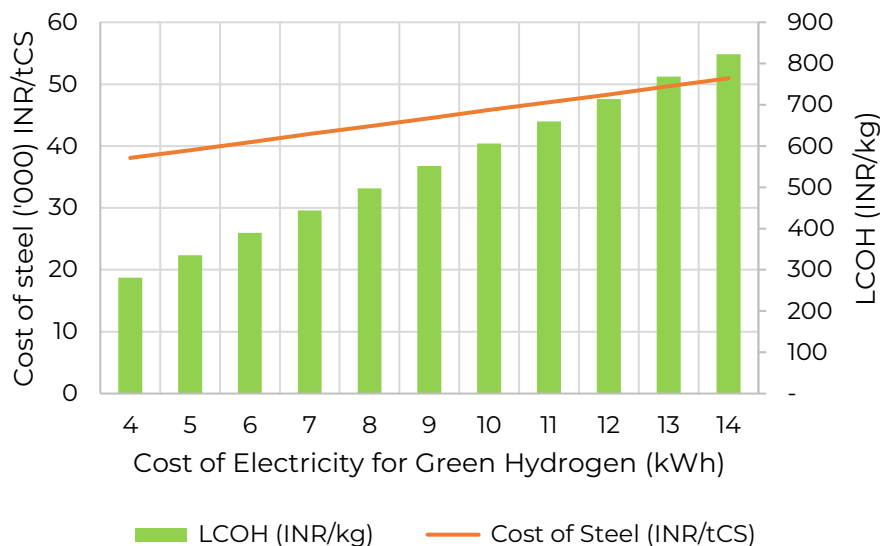
The premium associated (Figure 24) with the injection of hydrogen to the BF-BOF process was computed to be 39%.

Figure 24: Cost of steel (hydrogen injection)



The cost of hydrogen is contingent on the cost of renewable electricity and its storage. The base case assumed an electricity cost as INR 7 /kWh. The impact of the cost of electricity for hydrogen production on the cost of steel is shown in Figure 25.

Figure 25: Steel price variation with green hydrogen electricity cost



The incentives provided under the Strategic Interventions for Green Hydrogen Transition (SIGHT) scheme were also accounted for in the analysis, where the incentives for the first 3 years of production of green hydrogen were provided along the lines of INR 50/kg, INR 40/kg, and INR 30/kg for the first, second, and third years, respectively.

The impact of the SIGHT scheme was found to be marginal, with a ~2% drop in the per-tonne steel cost.

2.6. Limitations

Several limitations have been identified that need to be addressed to ensure more robust and scalable findings. One significant limitation involves the slag content, which in the study was observed to be lower than typical industry benchmarks. This discrepancy could impact the understanding of slag-metal reactions and the thermal balance in a blast furnace operation, potentially leading to incorrect conclusions regarding hydrogen's impact on furnace stability and efficiency. For a practical and scalable application, more granular data of the charge composition for the representation of slag chemistry and quantity, reflective of industrial conditions, are necessary.

Another notable limitation pertains to the reference literature, which often cites data from pilot-scale blast furnaces (12 m³; Kamijo et al., 2022). The use of pilot data presents inherent challenges because the dynamics in a full-scale blast furnace are more complex and sensitive to variations in operational parameters. Scaling these results to an industrial level could introduce significant errors because of differences in flow patterns, heat distribution, and gas-solid reactions. The results obtained in controlled, small-scale environments may not directly translate to full-scale operations, limiting the reliability of conclusions drawn from the current research.

Further, the introduction of hydrogen into the BF-BOF process will notably influence the composition of blast furnace gas. Traditionally, blast furnace gas is utilised in an

integrated steel plant in combination with coke oven gas, converter gas, or both, and serves as a fuel in various furnaces, such as blast furnace stoves, soaking pits, and annealing furnaces. It is also used in applications such as foundry core ovens, gas engines for blowing, boilers, gas turbines, and sinter plant furnaces (ISPAT Guru, 2013).

The injection of hydrogen into the blast furnace will alter the chemical composition of blast furnace gas, potentially affecting its calorific value and compatibility with different downstream uses. The changes brought by hydrogen injection need to be thoroughly investigated to understand their impact on the efficiency and feasibility of utilising blast furnace gas for various applications within the integrated steel plant.

Additionally, the scope of this study is confined to blast furnace technology and does not include DRI processes. While hydrogen application in the blast furnace route shows promise in reducing carbon emissions, the DRI process, which inherently has a lower carbon footprint and is more amenable to hydrogen usage, could potentially offer different insights or better optimisation routes. Sufficient literature and pilots are available detailing the use of hydrogen and hydrogen-rich gases in the DRI process. This work was constrained to the BF operation.

Another challenge encountered in this research is related to the use of HOMER software for determining LCOH. Although HOMER is widely used for energy system analysis, its algorithm limitations affect its ability to provide precise LCOH estimates under certain conditions, especially when considering novel hydrogen production routes and the integration of fluctuating renewable energy sources. The simplified assumptions and the linear optimisation model used by HOMER may fail to capture the complex interdependencies of production, storage, and consumption cycles when applied to hydrogen's role in ironmaking. This limitation restricts the accuracy and reliability of economic analyses presented in the current study.

Further uncertainties arise in determining the levelised cost of steel, especially concerning capex for steel plants. Key input data, such as coal and power consumption, were sourced from secondary literature and interactions with industry representatives, which may not accurately reflect the specific conditions of individual plants. This variability can influence both the necessary capital investments and the associated operational costs, particularly when factoring in the associated rise in the cost of steel when hydrogen is injected.

Additionally, the lack of available plant-level fuel prices for steel plants and captive units forces reliance on broad assumptions for these parameters. Such generalised assumptions introduce considerable uncertainties in the levelised cost of steel estimations as actual fuel prices and consumption patterns can differ significantly between plants. Factors such as location, technology, and energy efficiency measures implemented in plants play a crucial role in these variations, further impacting the accuracy of cost assessments.

These limitations highlight areas where future research could improve, particularly in adopting larger-scale, industry-representative models, expanding the scope to include alternative processes such as DRI and using more advanced simulation tools (Aspen Plus) for technical and economic evaluation at a plant level. Addressing these gaps will provide more comprehensive insights into hydrogen's role in transforming ironmaking towards a low-carbon future.



3. Cement

3.1. Cement manufacturing process

To effectively decarbonise the cement industry, it is necessary to have an in-depth understanding of the cement manufacturing process because of the following reasons:

1. Each sub-process of the cement manufacturing process, starting from the extraction of raw materials such as limestone and clay to the final production of cement, contributes to GHGs, primarily CO₂. Therefore, assessing emissions from each sub-process is necessary for an effective decarbonisation.
2. Decarbonisation efforts can be more targeted when the entire process is understood. For instance, reducing the clinker content in cement, which is a significant source of emissions, can be achieved by incorporating supplementary cementitious materials (SCMs). Knowledge of the manufacturing process allows for the optimisation of these materials at the blending stage, thereby reducing the carbon footprint.
3. Thorough understanding of the process helps identify inefficiencies and opportunities for innovation such as energy-efficiency measures and use of alternative fuels such as hydrogen and CCUS. These measures should be integrated into existing processes without compromising product quality.

The entire cement manufacturing process (irrespective of the type of cement) can be categorised into six main phases.

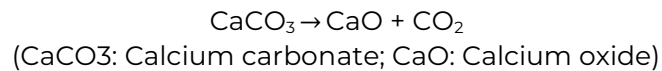
1. *Raw material extraction*: Limestone, the primary raw material for cement production, is typically sourced from a limestone mine in the proximity. Coal, which acts as the primary fuel to meet the thermal requirements of the cement plant, is also either sourced from coal mines in the country or imported.
2. *Raw material homogenisation*: The large rocks of the quarried limestone and other raw materials (clay, iron ore, bauxite, and sand) are crushed to products of sizes 25–75 mm (CII, 2021). These crushed materials are then transported to raw material blending and storage beds (stack and reclaimers) for homogenisation with the help of conveyor belts, railways, cableways, or trucks. Here, the desired raw mix of crushed materials and additional components as required is prepared using metering devices.

Before entering the pyroprocessing unit (pre-heater, pre-calciner, rotary kiln, and grate cooler), the raw materials are further powdered to approximately 90 microns with the help of grinding mills (usually ball mills or high-pressure roller grinders for limestone and vertical roller mills [VRMs] for coal). This helps in increasing the surface area of the raw meal (or the ground and homogenised raw material), facilitating more efficient chemical reactions. It also ensures homogeneity of the raw meal and helps improve energy efficiency.

3. *Pyroprocessing*: The resulting powdered material (raw meal) is directed to the pyroprocessing section, comprising of the following:
 - a. *Pre-heaters*: A string of cyclone separators (usually 5 or 6 stages in a large-scale cement plant) used as heat exchangers to transfer the heat from the

emerging hot exhaust gases from the kiln to the inflowing raw materials in a counter current manner (Figure 26). This process heats the raw meal to approximately 900 °C.

- b. Pre-calciner or pyro-clone: Approximately 90% of the calcination reaction occurs here.



Moreover, approximately 60% to 75% of the total thermal energy requirements (fuel injection) goes into meeting the heat requirements of the reactions happening in the pre-calciner. This reduces the load in the cement kiln. It also reduces sulphur oxides (SO_x) and nitrogen oxides (NO_x) emissions as incomplete combustion of the gases in the kiln are often completed in the pre-calciner.

- c. Rotary kiln: The remaining 10% of the calcination and the formation of alite (C₃S), belite (C₂S), and other compounds, such as tricalcium aluminate (C₃A) and tetracalcium aluminoferrite (C₄AF), occurs in the rotary kiln, ultimately producing clinker. During pre-calcination, the material undergoes heating at 900 °C, while clinker formation in the kiln involves heating the material at a temperature of 1,450 °C.
- d. Grate cooler: The hot clinker generated in the kiln is subsequently cooled to 150 °C in the grate cooler with the help of fans and blowers and stored in clinker silos.

The various reactions that occur in the pyroprocessing system are listed in Table 15 (GCCA, 2022; Krishnan et al., 2012).

Table 15: Various reactions occurring within the pyroprocessing system

Location	Reaction	Product	Significance	Temperature (°C)
Pre-calciner	$\text{CaCO}_3 \rightarrow \text{CaO} + \text{CO}_2$	CaO (lime), CO ₂	Calcination of limestone: Releases CO ₂ , producing reactive lime for further reactions.	900–1,000
	$\text{MgCO}_3 \rightarrow \text{MgO} + \text{CO}_2$	MgO, CO ₂	Calcination of magnesite (if present): Similar to limestone calcination.	900–1,000
Rotary kiln	$2\text{CaO} + \text{SiO}_2 \rightarrow$ $2\text{CaO}.\text{SiO}_2 \text{ (C}_2\text{S)}$	C ₂ S	Contributes to long- term strength development in cement.	1,200–1,450
	$3\text{CaO} + \text{SiO}_2 \rightarrow$ $3\text{CaO}.\text{SiO}_2 \text{ (C}_3\text{S)}$	C ₃ S	Primary clinker phase responsible for early strength gain in cement.	1,200–1,450
	$3\text{CaO} + \text{Al}_2\text{O}_3 \rightarrow$ $3\text{CaO}.\text{Al}_2\text{O}_3 \text{ (C}_3\text{A)}$	Tricalcium aluminate	Contributes to early hydration but can increase susceptibility to sulphate attack.	1,200–1,450
	$4\text{CaO} + \text{Al}_2\text{O}_3 + \text{Fe}_2\text{O}_3$ $\rightarrow 4\text{CaO}.\text{Al}_2\text{O}_3.\text{Fe}_2\text{O}_3$ $\text{(C}_4\text{AF)}$	Tetracalcium aluminoferrite (ferrite phase)	Acts as a flux, lowering the melting point and promoting the formation of other clinker phases.	1,200–1,450

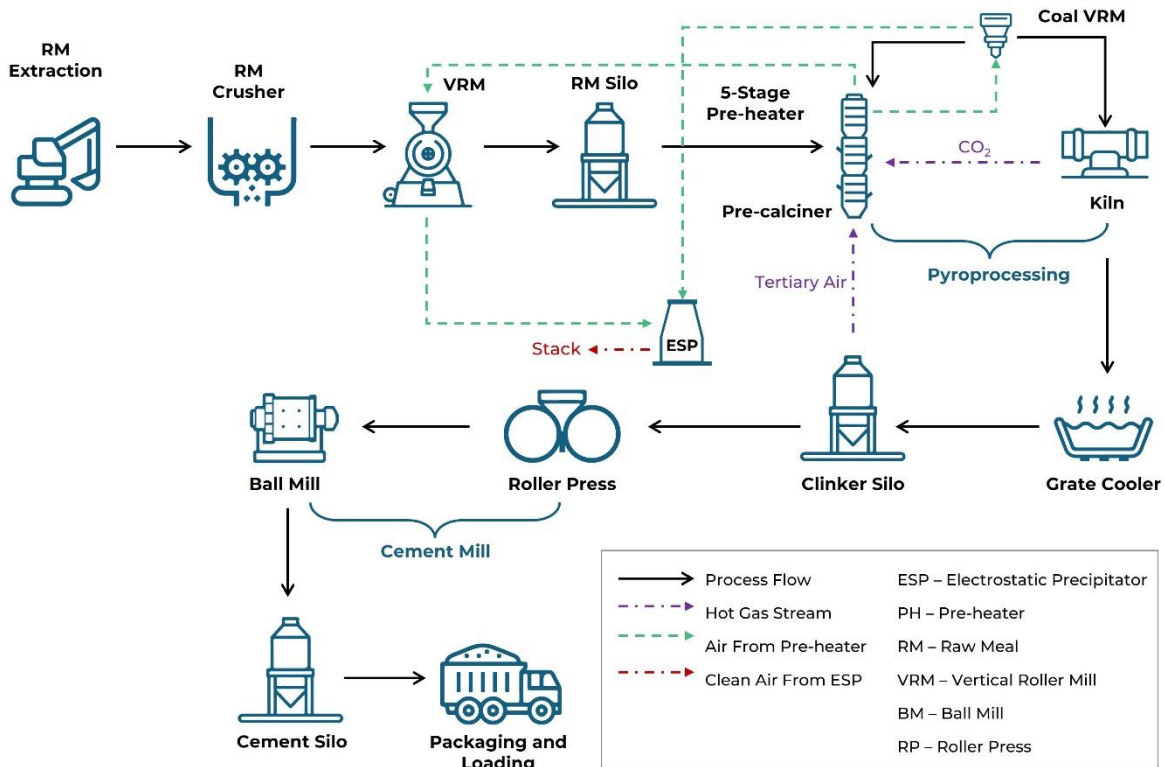
4. ***Cement manufacturing:*** The clinker that is stored in the clinker silos is then conveyed to the cement grinding units (usually vertical roller mills), where it is ground to fine powder and blended with different kinds of additives, such as gypsum, blast furnace slag, fly ash, and other materials, to create diversified cement grades and types such as Ordinary Portland cement (OPC), Portland Pozzolana cement (PPC), and Portland Slag cement (PSC).
5. ***Packaging and dispatch:*** The finished cement product is stored in cement silos, from where it is conveyed to a cement packaging plant. Here, the cement is packed in bags and dispatched through trucks.

Table 16 lists the different types of cements manufactured in India, as well as their energy requirements and emissions (GCCA, 2022; Nitturu et al., 2023).

Table 16: Types of cement and their properties

Cement type	Property	Clinker factor (CF)	Thermal specific energy consumption (SEC; kcal/kg clinker)	Electrical SEC (kWh/t cement)	Emission (kg CO ₂ /t cement)
OPC	<ul style="list-style-type: none"> * High early strength, suitable for fast-paced construction. * Most common cement type globally. * Susceptible to sulphate attack and chemical corrosion. 	0.9	724	87	740
PPC	<ul style="list-style-type: none"> * Low heat of hydration, beneficial for large concrete structures. * Improved durability and resistance against chemical attacks. * Low initial strength compared with OPC, but eventually achieves comparable strength. 	0.68	495	64	507
PSC	<ul style="list-style-type: none"> * Low heat of hydration, similar to PPC. * Exceptional resistance to chemical attack, particularly sulphate attack. * Slow strength gain compared with OPC, but reaches similar strength over time. 	0.55	305	59	312
Composite cement (CC)	<ul style="list-style-type: none"> * Combines advantageous properties of fly ash and slag. * Standardised in India in 2015. 	0.45	343	57	351

Figure 26: Cement plant layout



3.2. Energy requirements in a cement plant

The energy requirements in a cement plant can be categorised into thermal (heat) for the entire pyroprocessing system and electrical to run the crushing and grinding units, packaging plant, conveyor system, and auxiliaries that are required to run the pyroprocessing unit such as fans and motors and lighting.

3.2.1. Thermal energy requirement

The thermal energy requirements within a cement plant represents the largest share of energy consumed in the cement manufacturing process. This is primarily due to the energy-intensive nature of the pyroprocessing system, where the raw meal is heated to temperatures as high as 1,450 °C. The average thermal SEC in the Indian cement industry is 3.1 GJ/t clinker (741 kcal/kg clinker; Nitturu et al., 2023). This value is lower than the global average of 3.5 GJ/t clinker, indicating the advancements made in the Indian cement sector over the years to improve energy efficiency.

Within the pyroprocessing system, the calcination process is the most energy-intensive process as approximately 60% of the thermal energy is supplied to the calciner to achieve 90% calcination. This is followed by the kiln, where 40% of the thermal energy is supplied and rest of the clinkerisation reaction occurs.

Today, almost all of the thermal energy requirements in a cement plant is met by burning coal. Cement plants often use a combination of pet coke and imported coal from other countries to meet their thermal energy requirements. However, in efforts to decarbonise their fuel-based emissions, cement plants have increased the use of alternative fuel resources (AFRs) such as biomass, municipal solid waste (MSW), pharmaceutical sludge, paint sludge, car tyres, and other combustible materials to meet the thermal energy

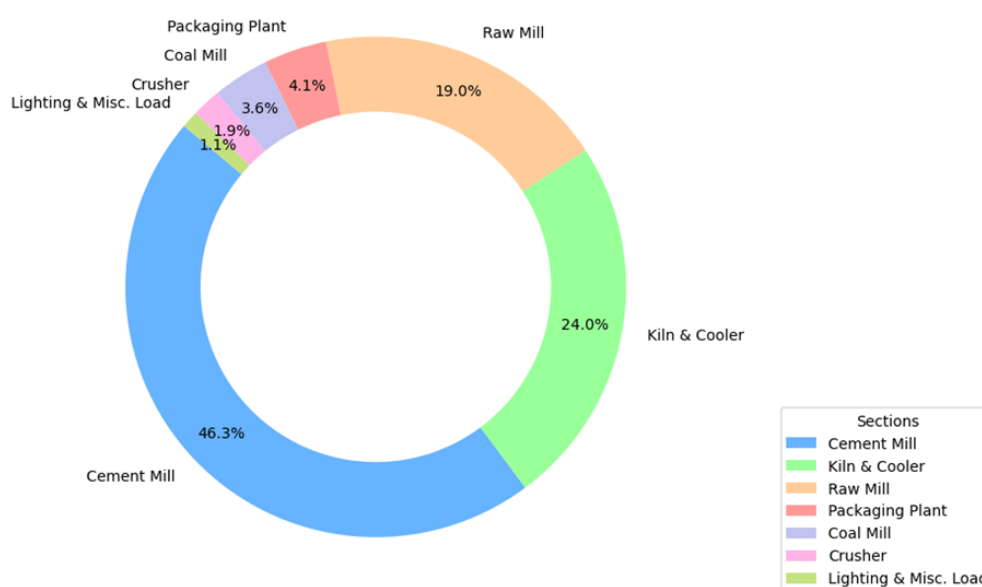
requirements. Cement plants in India have also gone far to achieve up to 35% thermal substitution rate (TSR; 35% of the fuel-need met with AFRs), with a TSR of up to 40% tested.

3.2.2. Electrical energy requirement

The average electrical SEC requirement for cement plants in India is 83.7 kWh/t cement, which is slightly lower than the global average of 91 kWh/t cement (Nitturu et al., 2023). However, some cement plants in India have SECs as low as 65 kWh/t cement (CII, 2021).

Cement grinding is the most energy-intensive sub-process, consuming approximately 27.6 to 45.7 kWh/t cement (GCCA, 2022). This can be attributed to the grinding of the already small clinker into fine cement, which requires significant comminution energy. The kiln and cooler operations follow, consuming approximately 24% of the energy usage. Moreover, the raw mill is responsible for 19% of the energy usage. Smaller contributions come from the packaging plant at 4.1%, lighting and miscellaneous loads at 3.6%, the coal mill at 1.9%, and the crusher at 1.1% (Figure 27).

Figure 27: Electrical SEC breakup



3.3. Need for decarbonising the Indian cement industry

Cement manufacturing is an energy- and emission-intensive process often requiring temperatures as high as 1,450 °C. In 2020–21, the average emission intensity of the Indian cement industry was 0.617 t CO₂/t cement, necessitating the need for decarbonising the cement manufacturing process (GCCA & Global CCS Institute, 2024). This would also help in balancing the increasing cement production in India with sustainable practices, thereby meeting climate goals.

Approximately, 56% of the emissions from the cement industry are mainly due to the decarbonisation of limestone (Nitturu et al., 2023). Moreover, the high temperature levels and other industrial heating requirements are often met by burning fossil fuels, especially pet coke and imported coal, contributing to 32% of the emissions (Nitturu et al., 2023).

The following sub-section discusses some of the decarbonisation measures for the cement industry.

3.4. AFRs and hydrogen

One of the decarbonisation options that most cement industries in India are looking at is the utilisation of AFRs. Industry giants such as Dalmia Bharat Limited claim to have achieved 17% TSR by substituting raw materials with industrial waste, renewable biomass, and hazardous and MSW (CRISIL, 2024). Although achieving 100% TSR in cement plants can abate up to 32% of their CO₂ emissions, including SO_x, NO_x, and other accompanied GHGs from coal combustion, 100% TSR is a utopian scenario. The challenges associated with the energy content of these AFRs (usually less than coal) and their composition (chlorine, moisture, and other impurities) can increase the thermal energy requirements of clinkerisation. As an industrial rule of thumb, for every 1% increase in TSR, the required energy content rises by approximately 2 to 3 kcal, setting a cap to achieving 100% TSR (Nitturu et al., 2023). Therefore, the Indian government has set a modest target of approximately 25% TSR by 2030.

Some of the most preferred AFRs and their calorific values are given below (Table 17).

Table 17: Calorific values of different AFRs

Fuel	GCV (kcal/kg)
Glycerine	4,624.8 (Bala-Litwiniak & Radomiak, 2019)
Meat and bone meal (MBM)	3,967.5 (Kantorek et al., 2021)
Hydrogen	33,910.1 (Engineering ToolBox, 2003)
Paint sludge	4,330 (Gautam et al., 2010)
MSW	2,993.0 (CSE, 2019)
Biomass	4,000.0 (Ministry of Power, 2021a),

Hydrogen holds significant promise as an AFR due to its unique advantages over other AFRs. Its combustion in cement kilns generates zero CO₂ emissions, positioning hydrogen as a key player in the industry's decarbonisation efforts. With India's ambitious plan to produce 5 million t of green hydrogen annually by 2030, the cement industry stands to benefit from increased availability and reduced costs (MNRE, 2023). Hydrogen also offers operational flexibility as it can be blended with other AFRs to create climate-neutral fuel mixes. Moreover, some trials have confirmed its feasibility in cement production without operational disruption (Perilli, 2022). Green hydrogen production near cement plants could enhance efficiency by providing both hydrogen and oxygen. While the hydrogen can be used as a clean fuel, the oxygen can be used to enhance the combustion process, which can improve clinker quality.

3.5. Other decarbonisation measures

In addition to AFRs and hydrogen, decarbonisation measures such as energy-efficiency improvements, WHR, clinker substitution, and CCUS can play a significant role in decarbonising the cement sector. These efforts along with other novel approaches such as calcium looping (CaL) and molten carbonate fuel cells (MCFCs) are discussed below.

3.5.1. Energy and feedstock efficiency improvements

While cement production is already a relatively efficient process, there are still opportunities for improvements across sub-processes such as raw meal grinding, pre-heating, calcination, clinkerisation, and grinding (Cavalett et al., 2024; Krishnan et al., 2012). Moreover, WHR can be used to convert heat losses from the plant into electricity, offsetting a significant portion of the plant's electricity demand. This is crucial as approximately 35% to 40% heat supplied to the plant is lost as waste heat (Fennell et al., 2021).

3.5.2. CF reduction

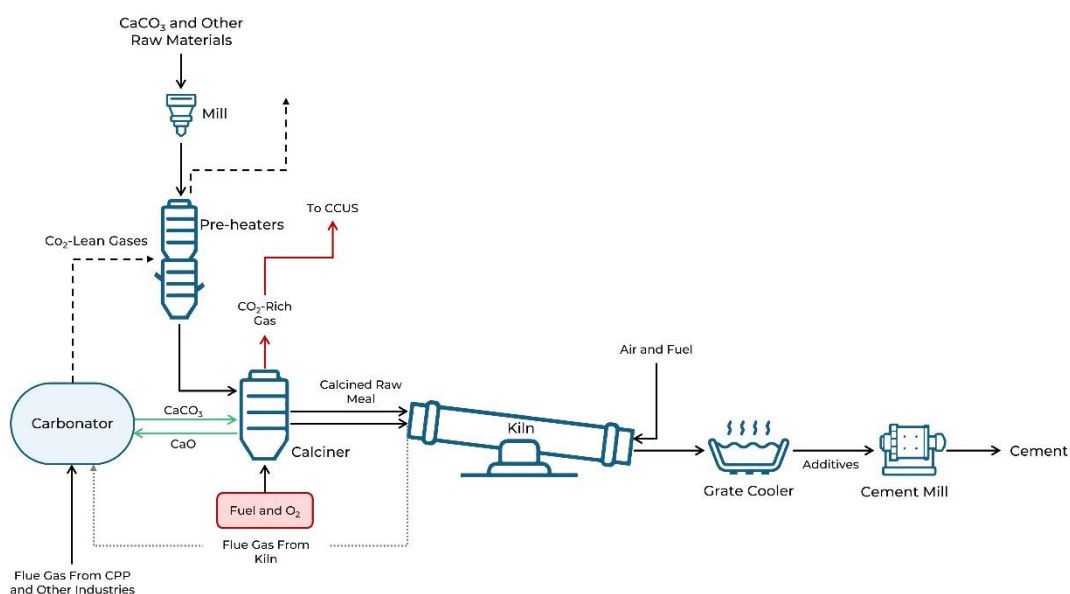
As mentioned previously, CF reduction can be achieved by increasing the use of SCMs such as fly ash, slag, silica fume, and calcined clay (Nitturu et al., 2023). Developing low-carbon cements such as blended cements and novel binders also contribute to reducing clinker reliance.

3.5.3. Carbon management

CCUS technologies: These are essential for addressing both process and energy emissions. CCS involves capturing CO₂ emissions and storing them underground or utilising them in other industrial processes (Cavalett et al., 2024). CCU, on the other hand, focuses on converting captured CO₂ into valuable products such as methanol (Barbhuiya et al., 2024; Rumayor et al., 2022).

CaL: This is a promising technology for decarbonising cement plants. This cyclic process involves the capturing of CO₂ from the cement flue gas by reacting it with CaO to produce CaCO₃. Subsequently, CaCO₃ is decomposed back into CaO at higher temperatures, releasing a concentrated stream of CO₂ for capture and storage (De Silvestri et al., 2021). CaL in cement plants typically involves two interconnected fluidised bed reactors, a carbonator and a calciner. The entire process is depicted in Figure 28.

Figure 28: CaL in the cement industry



Unlike CCUS, the biggest advantage of CaL is that it can be easily integrated into the clinker manufacturing process. Moreover, the sorbent used (CaO) is derived from

limestone, which is an important raw material for clinker manufacturing. In addition to this, the flue gas from the captive power plant (CPP) inside the cement plant can be sent to the carbonator, increasing the emission removal potential.

MFCs: These offer a dual benefit: capturing and concentrating CO₂ while generating electricity. This technology utilises the CO₂-rich flue gas from the calciner at the cathode, while the anode is fuelled by hydrogen/natural gas. MFCs can be integrated with CaL systems for enhanced decarbonisation (Nhuchhen et al., 2022; Spinelli et al., 2014).

Afforestation: Planting trees is another measure for offsetting remaining emissions (Nitturu et al., 2023).

3.5.4. Other technologies

Electrification technology for cement manufacturing

The RotoDynamic Heater (RDH) is the only electrical heating technology that can reach 1,700 °C without burning fossil fuels. This technology developed by Coolbrook can replace fossil-fuel-fired furnaces and kilns with electrical heating (Coolbrook, n.d.). The RDH uses a multistep process to rapidly accelerate and decelerate the gases to heat them. This works exactly the opposite of how hot gases are used to turn a turbine for generating electricity. The electric motors are used to rotate the shaft, where the mechanical energy is converted to heat (Coolbrook, 2023). Gases such as air and nitrogen are heated inside the RDH and used outside to replace the burning of fossil fuels (Coolbrook, 2023).

The RDH finds multiple use cases in the cement industry, especially to meet heating requirements. For example, raw material drying in a dryer–crusher, drying in a raw mill, replacing fuels in pyroprocessing, and drying of AFRs (Coolbrook, n.d.). Industry giants such as UltraTech Cement Limited and JSW group are planning to explore the uses of Coolbrook’s RDH technology (Cemnet, 2023; Coolbrook, 2024), with UltraTech intending to use it for drying AFRs. Based on the learnings, the company will scale-up the technology adaptation.

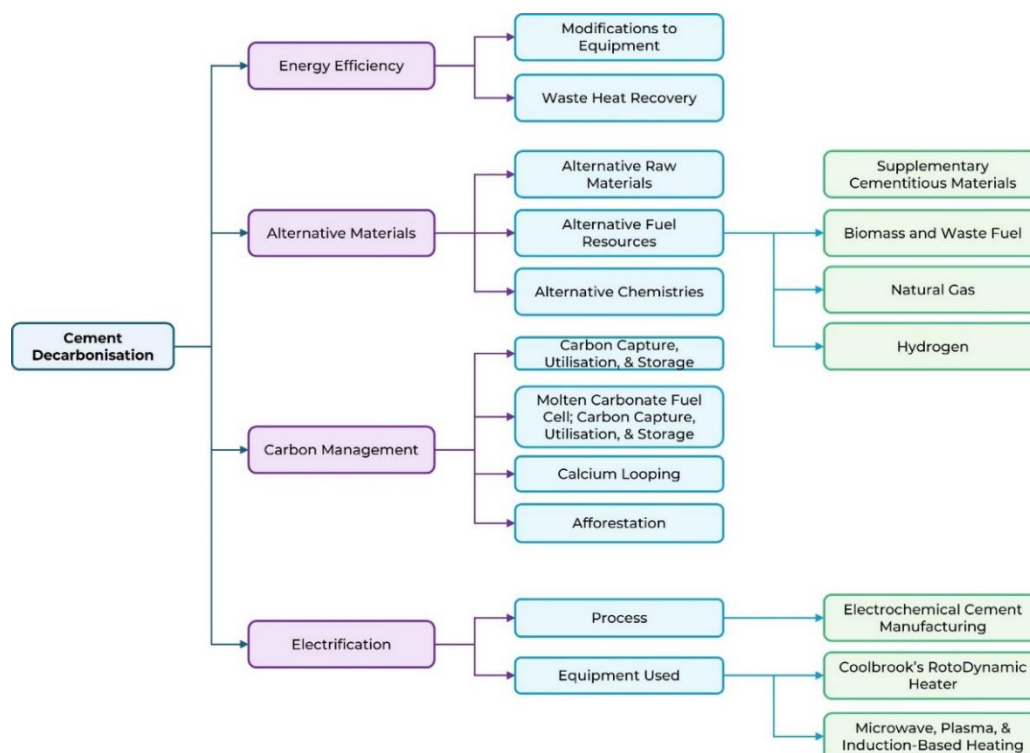
Some of the other electrification technologies that are being developed across the world are tabulated in the Appendix section (Table A 1).

Electrochemical technology for cement manufacturing

This emerging technology utilises an electrolysis process to decarbonate CaCO₃ and precipitate Ca(OH)₂, which can then react with SiO₂ to form cement (Ellis et al., 2020). Key advantage is the production of concentrated gas streams (H₂ and O₂ + CO₂) suitable for capture, utilisation, or power generation.

The figure below (Figure 29) summarises different decarbonisation measures in the cement industry.

Figure 29: Decarbonisation measures in the cement industry



The various decarbonisation measures and their emission reduction potential are tabulated in Table 18.

Table 18: Emission reduction potential of different decarbonisation measures

Decarbonisation measure	Emission reduction potential
Energy efficiency and WHR	9% (Nitturu et al., 2023)
CF reduction	11% (Nitturu et al., 2023)
Renewable energy and AFR (after applying energy efficiency and WHR measures)	13% (Nitturu et al., 2023)
CCUS	Up to 50%
100% TSR using AFRs	32%
CaL	90% (Ferrario et al., 2023)
MCFC	Concentrates CO ₂ from cement exit gases

3.6. Challenges to decarbonising the cement industry

While multiple decarbonisation solutions are being developed, the path to decarbonising cement plants is complex and multifaceted, requiring coordinated efforts across technology development, economic investment, and operational adjustments.

Here are some challenges to implementing decarbonisation measures in the cement industry.

3.6.1. Technical challenges

WHR: Installing WHR systems, particularly in old plants, can be challenging due to layout constraints and the need for significant retrofits (Ige et al., 2024; WBCSD, 2018). Moreover, the efficiency of WHR depends on factors such as plant utilisation rate.

AFRs: Some of the challenges in using AFRs are the following:

- **Fuel properties and pre-treatment:** AFRs often have different physical and chemical properties compared with conventional fuels. These differences, such as low calorific value, high moisture content, or high chlorine concentrations, often require pre-treatment to ensure optimal combustion. This pre-treatment adds complexity and cost to the process.
- **Kiln performance:** Introducing AFRs can negatively impact kiln production and SEC. Understanding the long-term effects of these fuels on cement performance requires further research and development (R&D).
- **Capacity limitations:** Some technologies such as roller presses for grinding have capacity limitations, while others such as advanced multi-channel burners involve high retrofitting costs and long payback periods.

Clinker substitution: Decarbonisation with clinker substitution also has challenges, which are discussed below.

- **Availability of SCMs:** Increasing the use of SCMs such as fly ash and slag to reduce clinker content remains challenging due to the declining availability of these materials. This is because more industries are decarbonising and generating fewer by-products.
- **Performance and standards:** Finding widely available clinker replacements (e.g. clinker clay) that meet performance standards is crucial. Moreover, the Bureau of Indian Standards (BIS) is yet to approve the production of a low-carbon alternative LC³ cement (limestone clay cement; 50% clinker, 30% clay, 15% limestone, and 5% gypsum), hindering its adoption (WBCSD, 2018).

CCUS: The following are some of the challenges of this technology:

- **Technical complexity and costs:** Implementing CCS technologies in cement plants presents significant technical challenges and high costs. These include the cost of capturing CO₂, transporting it to suitable storage sites, and ensuring the long-term integrity of those sites.
- **Energy penalty:** CCS technologies, particularly first-generation solutions, can increase energy consumption due to the energy required for CO₂ capture and compression.
- **Storage site availability and safety:** Identifying suitable geological formations for CO₂ storage, ensuring their long-term safety, and addressing potential leakage risks are crucial aspects of CCS implementation.

Electrochemical technology for cement manufacturing

- **Scaling challenges:** This emerging technology requires significant R&D to overcome scaling challenges and achieve commercially viable production rates.
- **Energy requirements:** While promising, electrochemical methods may have high energy demands, particularly for the electrolysis process. Ensuring access to low-cost, low-carbon electricity will be crucial for the sustainability of this approach.

3.6.2. *Economic challenges*

High investment costs: Many decarbonisation technologies require substantial upfront investments in new equipment, infrastructure modifications, and R&D. This is particularly challenging for old plants that might require extensive retrofits.

Operational costs: Implementing and maintaining these technologies can lead to increased operational costs, including energy consumption, maintenance, and workforce training.

Uncertain payback periods: The financial viability of these investments depends on uncertain payback periods, influenced by factors such as fluctuating energy prices, carbon pricing mechanisms, and market demand for low-carbon cement.

Financing constraints: Access to capital for these projects can be limited, especially for small and medium-sized enterprises. This is because traditional financiers are unfamiliar with sustainable construction practices and the perceived risks associated with new technologies.

3.6.3. *Policy and regulatory challenges*

Lack of supportive policies: The absence of clear and consistent policy frameworks that incentivise decarbonisation in the cement industry is a major barrier. This includes the lack of robust carbon pricing mechanisms, financial incentives such as tax breaks or subsidies, and clear regulatory standards for low-carbon cement production.

Inconsistent regulations: Inconsistent legislative requirements across regions regarding waste management, emissions standards, and AFR-use create uncertainty and hinder investment in decarbonisation technologies.

Social acceptance: Gaining public acceptance for technologies such as CCS and AFR-use can be challenging. CCS faces social acceptance challenges due to safety concerns over potential CO₂ leaks from pipelines or storage sites. Similarly, AFR-use can release toxic fumes, such as dioxins and heavy metals, during combustion, raising concerns about air quality and public health in nearby areas.

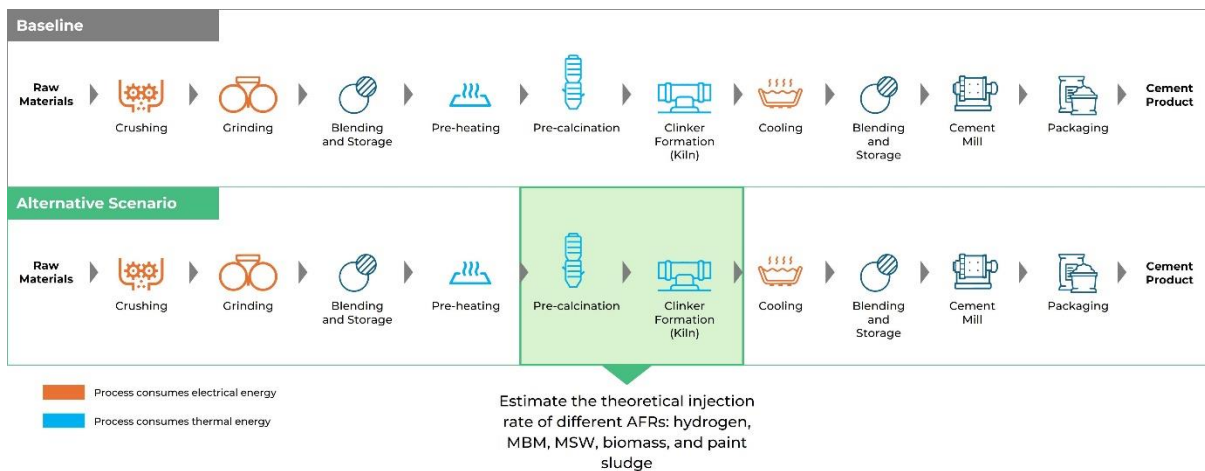
The detailed methodology followed for assessing the utilisation of hydrogen as an alternative fuel in the cement industry is discussed in the following sections.

3.7. **Process methodology**

Unlike in the steel sector, hydrogen cannot directly play the role of a reactant in the cement sector. However, it can play a critical role as a transitional fuel to pave way for electrification. To explore the utilisation of hydrogen as an AFR in cement manufacturing in India, we developed a **mass-and-energy-balance-based perturbation model** to provide a theoretical estimate of the amount of hydrogen that can be used.

Through literature study and data collection, we established a baseline value chain that represents cement manufacturing in India. The major unit operations and their energy consumption (thermal/electrical) are shown below (Figure 30).

Figure 30: Baseline value chain



As approximately 88% of the total emissions (56% from calcination and 32% from fuel combustion) in cement manufacturing comes from the pyroprocessing unit, the perturbation model was developed on basis of the cement plant’s pyroprocessing operation. The thermal SEC, which is confined to the heat requirements of the pyroprocessing system, was calculated and used to estimate the amount of hydrogen and other AFRs such as MBM, MSW, paint sludge, and biomass.

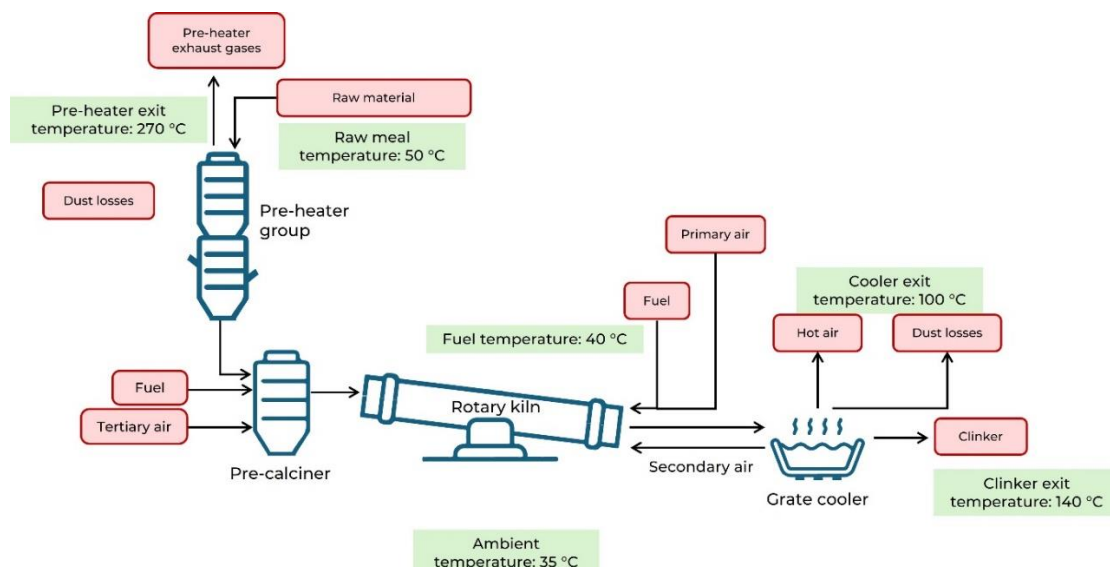
3.7.1. Perturbation model

To estimate the thermal SEC requirements of the cement plant, the mass and energy were balanced across the pyroprocessing unit. The detailed methodology and the key considerations to develop the model are listed below.

3.7.2. Key considerations

- Mass and energy balance was performed for **1 kg clinker**.
- Entire pyroprocessing operations was considered as a single system, with the boundary depicted in Figure 31.

Figure 31: System boundary of the pyroprocessing unit



- **Steady-state operation** was assumed throughout the process, with no accumulation of masses (mass in = mass out).
- Assumptions regarding the composition of the inlet ore, coal, and raw meal are based on discussions with industry experts and literature review (Figure 32 and Figure 33; Deolalkar, 2008).

Figure 32: Ore composition

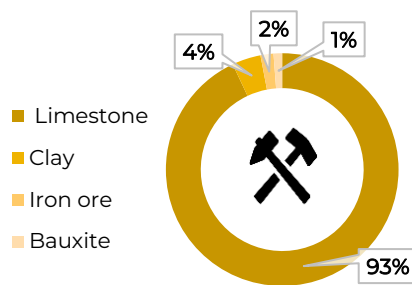


Figure 33: Raw meal composition

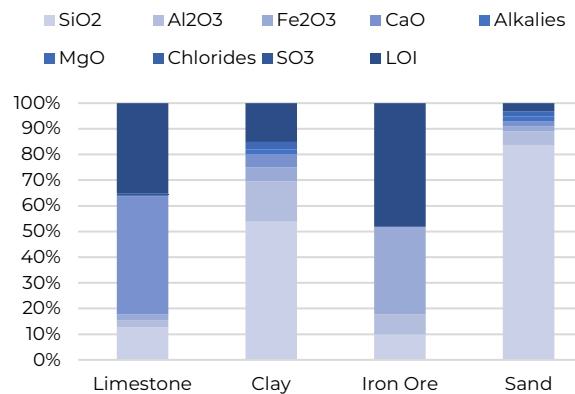
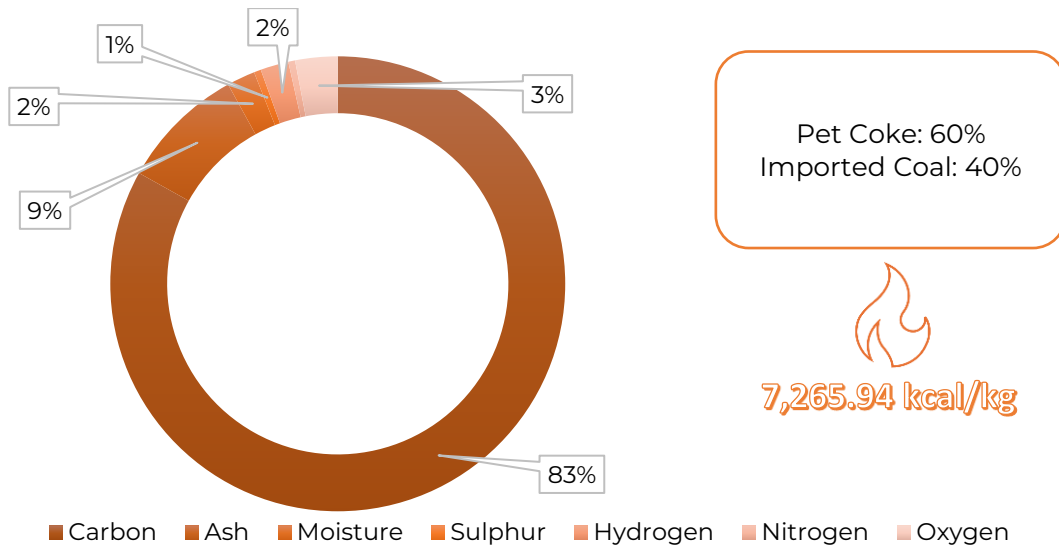


Figure 34: Coal composition



- Dulong formula was used to compute the GCV of coal by considering the coal compositions given in Figure 34 (CFD Flow Engineering, 2024).

$$GCV = (1/100) [8080C + 34500(H - O/8) + 2240S] \text{ kcal/kg}$$

- For computing dust losses, **cyclone pre-heater system efficiency** was assumed to be **94%**.
- Mass balance, based on the steady-state assumption, was used to compute the mass of different streams entering and leaving the system boundary.

- **Excess air** was assumed to be **5%**, and **10% of the cooling air** was assumed to be diverted into the kiln as **secondary air**. Moreover, infiltration air was assumed to be zero as even a tiny fraction of air ingress can tamper the optimality of the ongoing reactions.
- Raw-meal-to-clinker ratio, based on which the entire mass balance is achieved, was computed considering the loss on ignition value of the ore mix as suggested in the literature (Deolalkar, S., 2008).
- Compositions of the clinker stream's major constituents, namely C₃S, C₂S, C₃A, and C₄AF, were calculated using the constituents' mass percentages; the Bogue formula was used for the calculation (Table 19; Peray, 1979).

Table 19: Bogue formula

Constituent	Formula (A/F* > 0.64)	Formula (A/F ≤ 0.64)
C ₃ S	4.071CaO - (7.602SiO ₂ + 6.718Al ₂ O ₃ + 1.43Fe ₂ O ₃ + 2.852SO ₃)	4.071CaO - (7.602SiO ₂ + 4.479Al ₂ O ₃ + 2.859Fe ₂ O ₃ + 2.852SO ₃)
C ₂ S	2.867SiO ₂ - 0.7544C ₃ S	2.867SiO ₂ - 0.7544C ₃ S
C ₃ A	2.65Al ₂ O ₃ - 1.692Fe ₂ O ₃	0
C ₄ AF	3.043Fe ₂ O ₃	-
C ₄ AF + C ₂ F	-	2.1Al ₂ O ₃ + 1.702Fe ₂ O ₃

* Where A/F is the alumina-to-iron ratio (Peray, 1979)

- Constituents of the pre-heater exit gases, namely CO₂ (assuming only trace amount of CO is formed due to incomplete combustion), N₂, H₂O, SO₂, and O₂ (due to excess air), were calculated using mass ratios as suggested in the literature (Peray, 1979).
- Results from the mass balance were wetted using the cement quality control formulas (Table 20), which are based on the mass percentage of the cementitious compounds in the product stream as given in the literature (Peray, 1979). If the lime saturation factor (LSF) exceeds 0.97, it means that the clinker is over limed, leading to increased free lime, hydration issues, and reduced cement strength. It complicates the burning process, raising energy consumption and quality control challenges. Moreover, it can result in undesirable mineral phases, compromising cement performance and operational efficiency.

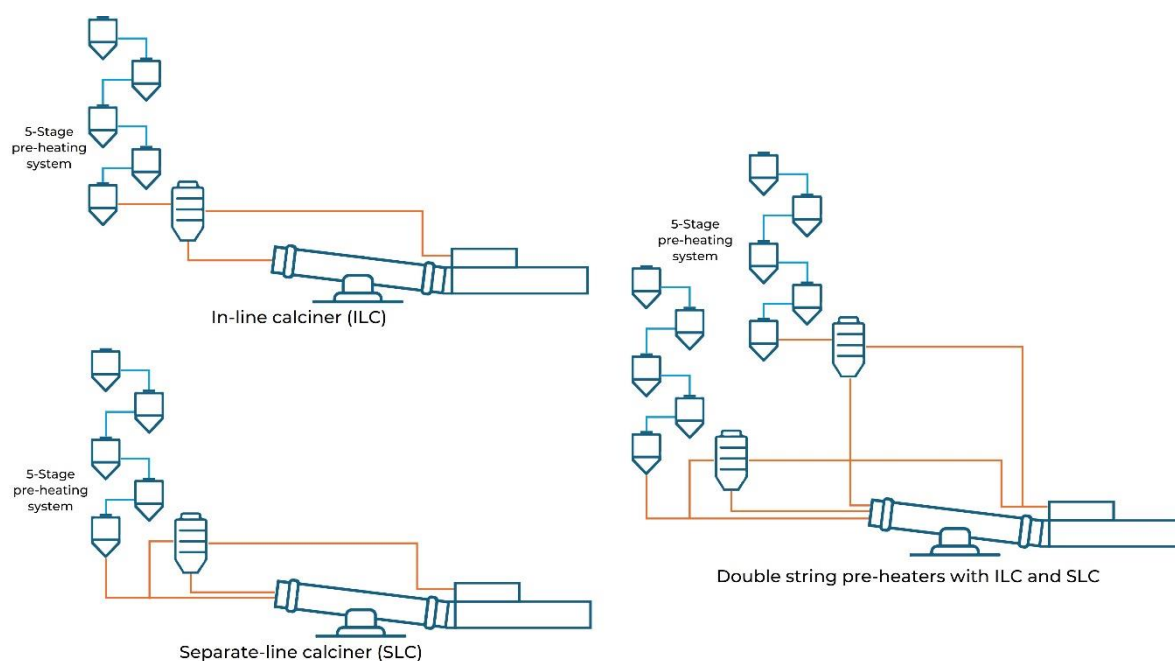
Table 20: Cement quality control formula

Quality control parameter	Formula
Silica ratio (SR)	SiO ₂ /(Al ₂ O ₃ + Fe ₂ O ₃)
A/F	Al ₂ O ₃ /Fe ₂ O ₃
LSF (A/F > 0.64)	CaO/(2.8SiO ₂ + 1.65Al ₂ O ₃ + 0.35Fe ₂ O ₃)
LSF (A/F ≤ 0.64)	CaO/(2.8SiO ₂ + 1.1Al ₂ O ₃ + 0.7Fe ₂ O ₃)

3.7.3. Thermal SEC

Subsequently, the mass flows of the compounds were used to calculate the theoretical reaction heat required for clinker formation based on the empirical relation given in the literature (Peray, 1979). The burning efficiency of cement plants are often very low, typically approximately 54% (Moses, 2023). Therefore, the actual thermal SEC of the plant can be up to two times higher than the calculated number. The thermal efficiency of a cement plant is dependent on several factors such as the plant capacity, fuel type, and number of pre-heater stages (usually 5 or 6). It also depends upon whether the calciner set-up is used in-line (along with the pre-heater chain) or as a separate line and whether a single or double pre-heater string set-up is used (Figure 35).

Figure 35: Pre-heater configurations



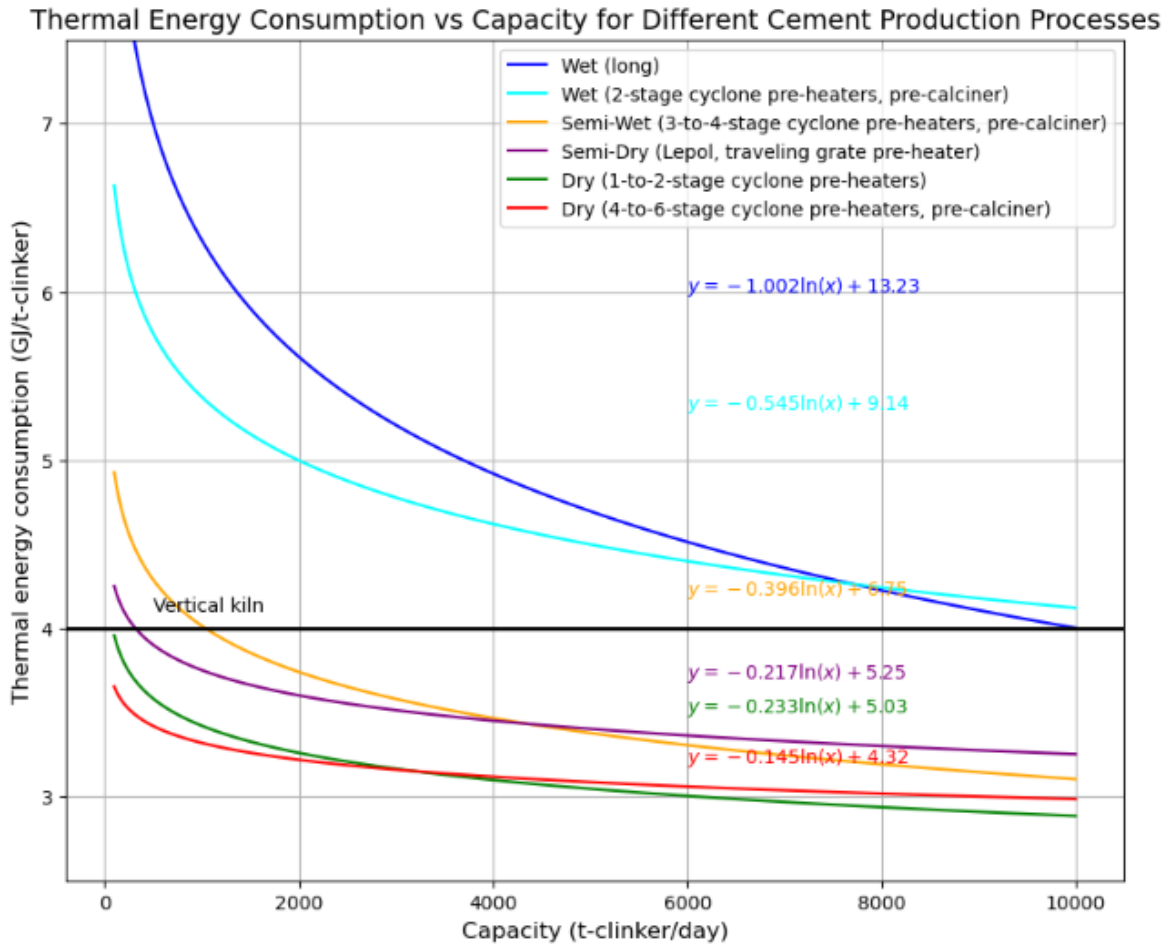
Although the actual thermal SEC is dependent on several factors, a study estimated the thermal SEC of a cement plant on the basis of its production capacity (Oda et al., 2012). This study adapted this estimation method of thermal SEC by considering both plant capacity and the type of cement manufacturing process (wet, semi-wet, semi-dry, and dry).

As most of the cement plants in India have shifted to the rotary kiln dry process with 4 to 6 stages of pre-heating and a pre-calciner, we used the corresponding relation by J. Oda et al. (2012) to estimate the thermal SEC and, thereby, calculate the energy balance (Figure 36). Further, **100% calcination** with no bypass losses was assumed for the calculation. Energy balance was computed using the following steady-state energy balance equation:

$$\text{Energy}_{in} = \text{Energy}_{out} + \text{Energy}_{consumed} + \text{Energy}_{lost}$$

Specific heat and latent heat to calculate the heat content of the different input and output streams were computed using empirical formulas and relations given in the literature (Ali Khalifa, 2019; Peray, 1979).

Figure 36: Plant capacity vs thermal SEC



3.7.4. Electrical SEC

Calculating the exact electrical energy consumption in cement plants is complex as the mill type, number of auxiliary equipment such as fans and motors, and conveying systems vary among these plants. Most of the electrical energy requirements in a cement plant comes from particle attrition. While theoretical calculations can provide estimates, the actual energy consumption may vary significantly due to real-world conditions and operational factors.

Bond's law for calculating energy attrition

The theoretical energy input required to achieve particle size reduction is calculated using the Bond's equation (McCabe et al., 1993).

$$E = 0.3162 * W_i * \left(\frac{1}{\sqrt{P}} - \frac{1}{\sqrt{F}} \right),$$

where

- E is the specific energy input in kWh/t (kilowatt-hours per metric tonne)
- W_i is the Bond Work Index, a measure of the resistance of the material-to-size reduction in kWh/t
- P is the product size (80% passing) in μm (microns)
- F is the feed size (80% passing) in μm

The Bond Work Index for the materials involved in the cement attrition operations is given below (Figure 37). For coal, the Hardgrove Grindability Index (assumed to be 65) is used for computing the work index as it provides a more accurate estimate (Hungary et al., 2019; Sahu, 2013).

Figure 37: Work indices of different materials (kWh/t)



The feed and product size specifications that were assumed for each attrition operation are provided in Table 21.

Table 21: Particle input and output sizes for various attrition equipment

Particle size assumed	Inlet (mm)	Outlet (mm)	Equipment
Limestone	1,500	50	Crusher
Cement raw material	250	0.09	Raw mill
Coal	100	0.09	Coal mill
Cement clinker	0.09	0.01	Cement mill

The theoretical energy requirement for the crusher and grinder drives was determined. This value was then added to the SEC of auxiliary equipment (motors, filter bags, fans, etc.), which is an average of data from 10 different plants. This SEC data accounts for both 5-stage and 6-stage pre-heater configurations, as provided in the Confederation of Indian Industry’s (CII’s) benchmarking data (CII, 2019). After obtaining the total SEC for each attrition operation (raw mill, coal mill, and cement mill), the energy consumption from other electrical processes, such as packaging and pyroprocessing, was included. By combining these energy contributions, the final electrical SEC for both 5-stage and 6-stage pre-heater configurations was arrived at.

3.7.5. AFR injection

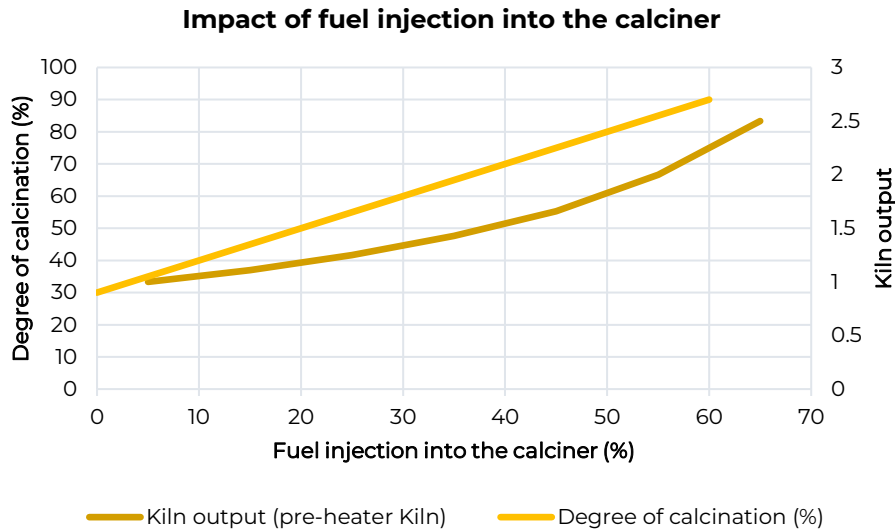
In modern cement plants, majority of the fuel is injected into the pre-calciner, where 90% of the calcination takes place. In fact, the degree of calcination in the pre-calciner is a function of the percentage of fuel injected. Injecting a large quantum of fuel into the pre-calciner also offers the following benefits:

- **Improved thermal efficiency** due to better heat transfer (Verma, K., et al., 2020).
- **Extended refractory lifetime** as the thermal load on the rotary kiln decreases (Agico Cement, 2024).

- **Improved fuel combustion** resulting in emission reduction (reduction in SO_x, NO_x, as well as complete combustion of C to produce CO₂; Agico Cement, 2024).
- **Increased kiln capacity** (Deolalkar, S., 2008).

The impact of the fuel injection rate on the calcination degree and kiln capacity is illustrated below (Figure 38).

Figure 38: Degree of calcination vs fuel injection rate



One of the biggest advantages of the pre-calciner is that it can handle various kinds of fuels, including solid-, liquid-, and gas-based fuel, paving way to the utilisation of AFRs such as biomass, waste, and hydrogen. AFR injection in the calciner can allow up to 60% thermal substitution with climate-neutral fuels and minimal retrofits.

Although CSTEP’s perturbation model treats the cement pyroprocessing section as a single unit, it utilises the basic estimation where 60% of the thermal SEC requirements (fuel injection) are met in the pre-calciner and 40% in the kiln. This is for determining the quantity of AFR, particularly hydrogen, which can be introduced into the cement manufacturing process.

While estimating the theoretical injection rates of each fuel, their physical phase and combustion properties, such as heat transfer rate, burnability, and flame speed, were considered to compute the amount of fuel that can be injected into the calciner and kiln. The assumed system and fuel combustion efficiencies of the calciner and kiln are listed in Table 22.

Table 22: Pyroprocessing system assumptions

Assumption parameter	Calciner	Kiln
Fuel combustion efficiency	90%	80%
System efficiency	90%	85%

In addition to these assumptions, a safety factor of 1.1 was considered to arrive at the final fuel injection rate.

3.7.6. *Scaling up cement manufacturing*

While CSTEP's perturbation model computes material and energy requirements for 1 kg of clinker, the results can be scaled up to provide the material and energy requirements, as well as the emissions, of a large-scale cement plant.

3.7.7. *Scaling-up assumptions*

Scaling up the energy and material requirements from that for 1 kg of clinker to that for a 4,500-tonnes per day (TPD) plant is inherently complex due to the many variables involved. While direct scaling might not yield perfectly accurate results, it can still provide reasonably accurate estimates if the correct capacity utilisation factor (CUF) of the plant is considered. The accuracy of this scaling largely depends on how well the CUF reflects the specific configurations of the plant, specifically the pre-heater system used and its configuration. The assumptions for scaling are listed in Table 23.

Table 23: Scaled-up plant assumptions

Basis	Plant capacity of 4,500 TPD
CUF (ratio of operated capacity and designed capacity)	Function of the pre-heater configuration (no. of stages, type of calciner [ILC/SLC], and no. of pre-heater strings)
Cement type	70% OPC, 25% PPC, and 5% PSC

Modifying the pre-heater configurations, such as increasing the number of stages in the pre-heater from a 4-stage to a 5-stage or 6-stage configuration, can significantly enhance the CUF. The additional stages improve the efficiency of heat exchange between the hot gases and raw meal, leading to higher pre-heating temperatures. This in turn boosts thermal efficiency and reduces fuel consumption in the rotary kiln. Moreover, it allows a larger portion of the raw meal to be calcined in the pre-heater and pre-calciner set-up, easing the load on the kiln and enabling it to handle higher throughput without compromising clinker quality. With more calcination occurring in the pre-heater, the raw meal spends less time in the rotary kiln, thereby increasing kiln's processing capacity and overall production.

Derived from the CII benchmarking data, the typical CUFs of cement plants based on the number stages and configuration are listed in Table 24 (CII, 2019). While the actual plant CUF is an operational parameter, these figures can be used to provide a first-order estimate.

Table 24: Pre-heater configuration and plant CUF

Pre-heater stage	Pre-heater string	System type	CUF (%)
5-Stage	Single	ILC	114
5-Stage	Double	ILC	130
5-Stage	Single	SLC	100
6-Stage	Single	ILC	112
6-Stage	Double	ILC	102
6-Stage	Double	SLC	105
6-Stage	Double	Pyroclone	119

By calculating the CUF based on these configurations, a more reliable prediction of the plant's material and energy requirement at larger scales were arrived at.

Based on the above configuration vs CUF data, two extreme cases, the lowest CUF and the highest CUF, were modelled.

- **Case 1:** 4,500-TPD plant comprising of single string and a 5-stage pre-heater system with an SLC of 100% CUF.
- **Case 2:** 4,500-TPD plant comprising of double string and a 5-stage pre-heater system with an ILC of 130% CUF.

3.8. Results and discussion

In this study, the mass-and-energy-balance-based perturbation model was used to describe and analyse the pyroprocessing system to arrive at the thermal energy requirements for producing 1 kg of clinker. The results were then utilised to determine the thermal energy requirements of a 4,500-TPD plant. The impact of replacing the conventional fuel mix (imported coal and pet coke) with AFRs such as MBM, MSW, paint sludge, biomass, glycerine, and hydrogen was also analysed for 1 kg of clinker. The amount of hydrogen that can be injected into the calciner, the challenges that could be encountered, the modifications that may be required to the burners, and corresponding emissions were calculated to assess the impact of this substitution on CO₂ emissions profile of the scaled-up plant.

3.8.1. Mass and energy balance

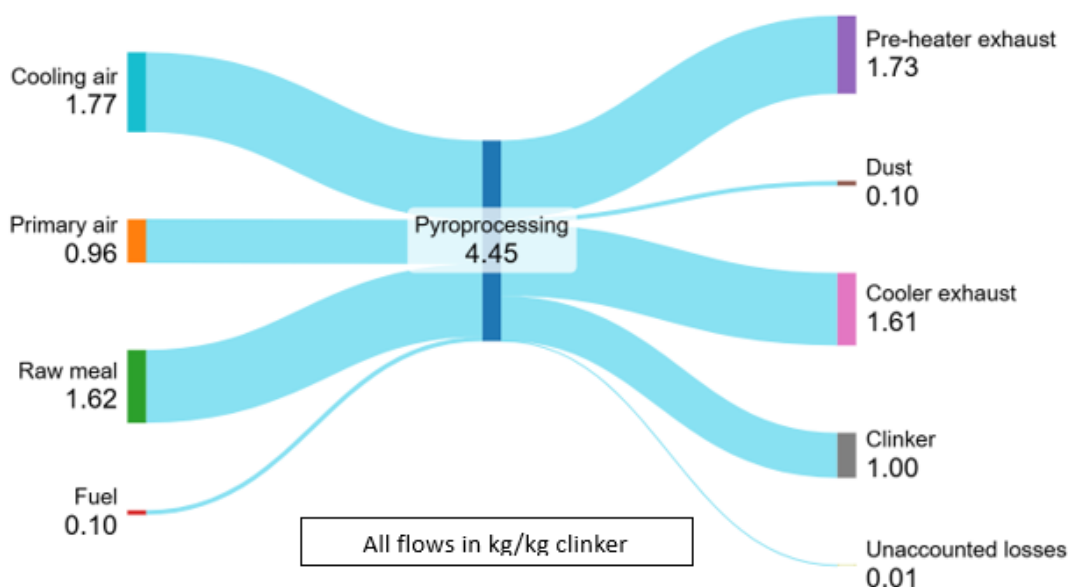
Table 25 lists the quantities required to produce 1 kg of clinker, which were arrived at by considering the assumed composition of raw materials (Section 3.7.2).

Table 25: Materials for producing 1 kg of clinker

Limestone	1.51 kg
Iron ore	0.03 kg
Sand	0.02 kg
Clay	0.06 kg
Coal	0.10 kcal

Based on the above raw material requirement and the different mass flows in and out of the system, the steady-state mass balance was established and the same is illustrated below (Figure 39).

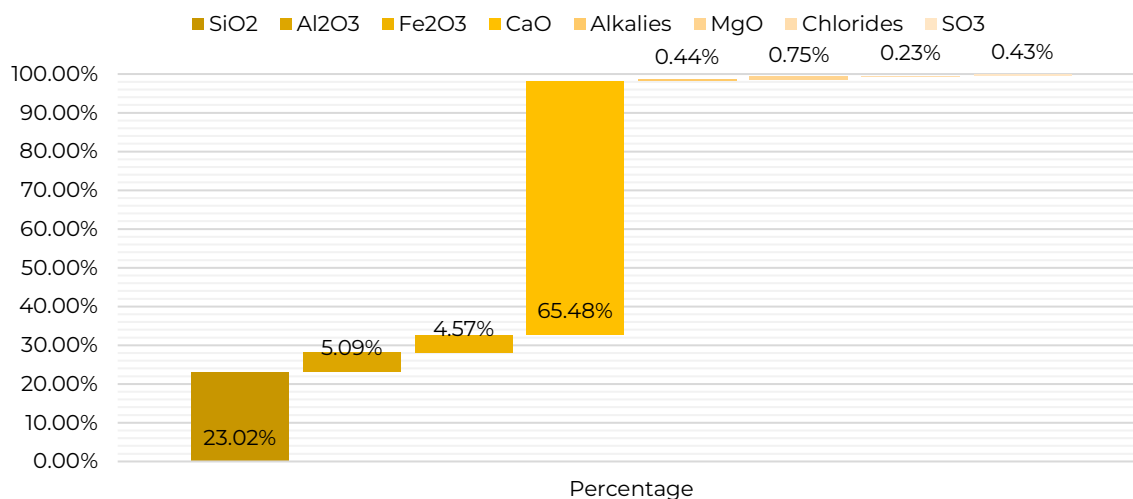
Figure 39: Mass balance for 1 kg of clinker



The air that is required for fuel combustion and cooling of the feed forms a major fraction of the mass flow. Moreover, due to the pre-heater system inefficiency (as discussed in Section 3.7.2), approximately 6% of the raw meal that is introduced into the pyroprocessing system is lost as dust.

The composition of the clinker in the exit streams is shown in Figure 40.

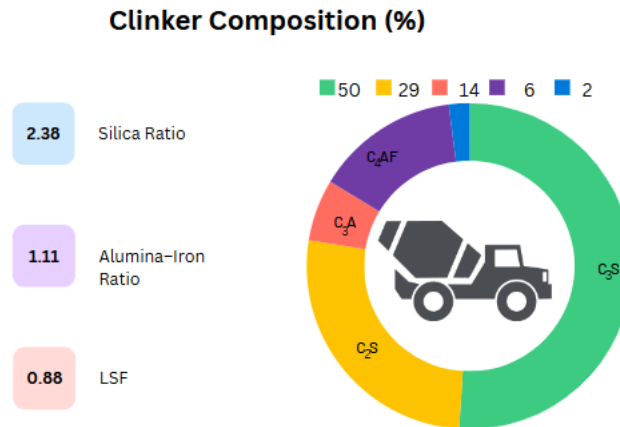
Figure 40: Clinker composition



CaO forms the major component of clinker, constituting approximately 65.48% of the clinker. It provides the primary source of calcium, which combines with silica, alumina, and iron oxide during the kiln process to form the main compounds in cement. These compounds, particularly C₃S, give cement its strength and durability, making lime essential for quality cement production. In addition to this, SiO₂ and Al₂O₃ play a crucial role in the formation of the major clinker compounds (C₃S, C₂S, C₃A, and C₄AF). Fe₂O₃ acts as the flux that lowers the temperature of clinker formation to a desirable phase (Herath Banda & Glasser, 1978).

Based on the above clinker composition, the quality control formulas, namely, silica ratio, A/F ratio, and the LSF were computed (Figure 41).

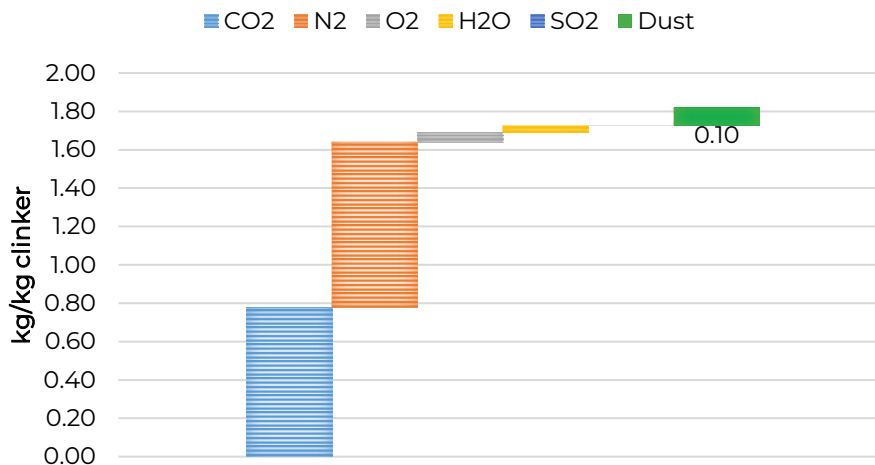
Figure 41: Clinker composition in terms of C_2S , C_3S , C_3A , and C_4AF



It was observed that the LSF was well below the 0.97 mark, and the silica ratio was between 2 and 3, indicating an acceptable clinker composition.

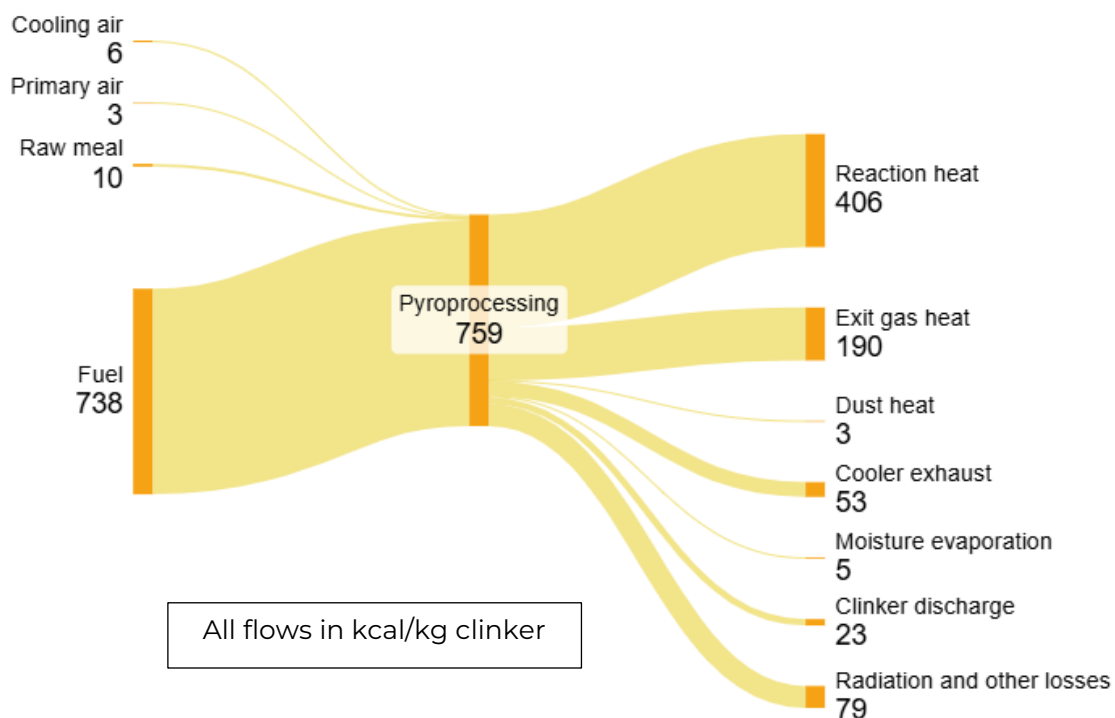
The pre-heater exhaust primarily contains gases such as CO_2 , H_2O , N_2 , SO_2 , unreacted O_2 , and NO_x . This study assumed that only trace amounts of NO_x are formed. This assumption is based on the idea that the multistage combustion process, involving both the pre-calciner and kiln, helps suppress the NO_x formation (Thomas, 2020). The pre-heater exhaust composition is given in Figure 42.

Figure 42: Pre-heater exhaust composition



The mass flows along with the sensible heat values of each of the streams were utilised to establish the energy flows as per the literature (Ali Khalifa, 2019). The theoretical reaction heat, which is based on the clinker composition mentioned above, was calculated and, subsequently, used to develop the energy balance of the pyroprocessing system (Figure 43).

Figure 43: Energy balance



As per our calculations, the theoretical reaction heat, which is the heat required to produce 1 kg of clinker, was 405.92 kcal. However, due to system inefficiencies, the heat requirements rise to approximately 600 to 800 kcal/kg clinker. This is mainly due to the loss of heat through the other streams as seen in Figure 41. The variation can be attributed to the type of pre-heater systems and fuels used.

3.8.2. Electrical SEC

The energy requirement for the various crushing and milling operations was calculated using the Bond's law and is tabulated in Table 26.

Table 26: Comparison of theoretical and practical drive requirement

Operation	Computed (kWh/t)	SEC data (kWh/t; CII, 2019)
Crusher	0.47	0.46
Ball mill	10.87	14.94
Coal mill	11.95	12.48
Cement mill	28.35	21.76

Based on these computed electrical energy requirements and the CII benchmarking, the electrical SEC was calculated for the various operations in the cement manufacturing process for 5-stage and 6-stage pre-heater configurations (Figure 44 and Figure 45).

Figure 44: 5-Stage pre-heater electrical SEC

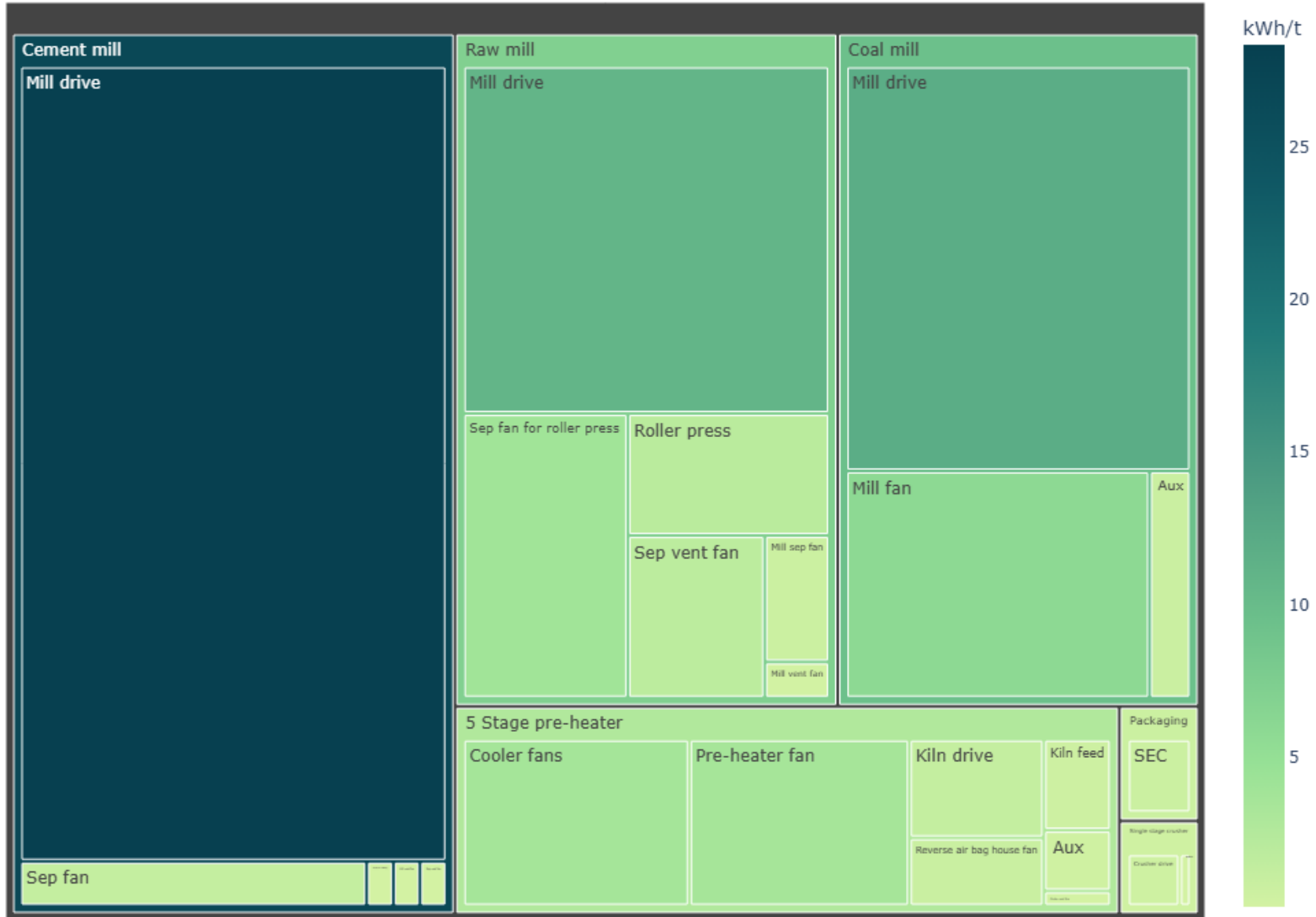
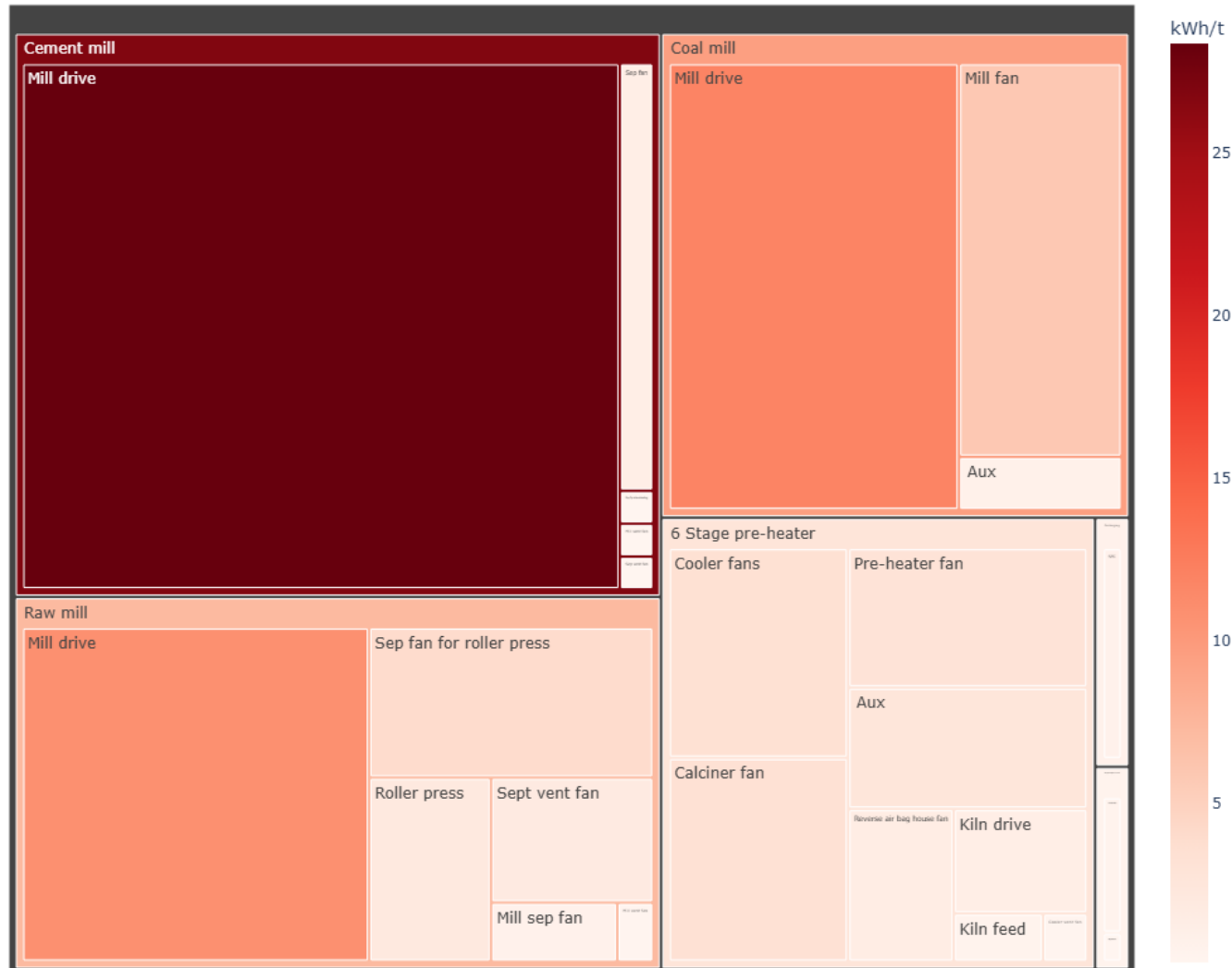


Figure 45. 6-Stage pre-heater electrical SEC



3.8.3. AFRs

The transition from coal to AFRs in clinker production presents several technical challenges, particularly in the context of heat transfer and fuel characteristics. The dominant mode of heat transfer in coal-fired rotary kilns is particle radiation, which plays a significant role in achieving the necessary temperatures for clinker formation. However, AFRs, such as biomass and MSW, have different particle characteristics compared with coal, leading to disruptions in heat distribution.

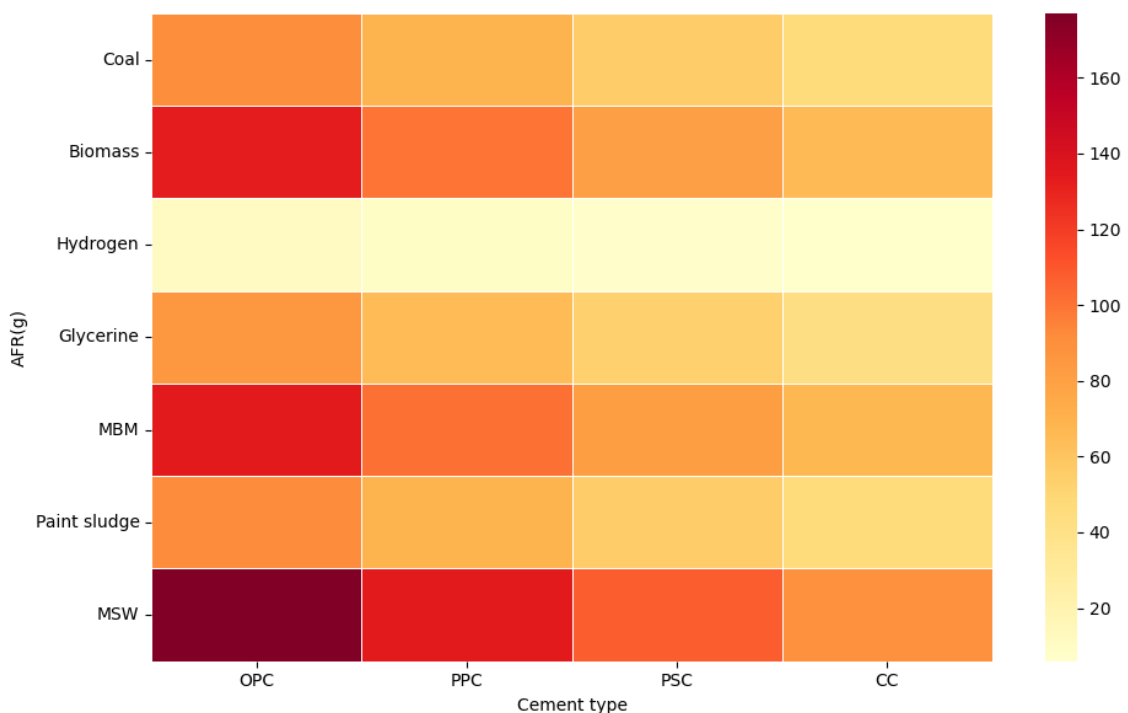
Biomass, for example, typically consists of larger particles than coal, which reduces the projected surface area for particle radiation (Bäckström et al., 2015). This results in a shorter flame length and potentially uneven heat distribution within the kiln, as seen with unignited biomass particles in the post-flame zone. Such flame characteristics can negatively affect clinker formation by causing uneven heating. Moreover, biomass co-firing introduces complexity in predicting radiative intensity due to factors such as fuel particle fragmentation and soot formation, which are not yet fully understood (Bäckström et al., 2015).

Moreover, natural gas (Bäckström et al., 2015) and hydrogen, despite their high flame temperatures, generate shorter flames, leading to uneven heating on the pellet bed and affecting the oxidation and sintering of pellets. Solid AFRs such as biomass, MSW, and MBM also pose challenges in clinker quality control due to their varying compositions, which can influence the thermal SEC and potentially compromise product quality.

Considering all these, only 60% of the energy requirement, which corresponds to 100% substitution in the calciner, can be effectively met by AFRs with minimal retrofits.

This study estimated the theoretical injection limits for various AFRs for the four main types of cement OPC, PPC, PSC, and CC based on their respective CFs (Figure 46).

Figure 46: Theoretical fuel requirement for different fuel



It was assumed that gaseous and liquid fuels can achieve only a maximum of 60% TSR corresponding to that of 100% substitution in the calciner. Solid fuels such as biomass, MSW, and MBM can achieve up to 80% TSR if they are co-fired with coal in the rotary kiln.

3.8.4. Hydrogen

Hydrogen as an AFR in cement production poses significant challenges due to its unique properties and the need for substantial retrofitting of existing systems. One of the key challenges is **hydrogen's fast-burning flame** compared with conventional hydrocarbon fuels such as methane and propane (Juangsa et al., 2022). Its higher burning velocity requires specialised pre-mixed burners to ensure safe and efficient combustion, which can prevent issues such as **flashback**. Moreover, the kiln design itself may need modifications to adjust for hydrogen's rapid combustion, such as changing the **residence time of the clinker** to allow for complete reactions.

Another challenge involves **NO_x emissions**, which can increase with hydrogen due to its higher flame temperature (Luzzo et al., 2021). While hydrogen combustion does not produce CO₂, the formation of NO_x can offset some of the environmental benefits as NO_x is a potent air pollutant.

Hydrogen's role in cement manufacturing is also limited in terms of CO₂ emissions reduction. While it eliminates CO₂ emissions from fuel combustion (32% of the total emission), the calcination process, which involves the decomposition of CaCO₃, still produces a significant amount of CO₂ (56%). Therefore, to fully decarbonise the cement manufacturing process, hydrogen must be used in conjunction with measures such as carbon capture or the use of AFRs.

Moreover, transitioning to hydrogen requires substantial retrofitting of cement plants. This includes replacing existing gas pipelines, burners, and possibly parts of the kiln to accommodate hydrogen's properties. Such modifications are expensive and complex. Moreover, the high cost of hydrogen production, especially green hydrogen, remains a significant economic barrier. While hydrogen presents a promising path to decarbonisation, these technical, economic, and environmental hurdles make its widespread adoption in cement production challenging in the near term.

Assumptions made for estimating the amount of hydrogen that can be injected into the cement manufacturing process are listed in Table 27.

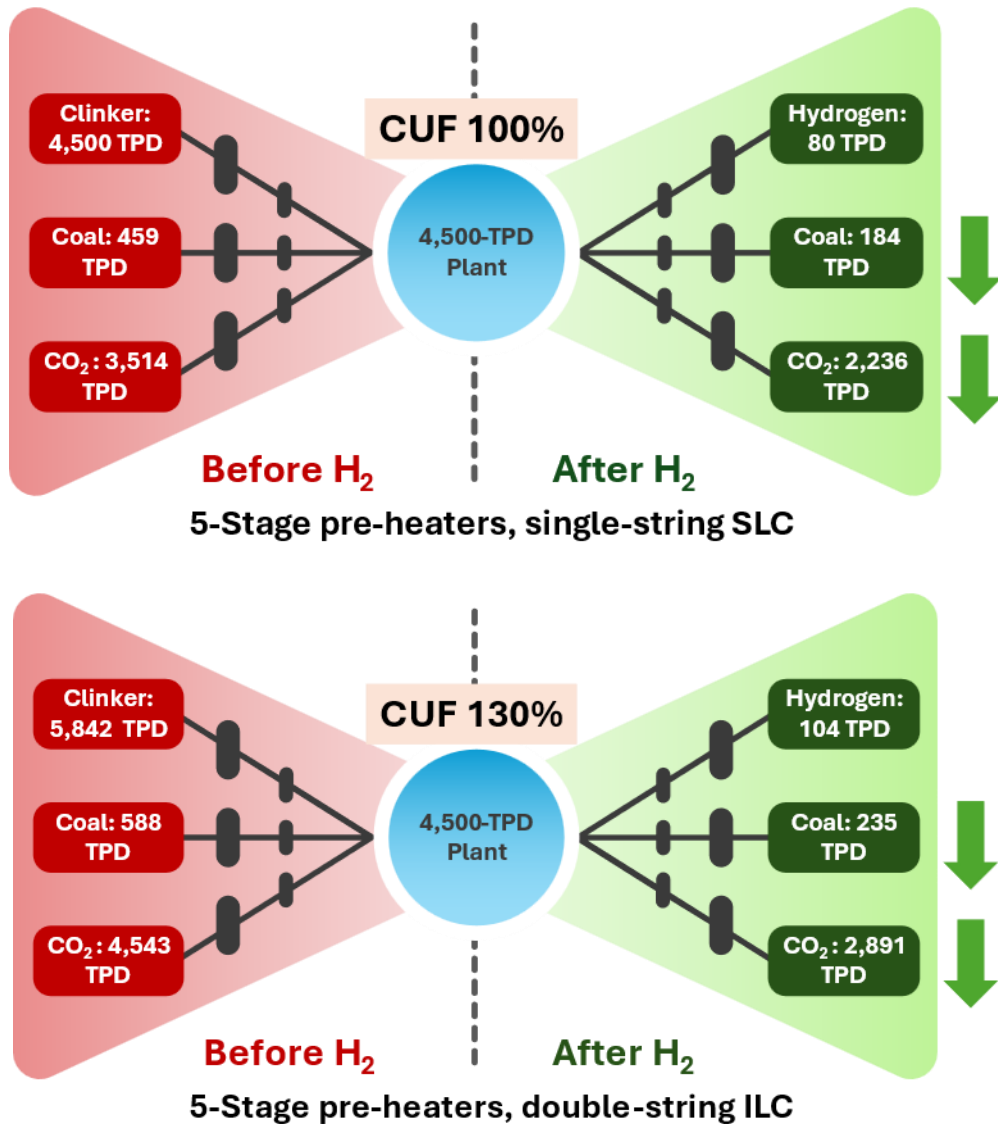
Table 27: Calciner assumptions

Fuel combustion efficiency (calcliner)	90%
System efficiency (calcliner)	90%
Safety factor	1.1
Hydrogen TSR	60%

Based on the above assumptions, the practical amount of hydrogen that can be injected into the cement manufacturing pyroprocessing system is **12 to 18 kg/t clinker**. This can result in a maximum emission reduction of 32% in a cement plant.

The impact of achieving 60% TSR in a scaled-up cement plant with hydrogen as an AFR is illustrated below (Figure 47).

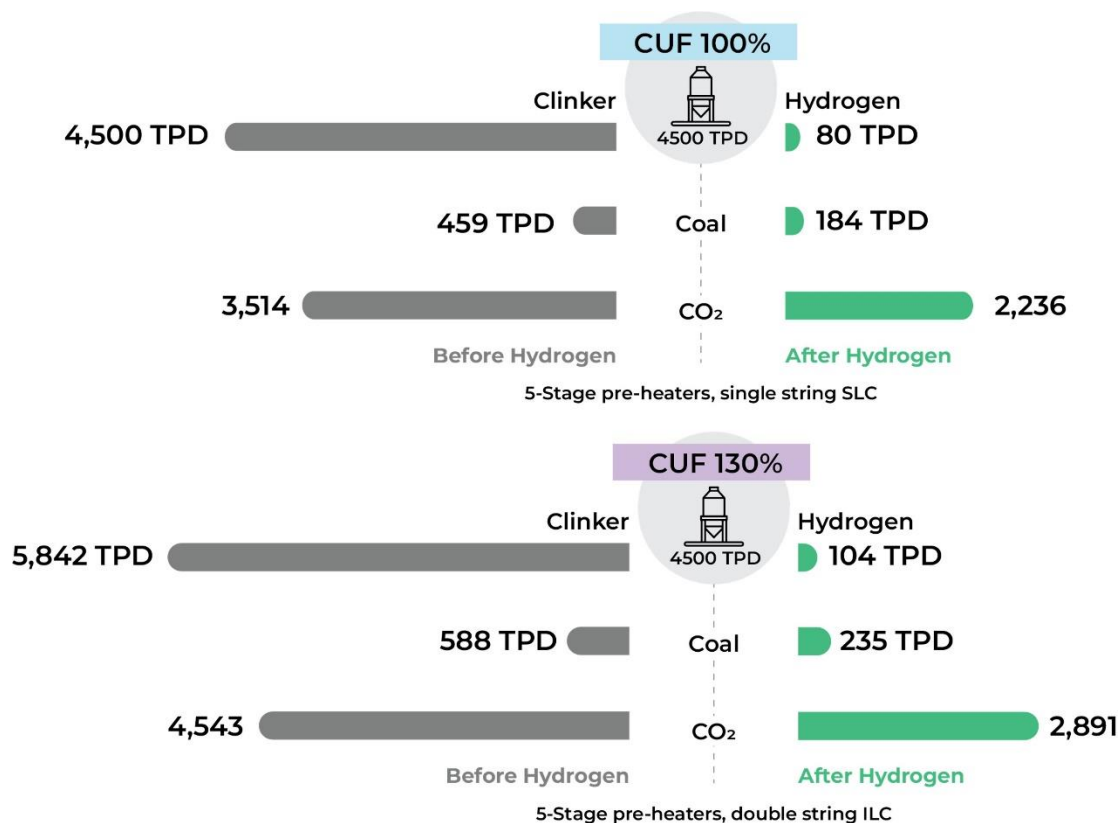
Figure 47: Impact of hydrogen injection



3.8.5. Scaled-up cement plant

The thermal and electrical SEC values from the perturbation model, along with the material requirements for producing 1 kg of clinker, was utilised to provide a plant-level material, energy, and emissions estimates (Figure 48). Analysis of the two extreme cases that were modelled (Section 3.7.7) reveals that the plant operated at a higher CUF required more raw materials and thermal and electrical energy. It also released a higher amount of CO₂ and dust emissions into the atmosphere.

Figure 48: Scaled-up cement plant



3.9. Limitations

This model for estimating hydrogen injection in cement production faces several key limitations rooted in both the theoretical assumptions and complexities of actual cement plant operations.

1. **Mass and energy balance (steady-state assumptions):** The model is built on steady-state mass and energy balance principles. However, in real-world cement plants, conditions often fluctuate due to various operational factors such as feed composition, environmental changes, and equipment-efficiency variations. This discrepancy between theoretical steady-state conditions and practical plant dynamics may lead to differences in hydrogen consumption and performance. As a result, the estimates provided by the model might not fully capture the variability seen in industrial environments. A transient model, on the other hand, can be developed using advanced process simulation modelling applications such as Aspen Plus. In fact, leading cement manufacturers use advanced version of this software to substantiate their research findings. The drawback is economically unviable pricing of the software, which hinders the possibility of its usage by think tanks and academic institutions.
2. **Thermal SEC:** The thermal SEC used in the model is highly dependent on factors such as the pre-heater configuration and kiln design. While this model relies on trends observed in specific plant capacities, the actual thermal energy requirements can vary significantly depending on the specific plant layout, equipment efficiency, and operational practices. This adds a level of uncertainty to the model's estimates, as not all plants follow the same design or operate under similar conditions. The type of fuel used by the plant also contributes to the

thermal SEC, with granular variables, such as composition, playing a significant role.

3. **Hydrogen estimation and clinker quality:** A key limitation of the work is the lack of detailed heat transfer modelling and by-product analysis, which are critical for understanding how hydrogen affects the clinker quality. Hydrogen combustion produces a different flame temperature and radiation profile compared with traditional fuels, potentially impacting the heat distribution in the kiln and the quality of the resulting clinker. Without incorporating detailed by-product analysis and heat transfer models (combination of Ansys and Aspen Plus), the estimation of hydrogen input could inadvertently compromise clinker properties and impact the throughput, which is closely linked with the batch size in every plant.

In summary, while this model provides a useful framework for estimating hydrogen injection in cement plants, its limitations in terms of mass and energy balance, thermal and electrical SEC assumptions, scalability, and clinker quality must be considered when applying it to the real-world scenarios.



4. Policy Discussions

Despite the limitations, the opportunity presented by green hydrogen in decarbonising steel and cement sectors is immense. However, to realise the opportunity, effective policy measures will play a pivotal role. Table 28 provides an overview of select current policies in steel, cement, and hydrogen sectors relevant for hydrogen adoption.

Table 28: Current policies in steel, cement, and hydrogen

Iron and steel	<p>National Steel Policy, 2017 The aim of this policy is to achieve a steel production capacity of 300 Mt by 2030. This will be achieved by enhancing domestic per capita steel consumption to 160 kg. Other goals pertain to increasing the domestic availability of washed coking coal to reduce import dependence of coking coal to 65%, as well as meeting the entire demand of high-grade automotive steel, electrical steel, special steel, and alloys.</p> <p>Production Linked Incentive (PLI) Scheme for Specialty Steel Under the aegis of the Ministry of Steel, the Government of India has approved an INR 6,322 crore outlay for a 5-year period to promote the manufacturing of specialty steel, thereby attracting investments and fostering technological advancements in the sector.</p> <p>Green Steel Making The Ministry of Steel constituted 13 Task Forces, with the engagement of industry, academia, think tanks, S&T (Science and Technology) bodies, and other key stakeholders, to delineate different levers of decarbonisation of the steel sector. The steel sector has been made a stakeholder in the National Green Hydrogen Mission (NGHM) for green hydrogen production and usage. Moreover, best available technology (BAT) available globally should be adopted in the modernisation and expansions projects (Ministry of New & Renewable Energy [MNRE], 2024) .</p> <p>Ministry's Engagement with PM Gati Shakti National Master Plan The Ministry of Steel has integrated BISAG-N's (Bhaskaracharya National Institute for Space Applications and Geo-informatics) capabilities into the PM Gati Shakti National Master Plan, uploading geolocations of more than 2 000 steel units to gain insights into steel production facilities.</p> <p>Steel Scrap Recycling Policy Notified in 2019, this policy provides a framework to facilitate and promote the establishment of metal scrapping centres in the country for scientific processing and recycling of ferrous scrap generated from various sources, including end-of-life vehicles (ELVs).</p>
-----------------------	---

<p>Cement</p>	<p>BIS for blending fly ash and other additives for cement production (14 types of cement; IS 1489 [Part 1]: 1991, 1993)</p> <p>CF reduction (IS 455:2015 [PSC] IS 1489:2015 [PPC] IS 164415:2015 [CC]) Around 29% blending with alternative raw materials has been already achieved.</p> <p>Guidelines for Co-processing of Plastic Waste in Cement Kilns issued by the Central Pollution Control Board (CPCB, 2017) Co-processing refers to the use of waste materials in industrial processes as AFRs to recover energy and materials. Owing to the high temperature in the cement kiln, different types of wastes can be effectively incinerated. As per the Basel Convention, different types of wastes, including hazardous wastes, can be disposed of in a safe way through co-processing in the kiln.</p>
<p>Hydrogen</p>	<p>NGHM</p> <p>With a goal to produce 5 Mt by 2030, the NGHM is expected to draw investments and create jobs in both hydrogen and allied sectors. Under the SIGHT scheme, two guidelines (tranches) have been issued. The first one is to incentivise domestic manufacturing of electrolyser and green hydrogen production. The second is the incentive scheme for green hydrogen production (0.45 Mt), with 40 Kt capacity reserved for biomass-based hydrogen production. Inter-state transmission (ISTS) charges to be waived off (at a varying progression of applicability for renewable electricity used to produce green hydrogen (Ministry of Power, 2021b; Ministry of Power, 2023;).</p>

4.1. Enabling policy measures

The integration of hydrogen into the cement and steel industries is essential for decarbonising these hard-to-abate sectors. However, a multifaceted policy approach is required to ensure the effective adoption of hydrogen.

A key aspect involves the beneficiation of iron slimes, which can enhance the sustainability of iron ore usage and ensure sufficient feedstock for hydrogen-based DRI production. With the requirement of iron ore expected to grow to around 440 Mt by 2030, from the current 250 Mt, beneficiation of ore is crucial to promote circular economy and maximise resource efficiency. Published literature suggests 48%–60% of iron content in tailings, making this a vital intervention (Padhi et al., 2022).

Further, the development of a green steel taxonomy, established through collaboration between producers and consumers, will help define, standardise, and certify green steel production, enabling its market acceptance and enhancing competitiveness. Addressing cost barriers is another priority; while consumers may be willing to pay a premium of up to 12% for green steel, a financial corpus could be created to bridge the remaining cost gap (Segal, 2023). Such a fund could be sourced from public investments, international green funds, or the carbon market. This would ensure that steel producers are incentivised to switch to hydrogen-based production. Policies should also promote green

procurement, possibly mandating the use of green steel in public infrastructure projects and providing tax incentives and subsidies to steel producers.

Based on interactions with industry experts, reducing the cost of renewable electricity to INR 2/kWh is crucial for green hydrogen adoption in the steel industry. To achieve this, policies could include streamlining regulatory frameworks, investing in grid infrastructure to improve renewable integration, and implementing long-term power purchase agreements to supply manufacturers with low-cost renewable energy, thereby making green hydrogen more viable.

Pull mechanisms, such as advanced market commitments (AMCs), can stimulate demand by offering price certainty for green products. This also reduces investment risk for producers and fosters early adoption. Public-private partnerships and collaborations with international organisations can further boost the effectiveness of AMCs in driving market demand.

To enhance energy efficiency in the steel and cement sectors, WHR systems should be promoted alongside hydrogen adoption to enhance energy efficiency in the steel and cement sectors. Policy incentives such as subsidies for WHR system installation or carbon credits for energy savings can help maximise energy efficiency while reducing emissions. Currently, the cement industry has implemented ~538 MW of WHR capacity. Approximately 70% of this capacity is concentrated in Rajasthan, Chattisgarh, and Madhya Pradesh. The high adoption in these states is attributed to supporting policies that place WHR systems at par with renewable energy, allowing WHR systems to meet renewable power obligations (RPOs; CMA, 2021).

In the cement industry, policies should support R&D in technologies such as CaL and RDH to make them viable for Indian conditions (NPC, 2017). Further, policies are required to establish long-term strategies, invest in infrastructure for hydrogen storage and distribution, and introduce carbon pricing to incentivise switching from traditional fuels to hydrogen. Initial efforts could involve co-firing hydrogen with alternative fuels.

Collectively, these policy measures will create a robust framework for supporting hydrogen integration into the cement and steel sectors, leading to substantial emissions reductions while enhancing economic sustainability and competitiveness.



H₂
GREEN
HYDROGEN

HYDROGEN

5. Way Forward and Conclusion

By 2050, the Indian steel industry is expected to undergo a significant transition in technology and production processes, largely driven by the need for decarbonisation. The steel production mix is anticipated to shift considerably, with a growing emphasis on low-carbon technologies such as enhanced secondary steel utilisation, hydrogen-based DRI, and hydrogen-enhanced BF-BOF systems. Moreover, steelmaking capacity by 2050 is projected to reach approximately 510 Mt (Sinha & Acharya, 2023).

Hydrogen demand for steel production

To meet the anticipated steel demand in 2050, the hydrogen requirements for BF-BOF and DRI technologies will be substantial. In the BF-BOF route, the amount of hydrogen to be used as a reducing agent in 2050 is projected to be approximately 18–25 kg/tHM, as emphasised in Section 2.4.3.3. Similarly, hydrogen injection in DRI is expected to play a central role in low-emission steel production, with a requirement of 54 kg/t of DRI (Shahabuddin et al., 2024). This translates to an overall annual hydrogen demand of 7.6–11 Mt for steel production.

Emission reductions and carbon abatement potential

The introduction of hydrogen into the BF-BOF process offers the potential for reducing carbon emissions in established plants. The extent of emissions abatement will further depend on factors such as the hydrogen injection rate and process efficiency. Our study suggests potential emission reductions of 8%–9% in BF-BOF operations. Moreover, hydrogen-based DRI production could reduce emissions by approximately 62%. These decarbonisation measures are projected to abate nearly 125 Mt of CO₂ annually. When combined with other strategies such as CCUS, the overall emission reductions could be further amplified.

Potential of alternative feedstocks: Biochar and hydrogen-rich gases

Hydrogen injection is just one aspect of the decarbonisation landscape for steel production. The use of alternative feedstocks such as biochar (produced from sustainable biomass) also presents a promising option. Biochar has the potential to act as a carbon-neutral reductant, further reducing reliance on fossil fuels in steelmaking. Moreover, hydrogen-rich gases, potentially derived from waste streams or other industrial processes, could serve as a viable alternative feedstock. These alternatives, when combined with hydrogen injection, could create a diversified portfolio of decarbonisation strategies for the BF-BOF process, optimising both cost and environmental performance.

The broader decarbonisation challenge: LCOH, levelised cost of energy (LCOE), and cement

The integration of hydrogen into steel production must also be viewed in the broader context of the decarbonisation challenge across industries such as cement and steel. As examined in this report, factors such as LCOH and LCOE will be critical in determining the economic viability of hydrogen-based processes. The price of hydrogen production, whether through electrolysis or other low-carbon pathways, will need to fall significantly for widespread adoption in steelmaking. This will increase the cost competitiveness of the process compared with traditional carbon-based methods.

While the injection of hydrogen into the BF–BOF process offers a clear pathway towards decarbonisation, the complexity of this transition demands careful planning and optimisation. The variability of hydrogen availability, the fluctuating cost of green energy, and the need to maintain operational efficiency in steel plants all require advanced dynamic process modelling. This will enable steelmakers to simulate and adapt to real-time conditions, optimising hydrogen use and balancing trade-offs between cost, emissions, and productivity. Such modelling will be vital to ensuring that hydrogen injection into blast furnaces contributes effectively to the broader decarbonisation goals of the steel industry.

Hydrogen demand for cement production

This study estimated that 12–18 kg of hydrogen can be injected (fuel) per tonne of clinker, reducing emissions by up to 32%. However, utilising hydrogen alone can be challenging as it may require retrofitting of burners, piping, and other infrastructure. While alternative fuels such as MBM, glycerine, and MSW can be used in conjunction with hydrogen, the operational challenges around using hydrogen as a fuel and how it affects the combustion property and clinker quality must be examined.

In summary, hydrogen-enhanced BF–BOF processes, in conjunction with complementary feedstocks and innovative modelling tools, are key components in the future of sustainable steel production. By leveraging these technologies, the steel industry can play a pivotal role in achieving global emissions reduction targets by 2050, while ensuring the long-term viability of one of the world's most essential industrial sectors. With a production target of 5 Mt per annum by 2030, green hydrogen is expected to be used primarily in refineries and fertilisers (MNRE, 2023). Having said that, the first foray into steel is expected to be in DRI units. Subsequently, large blast furnace units will start amending green hydrogen to reduce the overall emissions footprint. In due course of time, we expect cement sector to embrace green hydrogen considering the hard-to-abate nature of the decarbonation process.

6. References

- Abdul Quader, M., Ahmed, S., Dawal, S. Z., & Nukman, Y. (2016). Present needs, recent progress and future trends of energy-efficient Ultra-Low Carbon Dioxide (CO) Steelmaking (ULCOS) program. *Renewable and Sustainable Energy Reviews*, 55, 537–549. <https://doi.org/10.1016/j.rser.2015.10.101>
- Abhale, P. B., Viswanathan, N. N., & Saxén, H. (2020). Numerical modelling of blast furnace – Evolution and recent trends. *Mineral Processing and Extractive Metallurgy*, 129(2), 166–183. <https://doi.org/10.1080/25726641.2020.1733357>
- Alliance for an Energy Efficient Economy. (2021, February 4). *Emission Reduction Approaches for the Cement Industry*. <https://aeee.in/emission-reduction-approaches-for-the-cement-industry/>
- Agico Cement. (2024). *Advantages of precalciner*. <https://www.cement-plants.com/clinker-production/precalciner/>
- Agrawal, A., Das, K., Singh, B. K., Singh, R. S., Ranjan Tripathi, V., Kundu, S., Padmapal, Ramna, R. V., & Singh, M. K. (2020). Means to cope with the higher alumina burden in the blast furnace. *Ironmaking & Steelmaking*, 47(3), 238–245. <https://doi.org/10.1080/03019233.2019.1702828>
- Ali Khalifa, S. (2019). Heat balance analysis in cement rotary kiln. *Advances in Applied Sciences*, 4(2), 34. <https://doi.org/10.11648/j.aas.20190402.11>
- Aspen Plus. (n.d.). Aspen Tech. <https://www.aspentech.com/en/products/engineering/aspen-plus>
- Aspen Technology, Inc. (2001). *Physical Property Methods and Models 11.1*.
- Bäckström, D., Johansson, R., Andersson, K., Wiinikka, H., & Fredriksson, C. (2015). On the use of alternative fuels in rotary kiln burners—An experimental and modelling study of the effect on the radiative heat transfer conditions. *Fuel Processing Technology*, 138, 210–220. <https://doi.org/10.1016/j.fuproc.2015.05.021>
- Badgett, A., Brauch, J., Thatte, A., Rubin, R., Skangos, C., Wang, X., Ahluwalia, R., Pivovar, B., & Ruth, M. (2024). *Updated Manufactured Cost Analysis for Proton Exchange Membrane Water Electrolyzers* (NREL/TP-6A20-87625). National Renewable Energy Laboratory.
- Bailera, M., Nakagaki, T., & Kataoka, R. (2021). Revisiting the Rist diagram for predicting operating conditions in blast furnaces with multiple injections. *Open Research Europe*, 1, 141. <https://doi.org/10.12688/openreseurope.14275.1>
- Bala-Litwiniak, A., & Radomiak, H. (2019). Possibility of the utilization of waste glycerol as an addition to wood pellets. *Waste and Biomass Valorization*, 10(8), 2193–2199. <https://doi.org/10.1007/s12649-018-0260-7>
- Barbhuiya, S., Kanavaris, F., Das, B. B., & Idrees, M. (2024). Decarbonising cement and concrete production: Strategies, challenges and pathways for sustainable development. *Journal of Building Engineering*, 86, 108861. <https://doi.org/10.1016/j.jobee.2024.108861>
- Barrett, N., Mitra, S., Doostmohammadi, H., O’dea, D., Zulli, P., Chew, S., & Honeyands, T. (2022). Assessment of blast furnace operational constraints in the presence of

- hydrogen injection. *ISIJ International*, 62(6), 1168–1177.
<https://doi.org/10.2355/isijinternational.ISIJINT-2021-574>
- Battle, T., Srivastava, U., Kopfle, J., Hunter, R., & McClelland, J. (2014). The direct reduction of iron. In *Treatise on Process Metallurgy* (pp. 89–176). Elsevier.
<https://doi.org/10.1016/B978-0-08-096988-6.00016-X>
- Bhardwaj, N., Seethamraju, S., & Bandyopadhyay, S. (2024). Decarbonizing rotary kiln–induction furnace based sponge iron production. *Energy*, 306, 132516.
<https://doi.org/10.1016/j.energy.2024.132516>
- Bhaskar, A., Abhishek, R., Assadi, M., & Somehesaraei, H. N. (2022). Decarbonizing primary steel production: Techno-economic assessment of a hydrogen based green steel production plant in Norway. *Journal of Cleaner Production*, 350, 131339.
<https://doi.org/10.1016/j.jclepro.2022.131339>
- Biswas, A. K. (1981). *Principles of blast furnace ironmaking: Theory and practice* (Repr., (Students Edition)). SBA Publ.
- Cavalett, O., Watanabe, M. D. B., Voldsund, M., Roussanaly, S., & Cherubini, F. (2024). Paving the way for sustainable decarbonization of the European cement industry. *Nature Sustainability*, 7(5), 568–580. <https://doi.org/10.1038/s41893-024-01320-y>
- Cemnet. (2023, May 26). *UltraTech Cement to employ Coolbrook decarbonisation technology*. <https://www.cemnet.com/News/story/174902/ultratech-cement-to-employ-coolbrook-decarbonisation-technology.html>
- CFD Flow Engineering. (2024). *Calorific Value of Coal and Wood Calculations*. <https://cfdflowengineering.com/calorific-value-of-fuel-calculations/>
- Chattopadhyay, S., Mitra, R., & Kumar, Dr. N. (2019). *Resource efficiency in the steel and paper sectors: Evaluating the potential for circular economy*. Confederation of Indian Industry (CII). <https://shaktifoundation.in/wp-content/uploads/2020/03/Resource-efficiency-in-the-steel-and-paper-sectors.pdf>
- Confederation of Indian Industry. (2019). *Energy Benchmarking For Indian Cement Industry* [Benchmarking].
- Confederation of Indian Industry. (2021, November 27). *Cement Manufacturing Process*. <https://www.slideshare.net/slideshow/cement-manufacturing-process-250737684/250737684>
- Coolbrook. (n.d.). *RotoDynamic Heater*. Retrieved May 4, 2025, from <https://coolbrook.com/industrial-decarbonization-solutions/cement-industry-decarbonization/>
- Coolbrook. (2023). *Industrial Process Heating: Replacing Fossil Fuels with RotoDynamic Heater*. <https://coolbrook.com/electrification-solutions/rdh-industrial-process-heating/>
- Coolbrook. (2024, November 1). *JSW and Coolbrook ink strategic cooperation agreement for industrial electrification technology to drive decarbonisation*. <https://coolbrook.com/news/jsw-and-coolbrook-ink-strategic-cooperation-agreement-for-industrial-electrification-technology-to-drive-decarbonisation/>
- Central Pollution Control Board. (2017, May). *Guidelines for co-processing of plastic waste in cement kilns*. https://cpcb.nic.in/uploads/plasticwaste/Co-processing_Guidelines_Final_23.05.17.pdf

- Credit Rating Information Services of India Limited. (2024, June 6). *CRISIL Ratings- Dalmia Bharat Limited*.
https://www.crisil.com/mnt/winshare/Ratings/RatingList/RatingDocs/DalmiaBharat Limited_June%2006_%202024_RR_332280.html#:~:text=DBL%20aims%20to%20achieve%20a,hazardous%20and%20municipal%20solid%20waste.
- Centre for Science and Environment. (2019, July 2). *Solid waste in India*. CSE, India.
https://csestore.cse.org.in/pub/media/catalog/product/file/sample-to_burn_or_not_to_burn.pdf
- Davenport, W., Lefebvre, K., Sukhram, M., & Cameron, I. (2019). *Blast furnace ironmaking: Analysis, control and optimization* (1st edition). Elsevier.
- de Castro, J. A., de Medeiros, G. A., da Silva, L. M., Ferreira, I. L., de Campos, M. F., & de Oliveira, E. M. (2023). A numerical study of scenarios for the substitution of pulverized coal injection by blast furnace gas enriched by hydrogen and oxygen aiming at a reduction in CO₂ emissions in the blast furnace process. *Metals*, 13(5), 927. <https://doi.org/10.3390/met13050927>
- De Silvestri, A., Stendardo, S., Della Pietra, M., & Borello, D. (2021). Decarbonizing cement plants via a fully integrated calcium looping-molten carbonate fuel cell process: Assessment of a model for fuel cell performance predictions under different operating conditions. *International Journal of Hydrogen Energy*, 46(28), 14988–15007. <https://doi.org/10.1016/j.ijhydene.2020.12.024>
- Deolalkar, S. (2008). *Handbook for designing cement plants*.
https://www.bspublications.net/book_detail.php?bid=144
- Dowding, M. F., & Whiting, A. N. (n.d.). *The case for 100 000. Tonnes/year integrated iron and steel plants for emergent countries*. Retrieved October 17, 2024, from <https://eprints.nmlindia.org/5576/1/III-9-16.PDF>
- DWSIM. (n.d.). DWSIM. <https://dwsim.org/>
- El Haggag, S. M. (2005). Rural and developing country solutions. In *Environmental Solutions* (pp. 313–400). Elsevier. <https://doi.org/10.1016/B978-012088441-4/50015-0>
- Ellis, L. D., Badel, A. F., Chiang, M. L., Park, R. J.-Y., & Chiang, Y.-M. (2020). Toward electrochemical synthesis of cement—An electrolyzer-based process for decarbonating CaCO₃ while producing useful gas streams. *Proceedings of the National Academy of Sciences*, 117(23), 12584–12591.
<https://doi.org/10.1073/pnas.1821673116>
- Emre Ertem, M., & Gürgen, S. (2006). Energy balance analysis for Erdemir blast furnace number one. *Applied Thermal Engineering*, 26(11–12), 1139–1148.
<https://doi.org/10.1016/j.applthermaleng.2005.10.044>
- Engineering ToolBox. (2003). *Engineering Toolbox- Fuels—Higher and Lower Calorific Values*. https://www.engineeringtoolbox.com/fuels-higher-calorific-values-d_169.html
- Essar Projects [India] Limited Engineering & Project Management. (2014). *Pre-feasibility report of replacement of electric arc furnaces(Eaf's) of steel making plant(Smp-1) by basic oxygen furnaces(BOFs)in Hazira facility* (Doc No:2715-H000-Z00000-0001-0120-0002 R0). <https://studylib.net/doc/18319526/essar-steel-india-limited---environmental-clearances>

- Fabian, A., Hoyt, J., Marques, F., Reiter, S., & Schulze, P. (2023, October 6). *Cementing your lead: The cement industry in the net-zero transition*. McKinsey & Company. <https://www.mckinsey.com/industries/engineering-construction-and-building-materials/our-insights/cementing-your-lead-the-cement-industry-in-the-net-zero-transition#/>
- Fan, Z., & Friedmann, S. J. (2021). Low-carbon production of iron and steel: Technology options, economic assessment, and policy. *Joule*, 5(4), 829–862. <https://doi.org/10.1016/j.joule.2021.02.018>
- Fennell, P. S., Davis, S. J., & Mohammed, A. (2021). Decarbonizing cement production. *Joule*, 5(6), 1305–1311. <https://doi.org/10.1016/j.joule.2021.04.011>
- Ferrario, D., Stendardo, S., Verda, V., & Lanzini, A. (2023). Solar-driven calcium looping system for carbon capture in cement plants: Process modelling and energy analysis. *Journal of Cleaner Production*, 394, 136367. <https://doi.org/10.1016/j.jclepro.2023.136367>
- Gao, X., Zhang, R., You, Z., Yu, W., Dang, J., & Bai, C. (2022). Use of hydrogen-rich gas in blast furnace ironmaking of V-bearing titanomagnetite: Mass and energy balance calculations. *Materials*, 15(17), 6078. <https://doi.org/10.3390/ma15176078>
- Gautam, S. P., Bundela, P. S., & Murumkar, M. (2010). *Paint sludge waste co-processing at the ACC Wadi Cement Works in Karnataka, India*. 57–66. <https://doi.org/10.2495/WM100061>
- Global Cement and Concrete Association. (2022). *Blended cement - green, durable & sustainable*. https://gccassociation.org/wp-content/uploads/2022/04/Report_Blended-Cement-Green-Durable-Sustainable_13Apr2022.pdf
- Global Cement and Concrete Association & Global CCS Institute. (2024). *CCUS in the Indian cement industry A review of CO2 hubs and storage facilities*. <https://gccassociation.org/wp-content/uploads/2024/06/CCS-in-Concrete-India-Report-14-June.pdf>
- Ghosh, A., & Chatterjee, A. (2010). *Ironmaking and steelmaking: Theory and practice* (3. print). PHI Learning.
- Gupta, K., Shaik, N., Garg, V., & Srivastava, S. (2023). *Steel Decarbonisation in India*. IEEFA, JMK Research & Analytics. https://ieefa.org/sites/default/files/2023-09/Steel%20Decarbonisation%20in%20India_September%202023_2.pdf
- Hall, W., Spencer, T., & Kumar, S. (2020). *Towards a low carbon steel sector: Overview of the changing market, technology and policy context for Indian steel*. The Energy and Resources Institute (TERI). <https://shaktifoundation.in/wp-content/uploads/2020/01/Towards-a-Low-Carbon-Steel-Sector-Report.pdf>
- Hasanbeigi, A. (2022). *Steel Climate Impact—An International Benchmarking of Energy and CO2 Intensities*. Global Efficiency Intelligence. <https://www.globalefficiencyintel.com/steel-climate-impact-international-benchmarking-energy-co2-intensities>
- Herath Banda, R. M., & Glasser, F. P. (1978). Role of iron and aluminum oxides as fluxes during the burning of Portland cement. *Cement and Concrete Research*, 8(3), 319–324. [https://doi.org/10.1016/0008-8846\(78\)90101-1](https://doi.org/10.1016/0008-8846(78)90101-1)

- HYBRIT. (n.d.). *Pilot scale direct reduction with hydrogen*. HYBRIT Fossil Free Steel. Retrieved October 16, 2024, from <https://www.hybritdevelopment.se/en/a-fossil-free-development/direct-reduction-hydrogen-pilotscale/>
- India Brand Equity Foundation. (2024). *Cement industry in India*. <https://www.ibef.org/industry/cement-india>
- International Energy Agency. (2020). *Iron and Steel Technology Roadmap*, <https://www.iea.org/reports/iron-and-steel-technology-roadmap>. IEA. <https://www.iea.org/reports/iron-and-steel-technology-roadmap>
- International Energy Agency. (2022). *Energy system of India*. <https://www.iea.org/Countries/India>. <https://www.iea.org/countries/india/emissions>
- Ige, O. E., Von Kallon, D. V., & Desai, D. (2024). Carbon emissions mitigation methods for cement industry using a systems dynamics model. *Clean Technologies and Environmental Policy*, 26(3), 579–597. <https://doi.org/10.1007/s10098-023-02683-0>
- Indian Bureau of Mines. (n.d.-a). *Indian minerals yearbook 2018 (Part- II : Metals and alloys)—Slag - iron and steel* (57th ed.). Ministry of Mines, Indian Bureau of Mines.
- Indian Bureau of Mines. (n.d.-b). *Iron and steel vision 2020*. https://ibm.gov.in/writereaddata/files/06062017100713Iron%20and%20Steel%202020_2.pdf
- Institute of Raw Material Preparation and Environmental Processing, University of Miskolc, 3515 Miskolc, Hungary, Mucsi, G., Rácz, Á. (2019). Volume based closed-cycle hardgrove grindability method. *Rudarsko-Geološko-Naftni Zbornik*, 34(4), 9–17. <https://doi.org/10.17794/rgn.2019.4.2>
- Bureau of Indian Standards. (1993, March). *Portland-Pozzolona Cement—Specifications part 1 fly ash based*. Bureau of Indian Standards. <https://law.resource.org/pub/in/bis/S03/is.1489.1.1991.pdf>
- ISPAT Guru. (2013, March 18). *Blast furnace gas generation and usage*. ISPAT Guru. <https://www.ispatguru.com/blast-furnace-gas-generation-and-usage/>
- Johnson, S., Deng, L., & Gençer, E. (2023). Environmental and economic evaluation of decarbonization strategies for the Indian steel industry. *Energy Conversion and Management*, 293, 117511. <https://doi.org/10.1016/j.enconman.2023.117511>
- JSW Steel. (n.d.). *Steel and Indian Economy: An Upward Curve*. <https://www.jsw.in/steel/steel-and-indian-economy-upward-curve?ref=blog.fleetx.io#:~:text=Steel%20now%20contributes%20about%20,in%20the%20global%20steel%20market.>
- Juangsa, F. B., Cezeliano, A. S., Darmanto, P. S., & Aziz, M. (2022). Thermodynamic analysis of hydrogen utilization as alternative fuel in cement production. *South African Journal of Chemical Engineering*, 42, 23–31. <https://doi.org/10.1016/j.sajce.2022.07.003>
- Kamijo, C., Matsukura, Y., Yokoyama, H., Sunahara, K., Kakiuchi, K., Sakai, H., Nakano, K., Ujisawa, Y., & Nishioka, K. (2022). Influence of large amount of hydrogen containing gaseous reductant injection on carbon consumption and operation conditions of blast furnace - development of low carbon blast furnace operation technology by using experimental blast furnace: Part II -. *ISIJ International*, 62(12), 2433–2441. <https://doi.org/10.2355/isijinternational.ISIJINT-2022-099>

- Kantorek, M., Jesionek, K., Polesek-Karczewska, S., Ziółkowski, P., Stajnke, M., & Badur, J. (2021). Thermal utilization of meat-and-bone meal using the rotary kiln pyrolyzer and the fluidized bed boiler – The performance of pilot-scale installation. *Renewable Energy*, 164, 1447–1456. <https://doi.org/10.1016/j.renene.2020.10.124>
- Kildahl, H., Wang, L., Tong, L., & Ding, Y. (2023). Cost effective decarbonisation of blast furnace – basic oxygen furnace steel production through thermochemical sector coupling. *Journal of Cleaner Production*, 389, 135963. <https://doi.org/10.1016/j.jclepro.2023.135963>
- Krishnan, S. S., Venkatesh, V., Shyam Sunder, P., Murali Ramakrishnan, A., & Ramakrishna, G. (2012). *A study of energy efficiency in the Indian cement industry*. https://cstep.in/drupal/sites/default/files/2019-02/CSTEP_Energy_Efficiency_in_Indian_Cement_Industry_Report_2012.pdf
- Krishnan, S. S., Vunnam, V., Sunder P, S., J V, S., & Murali, R. (2013). *A study of energy efficiency in the Indian iron and steel industry*. Center for Study of Science, Technology and Policy. http://www.cstep.in/uploads/default/files/publications/stuff/CSTEP_A_Study_of_Energy_Efficiency_in_the_Iron_and_Steel_Industry_Report_2013.pdf
- Kumar Verma, Y., Mazumdar, B., & Ghosh, P. (2020). Thermal energy consumption and its conservation for a cement production unit. *Environmental Engineering Research*. <https://doi.org/10.4491/eer.2020.111>
- Kundrat, D. M., Miwa, T., & Rist, A. (1991). Injections in the iron blast furnace: A graphics study by means of the rist operating diagram. *Metallurgical Transactions B*, 22(3), 363–383. <https://doi.org/10.1007/BF02651235>
- Leadership Group for Industry Transition. (n.d.). *Green Steel Tracker*. <https://www.industrytransition.org/green-steel-tracker/>
- Luzzo, I., Cirilli, F., Jochler, G., Gambato, A., Longhi, J., & Rampinini, G. (2021). Feasibility study for the utilization of natural gas and hydrogen blends on industrial furnaces. *Matériaux & Techniques*, 109(3–4), 306. <https://doi.org/10.1051/mattech/2022006>
- McCabe, W. L., Smith, J. C., & Harriott, P. (1993). *Unit operations of chemical engineering*. McGraw Hill. <https://evsujpiche.wordpress.com/wp-content/uploads/2014/06/unit-operations-of-chemical-engineering-5th-ed-mccabe-and-smith.pdf>
- Ministry of New & Renewable Energy. (2024, February 2). *Scheme guidelines for implementation of pilot projects for use of green hydrogen in steel sector under the National Green Hydrogen Mission (NGHM)*. Ministry of New & Renewable Energy (MNRE). <https://mnre.gov.in/notice/scheme-guidelines-for-implementation-of-pilot-projects-for-use-of-green-hydrogen-in-steel-sector-under-the-national-green-hydrogen-mission-nghm/>
- Ministry of Power. (2021a). *National mission on use of biomass in thermal power plants*. <https://samarth.powermin.gov.in/content/policies/80e5db53-014e-4dbf-ad85-a9d0ce9b654a.pdf>
- Ministry of Power. (2021b, November 23). *Waiver of ISTS on transmission of the electricity generated from solar and wind sources of energy*. Ministry of Power, Government of India. <https://powermin.gov.in/sites/default/files/uploads/Orders/B.4.3.pdf>

- Ministry of Power. (2023, May 29). The ISTS waiver of Green Hydrogen and Green Ammonia projects extended from 30 June 2025 to 31 Dec 2030. *PIB Delhi*.
<https://www.pib.gov.in/PressReleaseIframePage.aspx?PRID=1928128>
- Ministry of Steel. (n.d.-a). *An overview of steel sector*. Ministry of Steel. Retrieved October 16, 2024, from <https://xn--i1bj1gb1azjhs7cwndf1qg.xn--11b7cb3a6a.xn--h2brj9c/sites/default/files/ANOVERVIEWOFSTEELSECTOR-Updated%20December%202023.pdf>
- Ministry of Steel. (n.d.-b). *Annual report 2016-17*. Retrieved October 16, 2024, from https://steel.gov.in/sites/default/files/Annual%20Report%20%28English%29_0.pdf
- Ministry of Steel. (n.d.-c). *Annual report 2020-21*. Retrieved October 16, 2024, from <https://steel.gov.in/sites/default/files/Annual%20Report-Ministry%20of%20Steel%202020-21.pdf>
- Ministry of Steel. (2021, July 22). *Energy and Environment Management in Iron & Steel sector*. <https://steel.gov.in/technicalwing/energy-and-environment-management-iron-steel-sector>
- Ministry of Steel. (2022, December 26). Year-end review-2022 Ministry of Steel. *PIB Delhi*.
- Ministry of Steel. (2023). *Brief report of activities*. Ministry of Steel, GoI.
https://steel.gov.in/sites/default/files/Published%20Brief%20Report%20of%20Activities%202023%20%281%29_0.pdf
- Ministry of Steel. (2024a). *Annual report 2023-24*.
https://steel.gov.in/sites/default/files/Annual%20Report%202023-24%20Final_0.pdf
- Ministry of Steel. (2024b, July 30). *The Government acts as a facilitator, by creating Conducive Policy Environment for Development of the Steel Sector—India became the world's Second-Largest Producer*. *PIB Delhi*.
<https://pib.gov.in/PressReleasePage.aspx?PRID=2039000>
- Ministry of New and Renewable Energy. (2023). *National Green Hydrogen Mission*.
chrome-extension://efaidnbmnnnibpcajpcglclefindmkaj/https://mnre.gov.in/img/documents/uploads/file_f-1673581748609.pdf
- Ministry of Environment, Forest and Climate Change of India. (2021). *India third biennial update report to the United Nations framework convention on climate change*.
https://unfccc.int/sites/default/files/resource/INDIA_%20BUR-3_20.02.2021_High.pdf
- Moses, I. A. (2023). Review on thermal energy audit of pyro-processing unit of a cement plant. *International Journal of Energy and Environmental Research*, 11(1), 54–74.
<https://doi.org/10.37745/ijeer.13/vol11n15474>
- Ministry of Steel. (2017). National Steel Policy
- Nhuchhen, D. R., Sit, S. P., & Layzell, D. B. (2022). Towards net-zero emission cement and power production using Molten Carbonate Fuel Cells. *Applied Energy*, 306, 118001.
<https://doi.org/10.1016/j.apenergy.2021.118001>
- Nippon Steel Corporation. (2023). *Development Hydrogen Injection Technology into Blast Furnace (Super COURSE50) World's Highest Level of CO2 Emissions Reduction Effect of Heated Hydrogen Injection at 22% Verified in the Test Furnace*. Nippon Steel Corporation.
https://www.nipponsteel.com/en/news/20230804_200.html#:~:text=The%20hydrog

en%20injection%20demonstration%20using,blast%20furnace%20has%20been%20verified.

- Nishioka, K., Takatani, K., & Yutaka, U. (2018). *Development of mathematical models for blast furnaces* (120). Nippon Steel & Sumitomo Metal.
<https://www.nipponsteel.com/en/tech/report/nssmc/pdf/120-10.pdf>
- Nitturu, K., Sripathy, P., Yadav, D., Patidar, R., & Mallya, H. (2023). *Evaluating net-zero for the Indian cement industry marginal abatement cost curves of carbon mitigation technologies*. <https://www.ceew.in/sites/default/files/How-Can-India-Decarbonise-For-Net-Zero-Sustainable-Cement-Production-Industry.pdf>
- National Productivity Council. (2017). *Good practices manual- greenhouse gases emission reduction cement sector*. National Productivity Council, India.
<https://www.npcindia.gov.in/NPC/Uploads/Competencies/Manual%20Cement%20sector.pdf>
- Oda, J., Akimoto, K., Tomoda, T., Nagashima, M., Wada, K., & Sano, F. (2012). International comparisons of energy efficiency in power, steel, and cement industries. *Energy Policy*, 44, 118–129. <https://doi.org/10.1016/j.enpol.2012.01.024>
- Padhi, M., Vakamalla, T. R., & Mangadoddy, N. (2022). Iron ore slimes beneficiation using optimised hydrocyclone operation. *Chemosphere*, 301, 134513.
<https://doi.org/10.1016/j.chemosphere.2022.134513>
- Peacey, J. G., & Davenport, W. G. (1979). *The iron blast furnace: Theory and practice*. Pergamon Press.
- Peray, K. E. (1979). *Cement manufacturer's handbook*. Chemical Publishing Co., Inc.
<https://apsaripuspita.wordpress.com/wp-content/uploads/2012/08/cement-manufacturers-hand-book-by-kurt-e-peray.pdf>
- Perilli, D. (2022, September 14). *Update on hydrogen injection in cement plants*. <https://www.globalcement.com/news/item/14637-update-on-hydrogen-injection-in-cement-plants>
- Qiao-kun, S., Qing-chun, Y., Jia-hao, Z., Xiao-fei, Y., & Wei-jin, Y. (2023). Numerical simulation of the dolomite in-situ desulfurization in molten iron. *Materials Research Express*, 10(1), 016512. <https://doi.org/10.1088/2053-1591/acb123>
- Rumayor, M., Fernández-González, J., Domínguez-Ramos, A., & Irabien, A. (2022). Deep decarbonization of the cement sector: A prospective environmental assessment of CO₂ recycling to methanol. *ACS Sustainable Chemistry & Engineering*, 10(1), 267–278. <https://doi.org/10.1021/acssuschemeng.1c06118>
- Sahu, B. (2013). *Study of washability characteristics of some Indian coals* [National Institute of Technology Rourkela]. <http://ethesis.nitrkl.ac.in/5133/1/109MN0127.pdf>
- Sau, D. C., Murmu, R., Senapati, P., & Sutar, H. (2021). Optimization of raceway parameters in iron making blast furnace for maximizing the pulverized coal injection (PCI) rate. *Advances in Chemical Engineering and Science*, 11(02), 141–153.
<https://doi.org/10.4236/aces.2021.112009>
- Schultmann, F., Engels, B., & Rentz, O. (2004). Flowsheeting-based simulation of recycling concepts in the metal industry. *Journal of Cleaner Production*, 12(7), 737–751.
[https://doi.org/10.1016/S0959-6526\(03\)00050-7](https://doi.org/10.1016/S0959-6526(03)00050-7)

- Segal, M. (2023, November 14). *Consumers Willing to Pay 12% Premium for Sustainable Products: Bain Survey*. <https://www.esgtoday.com/>
<https://www.esgtoday.com/consumers-willing-to-pay-12-premium-for-sustainable-products-bain-survey/>
- Shahabuddin, M., Rahbari, A., Sabah, S., Brooks, G., Pye, J., & Rhamdhani, M. A. (2024). Process modelling for the production of hydrogen-based direct reduced iron in shaft furnaces using different ore grades. *Ironmaking & Steelmaking: Processes, Products and Applications*, 03019233241254666. <https://doi.org/10.1177/03019233241254666>
- Shatokha, V. (2022). Modeling of the effect of hydrogen injection on blast furnace operation and carbon dioxide emissions. *International Journal of Minerals, Metallurgy and Materials*, 29(10), 1851–1861. <https://doi.org/10.1007/s12613-022-2474-8>
- Sinha, A., & Acharya, A. (2023). *India net zero steel demand outlook report*. Climate Group. <https://www.theclimategroup.org/sites/default/files/2024-02/India%20Net%20Zero%20Steel%20Demand%20Outlook%20report%203.pdf>
- Spinelli, M., Romano, M. C., Consonni, S., Campanari, S., Marchi, M., & Cinti, G. (2014). Application of molten carbonate fuel cells in cement plants for CO₂ capture and clean power generation. *Energy Procedia*, 63, 6517–6526. <https://doi.org/10.1016/j.egypro.2014.11.687>
- TATA Steel. (2020). *HISARNA - Building a sustainable steel industry*. <https://products.tatasteelnederland.com/sites/producttsn/files/tata-steel-europe-factsheet-hisarna.pdf>
- TATA Steel. (2022, January 21). *Tata Steel initiates a 'first-of-its-kind in the world' trial for continuous injection of Coal Bed Methane (CBM) in Blast Furnace to reduce emissions*. <https://www.tatasteel.com/media/newsroom/press-releases/india/2022/tata-steel-initiates-a-first-of-its-kind-in-the-world-trial-for-continuous-injection-of-coal-bed-methane-cbm-in-blast-furnace-to-reduce-emissions/>
- Thomas, E. (2020, January 31). *The WCA discusses de-NOx technologies and their application in cement plants*. <https://www.worldcement.com/special-reports/31012020/the-wca-discusses-de-nox-technologies-and-application-in-cement-plants/>
- Vipin, M., Sharma, M., R I, A., & Pushkar, P. (2023). *Cement industry of India: Outlook and challenges*. <https://www.infomerics.com/admin/uploads/Cement-Industry-Report-May2023.pdf>
- World Business Council for Sustainable Development. (2018). *Low carbon technology roadmap for the Indian cement sector: Status review*. https://docs.wbcsd.org/2018/11/WBCSD_CSI_India_Review.pdf
- West, K. (2020). *Technology factsheet*. TNO. https://energy.nl/wp-content/uploads/ref-bof-steelmaking-technology-factsheet_080920-7.pdf
- World Steel Association. (n.d.). *World steel in figures—2024*. World Steel Association. <https://worldsteel.org/wp-content/uploads/World-Steel-in-Figures-2024.pdf>
- Yang, K., Choi, S., Chung, J., & Yagi, J. (2010). Numerical modeling of reaction and flow characteristics in a blast furnace with consideration of layered burden. *ISIJ International*, 50(7), 972–980. <https://doi.org/10.2355/isijinternational.50.972>

- Yang, Y., Raipala, K., & Holappa, L. (2014). Ironmaking. In *Treatise on Process Metallurgy* (pp. 2–88). Elsevier. <https://doi.org/10.1016/B978-0-08-096988-6.00017-1>
- Yilmaz, C., Wendelstorf, J., & Turek, T. (2017). Modeling and simulation of hydrogen injection into a blast furnace to reduce carbon dioxide emissions. *Journal of Cleaner Production*, 154, 488–501. <https://doi.org/10.1016/j.jclepro.2017.03.162>
- Zang, G., Sun, P., Elgowainy, A., Bobba, P., McMillan, C., Ma, O., Podkaminer, K., Rustagi, N., Melaina, M., & Koleva, M. (2023). Cost and life cycle analysis for deep CO₂ emissions reduction of steelmaking: Blast furnace-basic oxygen furnace and electric arc furnace technologies. *International Journal of Greenhouse Gas Control*, 128, 103958. <https://doi.org/10.1016/j.ijggc.2023.103958>
- Zhang, H., Li, H., Tang, Q., & Bao, W. (2010). Conceptual design and simulation analysis of thermal behaviors of TGR blast furnace and oxygen blast furnace. *Science in China Series E: Technological Sciences*, 53(1), 85–92. <https://doi.org/10.1007/s11431-010-0029-0>

7. Appendix

7.1. Types of cement

There are several types of cement being manufactured in India, with each having its own unique properties and applications. However, the most manufactured cement types are the following:

OPC: This is widely used for its strength and durability and is ideal for large infrastructure projects such as bridges and reinforced concrete structures.

PPC: Made by blending OPC with pozzolanic materials such as fly ash. This enhances its workability and durability, making it suitable for structures near water and masonry work.

PSC: Includes ground granulated blast furnace slag, offering strong, durable concrete for mass concrete applications and marine constructions.

PCC or CC: This is made by combining OPC with materials such as limestone or slag, which improves workability and durability across various construction needs.

As of 2019–20, blended cement accounted for 73% of the total cement production in India, while OPC formed the remaining 27% (GCCA, 2022). Among the blended cement, PPC is the most prevalent type in the country, accounting for approximately 65% of the total blended cement. This is followed by PSC at 10%. Blended cement production results in lower emission footprint as more clinker, which is the most energy-intensive and emissions-intensive product in the cement plant, is substituted. Blended cement also differs in its property as per the type of additive utilised and can contribute to a wide spectrum of applications.

7.2. Other electrification technologies

Table A 1: Electrification technologies in cement manufacturing

Technology	Country/company/institution	Description
Electric Arc Calciner (EAC)	SaltX (Sweden)	Originally developed for quicklime production, the EAC has been shown to produce clinker with similar mineral characteristics to conventional clinker. SaltX is collaborating with Dalmia Bharat Limited to incorporate the EAC into an existing cement plant and with ABB Limited to provide control and electrical systems.
Plasma heating	Various	This method uses electricity to generate a hot beam of ionised plasma from a flowing gas. Heat is transferred to the product through convection. The CemZero project, a collaboration between Vattenfall and Cementsa, identified plasma generators in a pre-heater/pre-calciner system as a promising technology path for future development.

Technology	Country/company/institution	Description
Induction heating	Various	This process generates heat within an object by using a rapidly alternating magnetic field to induce electrical currents (eddy currents). However, this method requires the material to be electrically conductive. As cement raw meal is not sufficiently conductive, induction heating would require indirect heat transfer.
Microwave heating	Various	This technology transmits heat through microwave radiation into the material being heated. However, cement raw meal has poor microwave absorbing capacity, making this method inefficient for cement production.
Resistive heating	Various	This process generates heat by passing an electric current through a resistive element. Heat transfer to the material occurs through convection, conduction, or radiation. The challenge with this method lies in finding materials that can withstand the cement kiln's high temperatures, oxidising environment, and dusty atmosphere.
Cambridge Electric Cement process	Cambridge Electric Cement	This innovative approach integrates cement production with steel production in an EAF. It utilises spent cement powder from concrete waste, which has a similar composition to EAF slag, as a replacement for traditional lime-flux. The high temperatures in the EAF reactivate the cement, decarbonising the cement manufacturing process.
Leilac Technology	Heidelberg Materials (Germany)	This technology redesigns the traditional calciner to separate combustion exhaust gases from process CO ₂ emissions, allowing for efficient CO ₂ capture. It utilises an indirectly heated tube reactor, offering flexibility in heating sources, including electricity and AFRs.
ECoClay	FLSmidth Cement (Denmark)	This project aims to electrify the clay calcination process, making calcined clay, a lower carbon alternative to clinker. Rondo Energy's Heat Battery technology, which captures intermittent renewable electricity and stores it as high-temperature heat, is being considered for this process.

7.3. Decentralised renewable energy sizing: Green hydrogen (HOMER Pro)

To meet the hydrogen demand for green steel production, plants have the option to either negotiate supply agreements with external hydrogen providers or establish their own on-site hydrogen production facilities. Steel plants can generate hydrogen through water electrolysis. These projects can be powered entirely by the grid for baseload energy, a combination of grid and solar photovoltaic (PV), or solar PV paired with battery storage.

In this study, solar PV sizing necessary to produce the hydrogen that can be injected into the blast furnace was performed for the following two distinct scales:

Base case: Baseload met through grid and solar PV

100% Renewable energy case: Load met through 100% solar PV + battery storage

The systems were designed and optimised to estimate the corresponding LCOH that the steel manufacturer must bear.

To develop the models, certain assumptions were made (Table A 2).

Table A 2: Case set-up

Basis	1 MTPA crude steel production
Operational hours	24
Operational days	365
Hot metal: Crude steel	0.973
Amount of hydrogen injected into the blast furnace	21 kg/tHM
Annual hydrogen load (kg)	22,096,627
Electrolyser capacity (kW)	142,138

In addition to this, the capital, replacement and operating costs, and lifetime of the various components such as PV panels, converter, electrolyser, and battery that were fed to HOMER Pro for cost optimisation are tabulated in Table A 3.

Table A 3: Assumptions

SI No.	Component	Capital cost (INR)	Replacement cost (INR)	O&M (INR)	Lifetime (year)
1	Electrolyser	66,400/ kW	29,880	1,020/kW	7
2	Solar PV panel	54,000/ kW	–	350/kW	25
3	Converter	6,000/kW	6,000/kW	–	15
4	Li-ion battery	14,000/kW	14,000/kW	1,400	6
5	Hydrogen storage tank	42,278/ kg	–	–	25

The schematic diagrams from HOMER Pro provide a concise illustration of energy system configurations. These diagrams map the interactions between various components, helping in the design, optimisation, and analysis of hybrid energy systems. The schematic diagram for the two designed cases of hydrogen generation is shown below (Figure A 1 and Figure A 2).

Figure A 1: Base case (Grid + PV)

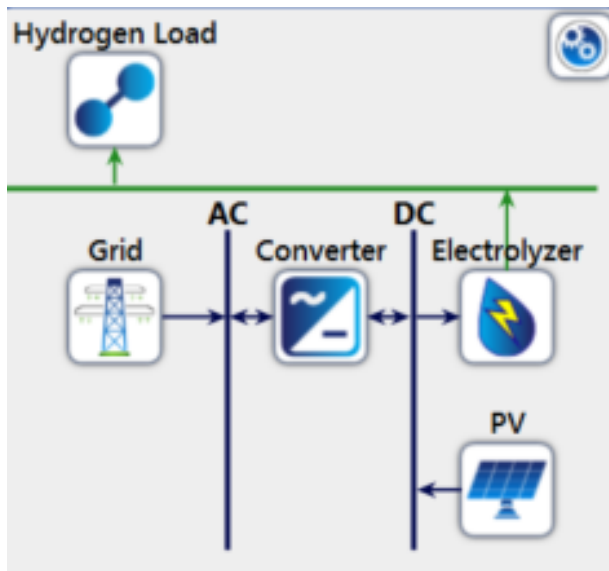
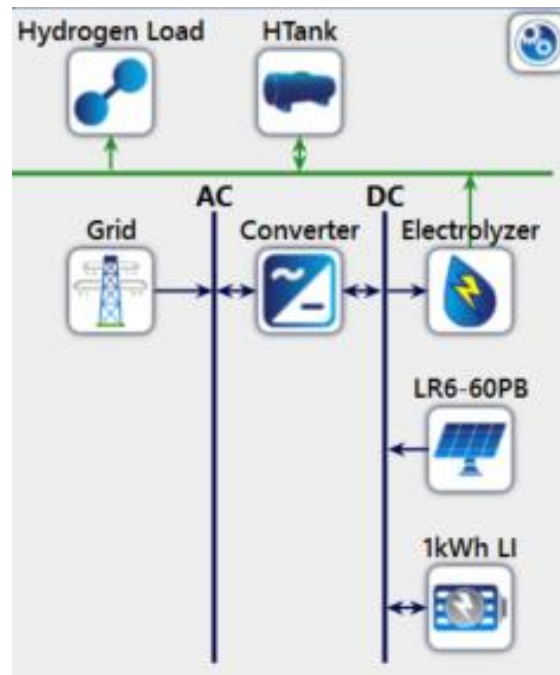


Figure A 2: 100% Renewable energy case



7.3.1. Base case

The base case is the most practical and achievable scenario for steel plants in the country. This involves relying on baseload (electrolyser load requirements necessary to generate the required hydrogen load) through the grid and PV panels. The solar panels were designed in HOMER Pro such that 75% of the total load is met by solar PV and the rest through the grid. This allowed for the excess electrical energy generated (kWh) to be sold to the grid during surplus and deficit bought from the grid during non-solar hours. The grid sellback price was set at INR 3/kWh while the purchase price was set at INR 6/kWh. Based on HOMER Pro's cost optimisation algorithm, the different results that were computed are listed below.

System architecture: The model specs are as follows: A PV system with a capacity of 1,385.8 MW and a converter rated at 1,150,000 kW.

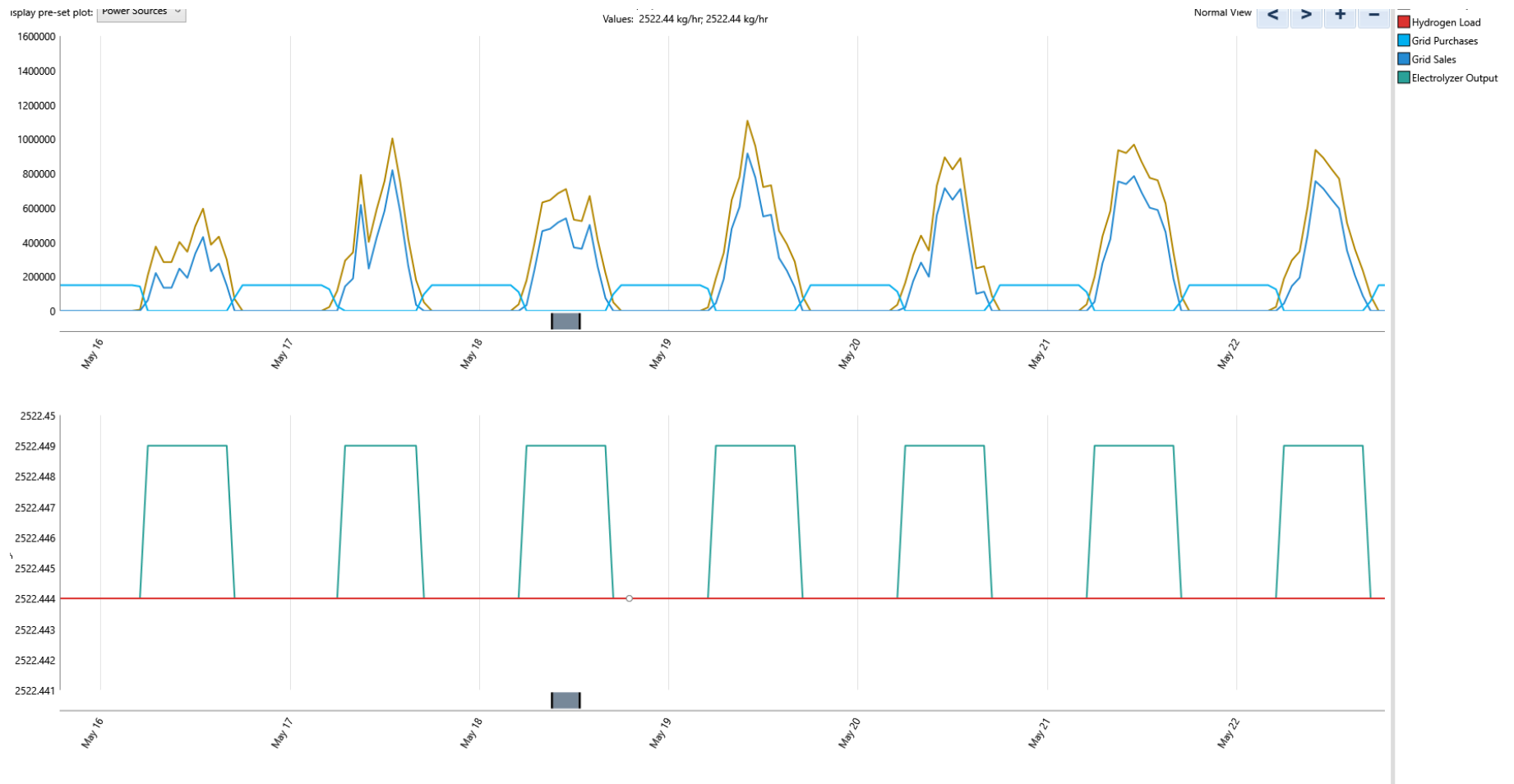
Table A 4: Energy balance - base case

Production (kWh/year)		Percentage
Generic flat plate PV	2,180,400,162	75%
Grid purchases	726,714,718	25%
Total	2,907,114,880	100%
Consumption (kWh/year)		Percentage
Grid sales	1,540,549,803	55.30%
Electrolyser consumption	1,245,127,382	44.70%
Total	2,785,677,185	100%

Due to the assumption that 75% of the baseload requirements will be met through renewable energy, a significant amount of excess electricity (55%; Table A 4) is being generated, which is sold to the grid. The LCOH was computed as INR 395/kg.

A representative time series plot depicting the solar load generation profile, electrolyser output, hydrogen load, grid sales, and grid purchase is given in Figure A 3.

Figure A 3: Time series plot - base case (screenshot)



7.3.2. 100% Renewable energy

To meet the load during non-solar hours, a lithium-ion-based battery set-up was introduced. The grid acts as a sink to which the excess energy that is generated from the solar PV system is sold.

System architecture: The system includes a solar panel array (LR6-60PB) with a total capacity of 2,984.8 MW, a battery storage system with a capacity of 10 GWh, and a hydrogen tank with a capacity of 1,000 t. The energy flows are listed in Table A 5.

Table A 5: Energy balance - 100% renewable energy case

Production (kWh/year)		Percentage
LONGi solar LR6-60PB	4,360,977,076	100%
Total	4,360,977,076	100%
Consumption (kWh/year)		Percentage
Grid sales	2,216,555,470	67.00%
Electrolyser consumption	1,091,700,000	33.00%
Total	3,308,255,470	100%

It was observed that the electrolyser was run at only about 83% of its capacity, resulting in approximately 10% of the total hydrogen requirement remaining unmet. The LCOH also increased more than seven times to 2,849 INR/kg because of the incurring battery and hydrogen storage costs.

A representative time series plot depicting the solar load generation profile, electrolyser output, hydrogen load, grid sales, battery discharge, and charge profile, as well as the hydrogen tank utilisation, is given in Figure A 4.

Figure A 4: Time series plot - 100% renewable energy (screens)





विज्ञान एवं प्रौद्योगिकी विभाग
DEPARTMENT OF
SCIENCE & TECHNOLOGY

**Climate, Energy and Sustainable Technology (CEST) Division
Department of Science & Technology (DST)
Ministry of Science & Technology – Government of India**

Technology Bhavan, New Mehrauli Road,
New Delhi – 110016, India
Website: www.dst.gov.in



CENTER FOR STUDY OF SCIENCE, TECHNOLOGY AND POLICY

Bengaluru

No. 18, 10th Cross, Mayura Street,
Papanna Layout,
Nagashettyhalli (RMV II Stage),
Bengaluru-560094
Karnataka, India

Noida

1st Floor, Tower-A, Smartworks Corporate
Park, Sector-125,
Noida-201303, Uttar Pradesh, India



www.cstep.in



+91-8066902500



cpe@cstep.in



[@cstep_India](https://twitter.com/cstep_India)